

Appendix D
2019 Groundwater Modeling Report



Grain Handling Facility at Freeman, Freeman, Washington

2019 Groundwater Modeling Report

Revised Draft

June 2020

Union Pacific Railroad



Grain Handling Facility at Freeman, Freeman, Washington

Project No: 661508
Document Title: 2019 Groundwater Modeling Report
Document No.: GES1120191147PDX
Revision: Revised Draft
Date: June 2020
Client Name: Union Pacific Railroad
Project Manager: David Hodson
Author: Brian Boer

Jacobs Engineering Group Inc.

2020 SW Fourth Avenue, Third Floor
Portland, OR 97201
United States
T +1.503.235.5000
F +1.503.736.2000
www.jacobs.com

© Copyright 2020 Jacobs Engineering Group Inc. The concepts and information contained in this document are the property of Jacobs. Use or copying of this document in whole or in part without the written permission of Jacobs constitutes an infringement of copyright.

Limitation: This document has been prepared on behalf of, and for the exclusive use of Jacobs client, and is subject to, and issued in accordance with, the provisions of the contract between Jacobs and the client. Jacobs accepts no liability or responsibility whatsoever for, or in respect of, any use of, or reliance upon, this document by any third party.

Contents

Acronyms and Abbreviations	vii
1. Introduction	1-1
2. Conceptual Model	2-1
2.1 Physiography	2-1
2.1.1 Climate	2-1
2.1.2 Surface Water Characteristics	2-1
2.1.3 Geology	2-1
2.1.4 Hydrogeologic Characterization	2-2
2.2 Groundwater Elevations	2-4
2.2.1 Water Level Trends	2-4
2.2.2 Groundwater Flow Directions	2-4
2.2.3 Seasonal Response to School Well Operations	2-5
2.2.4 Short-term Response to School Well Operations	2-5
2.3 Water Budget Components	2-5
2.3.1 Primary Inflow Components	2-5
2.3.2 Primary Outflow Components	2-6
2.4 Conceptual Model Summary	2-6
3. Numerical Model Construction	3-1
3.1 Groundwater Model Code Selection	3-1
3.2 Groundwater Model Domain and Grid	3-2
3.3 Groundwater Model Parameters	3-2
3.4 Groundwater Model Boundary Conditions	3-3
3.4.1 No Flow	3-3
3.4.2 Specified Head	3-3
3.4.3 Specified Fluxes	3-3
3.5 Time Discretization	3-5
4. Numerical Model Calibration	4-1
4.1 Groundwater Model Calibration Approach	4-1
4.2 Groundwater Model Calibration Targets	4-1
4.2.1 Head Targets	4-1
4.2.2 Drawdown Targets	4-1
4.3 Groundwater Model Calibration Results	4-2
4.3.1 Calibration to Steady-state Heads	4-2
4.3.2 Calibration to Short-term Stresses	4-2
4.3.3 Calibration to Long-term Stresses	4-3
4.3.4 Sensitivity Analysis	4-3
4.3.5 Calibration Summary	4-3
5. Model Application	5-1
6. Summary and Conclusions	6-1
7. References	7-1

Appendix

A 2019 Slug Test AQTESOLV Results

Tables

- 2-1 Packer Test Results
- 2-2 Slug Test Results
- 4-1 Well Details and Groundwater Elevations
- 4-2 Sensitivity Evaluation Results
- 4-3 Summary of Layer Storage Properties
- 4-4 Summary of Layer Hydraulic Conductivity

Figures

- 1-1 Site Location
- 1-2 Site Details
- 2-1 Precipitation and Evapotranspiration Rates
- 2-2 Wells and Borings with Elevation Top of Granite
- 2-3 Wells and Borings with Elevation Top of Basalt
- 2-4 Aquifer Test and Monitoring Well Locations
- 2-5 Hydrographs, Overburden Wells
- 2-6 Hydrographs, Upper Basalt Wells
- 2-7 Hydrographs, Basalt Wells
- 2-8 Hydrographs, Deep Granite Wells
- 2-9 Hydrographs, Lower Basalt Wells
- 2-10 Groundwater Elevations, Shallow and Granite Wells
- 2-11 Groundwater Elevations, Deep Basalt Wells
- 2-12 Freeman School Well (WS5) Pumping Rates
- 2-13 Freeman School Pumping Rates and Deep Basalt Groundwater Elevations
- 2-14 Example Short-Term Groundwater Elevation Fluctuations
- 3-1 Model Domain and Streams
- 3-2 Model Cross Section
- 3-3 Simulated Pumping Wells
- 3-4 Computed Freeman School Field Irrigation Rates
- 4-1 Simulated vs Observed Steady State Groundwater Elevations
- 4-2A Steady State Groundwater Elevations and Residuals, Layers 1-4
- 4-2B Steady State Groundwater Elevations and Residuals, Layers 5-7
- 4-3A Observed and Simulated Drawdown, 2017 Aquifer Test, Model Layer 1
- 4-3B Observed and Simulated Drawdown, 2017 Aquifer Test, Model Layer 2
- 4-3C Observed and Simulated Drawdown, 2017 Aquifer Test, Model Layers 3, 5, and 6
- 4-4 Observed and Simulated Drawdown, Response to WS5
- 4-5 Simulated vs Observed Transient Groundwater Elevations
- 4-6A Observed and Simulated Groundwater Elevations, Model Layer 1
- 4-6B Observed and Simulated Groundwater Elevations, Model Layer 2
- 4-6C Observed and Simulated Groundwater Elevations, Model Layers 3 and 4
- 4-6D Observed and Simulated Groundwater Elevations, Model Layer 5
- 4-6E Observed and Simulated Groundwater Elevations, Model Layers 6 and 7
- 4-7A Hydraulic Conductivity Distribution, Layers 1-4
- 4-7B Hydraulic Conductivity Distribution, Layers 5-8
- 4-7C Hydraulic Conductivity Distribution, Layers 9-12
- 4-7D Hydraulic Conductivity Distribution, Layers 13-16
- 4-8A Vertical Hydraulic Conductivity Distribution, Layers 1-4
- 4-8B Vertical Hydraulic Conductivity Distribution, Layers 5-8
- 4-8C Vertical Hydraulic Conductivity Distribution, Layers 9-12

- 4-8D Vertical Hydraulic Conductivity Distribution, Layers 13-16
- 5-1 Remedial Scenario Well Locations
- 5-2 Reverse Particle Starting Location Protocol
- 5-3 Remedial Scenario Results, Groundwater Elevations and Particle Pathlines

Acronyms and Abbreviations

3D	three-dimensional
AF/yr	acre-feet per year
cm/s	centimeter(s) per second
DFN	discrete fracture network
ET	evapotranspiration
EPM	equivalent porous medium
ft/day	foot (feet) per day
GHFF	Grain Handling Facility at Freeman
gpm	gallon(s) per minute
Jacobs	Jacobs Engineering Group Inc.
K	hydraulic conductivity
K _h	horizontal hydraulic conductivity
K _v	vertical hydraulic conductivity
mya	million years ago
R ²	coefficient of determination
RMSE	root mean squared error
USBR	U.S. Bureau of Reclamation
USGS	U.S. Geological Survey

1. Introduction

This report documents modifications to the Groundwater Flow Model previously documented in the Aquifer Test and Groundwater Modeling Report (Jacobs, 2018) for the Grain Handling Facility at Freeman (GHFF) at 14603 Highway 27, Freeman Washington (site) (Figures 1-1 and 1-2). Modifications were based upon additional hydraulic and geologic data collected in 2019.

2. Conceptual Model

A conceptual model is a theoretical construct of a physical system developed by assimilating relevant site information. Ideally, a conceptual model is the simplest representation of a physical system that provides enough information to achieve the modeling objectives.

2.1 Physiography

Freeman, Washington sits at the eastern edge of the Columbia Plateau, a large intermontane basin spanning from the Cascade Range in the west and the Rocky Mountains in the east. In the Freeman area, lower elevations consist of dryland-farmed grasslands, with scattered rural development. Upper elevations are typically forested with scattered rural development.

2.1.1 Climate

The climate in the Spokane-Freeman area is generally very warm and dry in the summer and cool and moist during the winter, with average temperatures ranging from near freezing in winter to around 70 degrees Fahrenheit in summer (NOAA, 2019). During 2017-2018, precipitation at the Spokane International Airport, located 17 miles northwest of Freeman and at approximately 2,370 feet elevation, averaged 18.6 inches per year, while the longer term average is approximately 16.5 inches per year. At Plummer, Washington, located approximately 19 miles southeast of Freeman at approximately 2,750 feet elevation, precipitation averaged of 29.3 inches per year for 2017-2018.

Figure 2-1 shows daily precipitation rates for 2017 through June 2019 at both Spokane International Airport and Plummer, along with the average monthly potential evapotranspiration (ET) rate. The ET data are from the U.S. Bureau of Reclamation (USBR) Agrimet station at Chamokane, northwest of Spokane, the location nearest Freeman (USBR, 2017). Most precipitation occurs in the winter, spring, and fall, while the highest ET rates are in the summer. The timing of precipitation at Spokane International Airport and Plummer is very similar, with typically higher magnitudes at Plummer.

2.1.2 Surface Water Characteristics

The largest stream in the area is Rock Creek, approximately 3 miles southwest of the GHFF (Figure 1-2). Rock Creek flows to the northwest, where it enters Hangman Creek approximately 6 miles west of Freeman. The Rock Creek watershed (which includes Freeman) covers 179 square miles. Several smaller named and unnamed tributaries to Rock Creek drain the local Freeman area.

2.1.3 Geology

The basin is filled primarily with basalt of Cenozoic age. The basalt is often interbedded overlain by consolidated or unconsolidated sediments in the western portion of the basin. The basalt is underlain by igneous and metamorphic rocks of the Idaho Batholith.

There are four primary geologic units in the Freeman area:

1. Idaho Batholith – primarily granitic rocks
2. Columbia River Basalt – extensive flood basalts
3. Latah Formation – sedimentary deposits found overlaying or interbedded with basalt
4. Palouse Formation – loess and developed soils

Basement rocks of the Idaho Batholith consist of Pre-Tertiary (greater than 63 million years ago [mya]) gneiss and granite. These rocks are exposed on the hills east of Freeman and slope downward steeply to the west. Subsurface lithology was interpreted from 78 wells and borings installed specifically for the site and 155 private well boring logs available from the Washington State Department of Ecology (Ecology, 2017).

Data from these wells and borings were used to create contour plots of the buried granite surface (Figure 2-2). The granitic surface is well-defined near the GHFF and the hills to the northeast, but few borings or wells intersect the granitic surface southwest of the GHFF.

The Columbia River basalts erupted during the Miocene Period, 5 to 24 mya. The Priest Rapids member of the Wanapum Basalt erupted approximately 14.5 mya, and overlays the Idaho Batholith in most areas beneath Freeman and to the west. The lateral extent of the basalt is shown on Figure 2-3, extending underneath most of the town of Freeman. The basalt flows were typically intermittent and overlapping, and groundwater flow within a particular flow group can vary from dominantly horizontal to dominantly vertical over relatively short distances.

The wells and borings encountering basalt are shown on Figure 2-3. The interpreted granite surface is included on Figure 2-3, indicating that the thickness of basalt is typically 200 to 300 feet, thinning toward the northeast. There appear to be two distinct, vertically stacked basalt flows, separated by a thin (10 to 20 feet) interbed deposit containing soil and vegetative material. The contact appears at approximately 280 feet in the vicinity of well WS5 (the Freeman School well), and has not been detected closer to the GHFF. Some domestic wells encountered this interbed deposit.

The basalt flows filled the stream valleys and dammed the local streams, creating extensive ponds and wetlands along the eastern margin of the Columbia River basalts (USGS, 1969). Lacustrine deposits from these wetland features are known as the Latah Formation. The silts, sands, and clays were deposited between various basalt flows and occasionally overlay the uppermost basalts. The Latah Formation generally contains leaves and other organic matter that indicate quiet waters. However, in some areas, the formation consists of deposits created by mass wasting or landslides. Flora and fauna of the Latah Formation indicate a temperate climate with 30 to 40 inches annual rainfall, permitting deep weathering of exposed and buried rocks.

An important effect of ponding and wetland development along the eastern margins of the Columbia River basalts was the accelerated decomposition of saturated basalt and granitic bedrock. Thick saprolites (layers of highly decomposed rock) developed with properties dependent on the parent material. Generally, basalts decomposed into bluish gray clays (primarily halloysite) and granitic rocks decomposed into white clays (kaolinite), quartz, and muscovite micas (USGS, 1969).

Other clays are present in the area, including greenish gray silty clays from lacustrine deposits and brown silty clays of the Palouse. Locally, some residual clay deposits from granitic saprolites were mined for brick construction during the past century.

In the Freeman area, the shallow subsurface consists of the silty Palouse Formation, consisting primarily of loess, or eolian deposits believed to have originated from the scoured surface remaining following the Pleistocene glacial retreat. The thickness of the Palouse Formation varies from less than 10 feet to over 50 feet (USGS, 1969). The Palouse Formation is generally thin to non-existent on the hills east of Freeman.

Palagonites have been inferred at depth in some well boring logs. Palagonite is an alteration product created when basaltic lava enters open water or saturated terrain, and can result in fractured or shattered glassy deposits with orange to brown coloration. Palagonite and palagonite tuffs can have higher or lower permeabilities than typical fractured basalt, depending on the degree of solidification or the presence of clays (as may be expected if the basalt entered shallow ponds or wetlands).

2.1.4 Hydrogeologic Characterization

Several site-specific investigations have been undertaken to better understand site hydrogeology. These are summarized in Section 4.5 of the *Remedial Investigation/Feasibility Study Report, Grain Handling Facility at Freeman, Freeman, Washington* (Jacobs, 2019a) and in the *Basalt Aquifer Characterization, Grain Handling Facility at Freeman, Freeman, Washington* (Jacobs, 2019b; Appendix B of Jacobs, 2019a). Results pertaining to hydraulic conductivity assessments and slug test results from 2019 are presented in this section, along with hydraulic properties from the 2018 groundwater flow model (Jacobs, 2018).

Previous site investigation (Jacobs, 2019a; 2019b) and groundwater modeling (Jacobs, 2018) work identified zones of high contrasting basalt permeability, based upon observed potentiometric surface measurement in monitoring wells, aquifer testing, and numerical model calibration. In general, the basalt at and surrounding the site is more permeable in the area of the GHFF, and at depth to the southwest in the vicinity of Freeman School well WS5 in the lower fractured basalt. Water levels are relatively uniform throughout the basalt aquifer in the area of the GHFF. Steep hydraulic gradients exist between the shallow water-bearing zones (including upper basalt) and deeper fractured basalt in the vicinity of well WS5. Hydraulic gradients are also very steep between the fractured basalt aquifer near the GHFF and the deeper fractured basalt aquifer penetrated by well WS5.

Additional characterization of saturated basalt using borehole geophysics, hydrophysical logging, and packer testing was completed (Jacobs, 2019b; Appendix B of Jacobs, 2019a). This work provided additional corroborating evidence of a non-fractured basalt acting as a confining layer separating the upper and lower fractured basalt offsite (southwest) of the GHFF.

Site-specific estimates for hydraulic conductivity values based on previous groundwater model calibration are summarized here. The horizontal hydraulic conductivity (K_h) of the near-GHFF basalt aquifer was estimated to be 25 feet per day (ft/day) ($8.8E-3$ centimeters per second [cm/s]), and up to 20 ft/day ($7.1E-03$ cm/s) in the deeper fractured basalt aquifer to the southwest (Figure 3-6 in Jacobs, 2018). The hydraulic conductivity (K) of less-permeable basalt separating the GHFF aquifer from the downgradient aquifer was lower (K_h of 0.5 ft/day [$1.8E-4$ cm/s], K_v of 0.002 to 0.006 ft/day [$7.1 E-7$ to $2.1E-6$ cm/s]).

2.1.4.1 2019 Packer Testing

As part of a broad basalt aquifer characterization program, packer tests were performed in boring RC-2 and RC-4 (Figure 2-4). K_h values were derived from the packer tests and are summarized in Table 2-1. The highest values were in the deeper portions of RC-4 (near Freeman School well WS5) and the lowest values in the shallow basalt at both locations.

2.1.4.2 2019 Slug Testing

Between September 10 and 13, 2019, slug tests were performed in 10 newly installed monitoring wells to evaluate hydrogeologic characteristics of the site (Figure 2-4). All slug tests were performed according to the Jacobs Engineering Group Inc. (Jacobs) Slug Testing Standard Operating Procedure using a 0.057-cubic-foot slug volume. A rising- and falling-head test was performed in each well and an In-Situ Troll 700 transducer was used to log head displacement at 5-second intervals during each test. For consistency, the rising-head portion of each test was selected for analysis and evaluation of the slug test data. AQTESOLV v4.5 (Duffield, 2007) was used to analyze the slug test data and estimate the localized hydraulic conductivity surrounding each well screen interval.

Slug test transducer data were loaded into WinSitu 5 and exported to a comma-separated value format. The data were then processed with R programming code to extract the rising-head portion and convert the raw water levels into normalized head displacement. The two-dimensional time-displacement data were then loaded into AQTESOLV v4.5 to perform curve-fitting and estimate hydraulic conductivity.

Depending on the hydrogeologic conditions of each well, the appropriate analytical curve-fitting solution was selected for analyzing the slug test data. For wells screened in the unconfined aquifer with an overdamped (straight-line) head response, the Bouwer-Rice (1976) method was chosen. For wells screened in the confined aquifer with an overdamped head response, the Hvorslev (1951) method was chosen. For wells screened in the confined aquifer with an underdamped (oscillatory) head response, the Butler (2002) method was chosen. For wells screened in the unconfined aquifer with an underdamped head response, the Springer-Gelhar (1991) method was chosen. All solutions have the same basic set of the following assumptions :

- The aquifer has infinite areal extent.
- The aquifer is homogeneous and of uniform thickness.
- The aquifer potentiometric surface is initially horizontal.
- The slug test well is fully or partially penetrating the aquifer.

- The slug acts instantaneously upon the control well.
- Flow to well is in steady-state.

Slug test results are presented in Table 2-2. The estimated hydraulic conductivity among all 10 wells ranged over 4 orders of magnitude, from 0.02 ft/day (0.00001 cm/s) to 88 ft/day (0.31 cm/s). The highest values (over 10 ft/day [3.5E-03 cm/s]) are at the bottom of the younger basalt flow [MW-33] and just below at the top of the older basalt flow [MW-32], and in shallow basalt at MW-36). Wells screened in granitic material generally have the lowest values – less than 0.1 ft/day (3.5E-5 cm/s). The results at MW-34 are not considered representative of actual conditions because of the proximity of Freeman School well WS5 and violation of the basic assumption of steady-state ambient conditions and horizontal potentiometric surface. AQTESOLV analysis output for each well is presented in Appendix A.

2.1.4.3 Additional Characterization

A surface geophysical survey was undertaken in 2019 (ECA Geophysics, 2019), but the results of this study have not been incorporated in the conceptual site model or the groundwater flow model pending further review.

2.2 Groundwater Elevations

Groundwater elevation data have been collected at several monitoring wells since 2016 and 2017, both manual measurements and continuous data from pressure transducers. Figure 2-4 shows the locations of the monitoring wells.

2.2.1 Water Level Trends

Figures 2-5 through 2-9 show the groundwater elevation trends at these wells. Pressure transducer data were collected at 15-minute intervals and distilled to daily average for display in the figures. The vertical scale for these figures is kept constant at 12 feet, with the exception of well MW-6D (Figure 2-9), which exhibits the greatest measured overall fluctuations of over 16 feet.

Groundwater elevations typically fluctuate seasonally on the order of 1 to 8 feet, with the lower amplitudes occurring in wells MW-20D (Figure 2-7) and MW-5D (Figure 2-8), both of which are near the Freeman School irrigated fields (Figure 2-4). The seasonal pattern of the upper and lower wells is slightly offset, with the rises and falls occurring earlier in the deeper basalt wells closer to the school production well (Figure 2-9). The daily water level data at well MW-6D show considerable scatter, driven by the daily cycling of the Freeman School well operations.

No sitewide year-to-year trends are apparent, although water levels at some wells (W20, Figure 2-6, and MW-14D, Figure 2-8) and all deep basalt wells (Figure 2-9) appear to be overall increasing.

2.2.2 Groundwater Flow Directions

The groundwater system can be roughly divided into upper and lower regions. Figures 2-10 and 2-11 show average groundwater elevations at wells as grouped into these two regions, with the average data based solely upon manually measured historical data. The interpreted potentiometric surface (based on these averaged groundwater elevations) indicates that the groundwater flow direction in both depictions is generally toward the southwest. The groundwater elevations drop by about 80 feet between the upper region and the lower region in the vicinity and immediately upgradient of Freeman School well WS5, as well as laterally away from the GHFF at depth.

These steep vertical and horizontal hydraulic gradients separate the upper region and the GHFF basalt aquifer from the more extensive and deeper fractured basalt aquifer penetrated by the school production well and presumably extending south and westward. Groundwater conditions in the deep basalt (Figure 2-11) are based on a limited number of wells, and show very uniform groundwater elevations to the southwest of well WS5. Between this area and the deeper basalt at well MW-19D, the hydraulic gradient is very steep, indicating low permeability material over this interval (including unfractured basalt and

underlying low-permeability granite). The groundwater elevations at MW-19D are very similar to the shallow and granite wells in the same area, indicating weak vertical hydraulic gradients closer to the GHFF (Figure 2-10).

2.2.3 Seasonal Response to School Well Operations

Detailed pumping rate data were obtained from a recently installed totalizer in the Freeman School well (WS5) plumbing for the period from December 7, 2018, through June 24, 2019. Totalizer readings indicate that the well pumps between 54 and 55 gallons per minute (gpm) when the well is on. Variations likely have to do with both the ambient starting head in the aquifer and the total duration pumped, as both will affect the total head the pump needs to overcome to deliver water.

To get a more complete record of school well pumping operations, transducer-based groundwater elevations data at nearby wells MW-6D and MW-15D were evaluated to determine the percent of time WS5 was operating, as evident from the 15-minute transducer data (and rapid responses at observation wells to the pumping stress). Weekly average pumping rates were computed for the period from January 1, 2017, through August 2019 (Figure 2-12). Figure 2-12 also includes weekly average precipitation data (from Spokane) to illustrate the reciprocal relationship between pumping and precipitation rates. During the winter, when the schools' sports fields and landscaping are not being irrigated, the well pumps at an average daily rate of 3.95 gpm (rates range from 1.7 to 10.8 gpm). During the summer irrigation season, the well pumps nearly continuously, with a daily rate of 53.9 gpm (rates range from 47.3 to 55.0 gpm). The average annual rate is 20.6 gpm based on data from 2017 and 2018. The estimated data shown on Figure 2-12 are because of gaps in transducer and/or totalizer records. Three gap periods (January 1 to May 20, 2017, October 1, 2017 to April 7, 2018, and December 16, 2018 to January 5, 2019) occurred during periods of typical low water use, and were assigned the average low use rate of 3.95 gpm. A separate gap from June 6 through July 31, 2019, was assigned the high rate of 53.9 gpm.

Figure 2-13 overlays the Freeman School well pumping data with water level records from the deep basalt wells MW-4D, MW-6D, MW-15D, and MW-18D. The relationship is seen most clearly during the September-October 2018 transition from high-pumping to low-pumping, as water levels at the monitoring wells begin to recover. The day-to-day variability in MW-6D water levels is much more pronounced and of higher magnitude during this transition time because of the sporadic nature of well WS5 pumping durations.

2.2.4 Short-term Response to School Well Operations

The 15-minute transducer data, combined with pumping records taken from well WS5, enable evaluation of the hydraulic response to WS5 operations. Data from early June 2019 were normalized to water levels on June 6, 2019, at 3 a.m. (just before well WS5 turning on for a cycle). Figure 2-14 shows these data displayed as drawdown from this time, for all wells with transducers, combined with pumping rate data. Of these wells, four in the deep fractured basalt aquifer show a clear response to the pumping fluctuations: MW-6D, MW-4D, MW-15D, and MW-18D. The remaining wells do not appear to be affected by the short-term cycling at WS5. Other wells did detect unknown disturbances (MW-19D and W20 in particular), most likely because of nearby domestic well operations.

2.3 Water Budget Components

The following subsections describe the primary groundwater inflow and outflow components to the overall simulated groundwater balance in the study area.

2.3.1 Primary Inflow Components

On the basis of the dimensions and location of the study area and relevant and available hydrologic and water use data, the following primary components of water inflow to the study area can be logically assumed:

- Precipitation and subsequent infiltration into groundwater
- School irrigation return flow

- Wastewater from Freeman School water treatment

Although other sources of inflow might exist, it is assumed that consideration of these inflow components identified above is sufficient to further evaluate the water balance and develop the model.

2.3.2 Primary Outflow Components

On the basis of the dimensions and location of the study area and relevant and available hydrologic and water use data, the following primary components of water outflow from the study can be logically assumed:

- Groundwater extraction
- ET
- Subsurface outflow to adjacent areas
- Discharge to surface water drains and streams

As with the primary components of water inflow, it is assumed that consideration of these outflow components is sufficient to further evaluate the groundwater balance and develop the model.

2.4 Conceptual Model Summary

The Freeman area is characterized by a complex geologic setting, with three distinct parent materials (loess, basalt, and granitic bedrock) in various states of competency (competent to highly weathered saprolites). The hydrogeology of the site includes productive aquifers in the shallow basalt in the GHFF area and in the downgradient deep fractured basalt. These two productive areas are separated both vertically and laterally by tight, unfractured basalt, leading to steep hydraulic gradients both vertically and laterally.

The hydrologic cycle is seasonal in nature, driven by precipitation. No surface water enters the area, and surface water features serve to drain the landscape. The primary groundwater stress is the Freeman School well, which operates in a seasonal fashion somewhat tied to precipitation patterns, as most pumped water is used for sports field and landscape irrigation (less irrigation is required when it rains, and vice versa). Well WS5 operations appear to drive seasonal changes in deep basalt groundwater elevations, as well as to cause short-term perturbations recorded in monitoring wells. Seasonal groundwater trends in shallow and deep wells upgradient of the deep productive basalt appear to be driven by precipitation cycles.

3. Numerical Model Construction

Three-dimensional groundwater flow modeling was performed to evaluate hydrogeologic characteristics at the site and surrounding area with the goal of aiding in the understanding of site hydrogeology and development of remedial strategies at the site. Remedial option evaluations will include particle tracking with the groundwater flow model. The groundwater model uses meteorological data, hydrological data, and estimated aquifer characteristics to simulate groundwater flows, groundwater elevations (heads), and groundwater exchange rates with surface water under specific hydrogeological and operational conditions.

The overall approach to groundwater flow model development includes constructing, calibrating, and applying a three-dimensional (3D), physically based, spatially distributed numerical model. The model simulates average, or steady-state, conditions as well as the transient aquifer test at extraction well EW-9U.

Numerical model development is the result of translating understanding of the physical system into a form that is suitable for numerical modeling. The groundwater flow model for the site was developed using the following steps:

1. Selecting numerical groundwater flow model code
2. Establishing a model domain and developing a model grid
3. Specifying subsurface hydraulic parameter values
4. Establishing boundary conditions for groundwater flow
5. Selecting a time discretization approach appropriate for evaluating the field problem

The following sections describe the methodology for executing these five design steps.

3.1 Groundwater Model Code Selection

Groundwater flow in fractured rock aquifers can be simulated using two basic modeling approaches: discrete fracture networks (DFN) and equivalent porous medium (EPM) (ITRC, 2017). DFN models explicitly represent individual fractures, incorporating 3D spatial relationships and interconnectedness between fractures in rock matrices. EPN models treat fractured media as traditional porous media (as with an alluvial sedimentary or similar environment). EPM models use hydraulic properties data (K, storativity) from field observations and available hydraulic stress data, and are generally much less computationally demanding than DFN models. DFN applications typically are used at much smaller scale than EPM models because of the difficulty of obtaining information on fracture distribution and properties (length, aperture, and roughness) at the scale typically required for sitewide modeling. EPM models have limitations, such as the inability to characterize small-scale hydrogeology that may be dominated by a small number of fractures, but are generally considered suitable for evaluating hillslope- or catchment-sized problems.

An EPM approach was determined to be suitable for sitewide groundwater modeling at the site because of both the intense data needs of DFN modelling and the ability to characterize the fractured media using macro-scale classification. Specifically, basalt flows at the GHFF have been characterized as having relatively large-scale features (fractured and unfractured zones, distinctions between flow tops/bottoms and flow cores, and palagonites zones) that can be simulated using an EPM approach. The model also needs to include unconsolidated overburden (loess), which is an important element of the groundwater system at the site. However, the limitations of the EPM approach for fractured basalt are recognized, and an EPM model may not be suitable for characterizing small-scale phenomena, for estimating groundwater velocities on small scales, or for contaminant transport.

After determining to implement an EPM approach, the MODFLOW 2005 code with the NWT configuration (MODFLOW-NWT) (Niswonger et al., 2011) was selected for the following reasons:

- The code is an improvement on MODFLOW with respect to drying and rewetting of cells (which occurs during simulation of aquifer testing).

- MODFLOW-NWT is built on the U.S. Geological Survey (USGS) MODFLOW model (Harbaugh et al., 2000). MODFLOW-NWT has been benchmarked and verified, meaning that the numerical solutions generated by the code have been compared with one or more analytical solutions, subjected to scientific review, and used on previous modeling projects. Verification of the code confirms that MODFLOW 2005-NWT can accurately solve the governing equations that constitute the mathematical model (Niswonger et al., 2011).

3.2 Groundwater Model Domain and Grid

The lateral extent of the groundwater flow model was determined by evaluating surface topography and, if possible, extending the model boundaries to local topographic divides. The model domain was selected to include most of the local watershed, draining toward Rock Creek in the southwest (Figure 3-1). The model boundary thus follows topographic divides along all borders except along Rock Creek, the lower reaches of Ochlare Creek, and Cottonwood Creek.

To facilitate calculation of groundwater flows, the groundwater flow model domain is divided into discrete blocks of space called grid cells. The grid spacing is generally 100 by 100 feet, but is refined to 25- by 25-foot cells in the primary area of interest (Figure 3-1),

The model incorporates 16 vertically stacked model layers to provide a 3D representation of the subsurface system. Land surface topography with 10-foot resolution was downloaded in a digital elevation model file format from the USGS National Elevation Dataset (USGS, 2017). The land surface elevation data set was used to define the top of Layer 1 (Figure 1-2).

Ideally, model layers would represent geologic contacts or features. The geology of the site is complex and partially defined by the existing well logs. The general pattern includes thick basalt flows butting up against granitic bedrock, with well-developed saprolites at the interfaces and loess overburden. Generally, Layer 1 represents unconsolidated overburden, Layers 2 through 10 represent the upper basalt flow, Layer 11 represents the soil horizon separating the upper and lower basalt flows, Layers 12 through 14 represent the lower basalt flow, and Layers 15 and 16 represent granite. The model was constructed with somewhat horizontal layers that extend across the basalt-granite contact. At the contact, the hydraulic properties of the model layers transition from basalt to granite. Correlation of the various facies of a typical basalt flow (that is, porous flow top, tight entablature, and rubble zones at the base) between site boring logs resulted in a distribution of hydraulic properties that coarsely represent these features. In general, the model represents productive basalts in the source area basalt aquifer, tight relatively unproductive basalts south and west of the GHFF, and permeable basalts in the deeper portions of the upper basalt flow, near and surrounding the school production well. The properties (storage and hydraulic conductivity) of the basalt in these and other areas were varied during calibration to match observed groundwater levels.

3.3 Groundwater Model Parameters

After the structure of a model grid was established, cell-by-cell parameter values were distributed throughout the groundwater flow model domain. The groundwater flow model requires cell-by-cell K_h and K_v input values. These cell-by-cell K_h and K_v values are grouped into zones (K zones) that generally represent distinct geologic materials.

Data from aquifer tests and professional judgment formed the basis for the initial K_h and K_v values before calibration. These values were adjusted during the calibration process, which is discussed in Section 4. Figure 3-2 presents a cross section of the model grid passing roughly northeast to southwest through the GHFF (MW-9D) and the Freeman School Well (WS5), and generally aligned with the centerline of carbon tetrachloride-impacted groundwater. Figure 3-2 identifies various interpreted geologic features within the model structure and post-calibration (calibration discussed in Section 4) horizontal hydraulic conductivity values along the specific section alignment. Hydraulic conductivity values vary widely in the horizontal dimension for each model layer, and a more detailed layer-by-layer distribution of post-calibration values is presented in Section 4.

3.4 Groundwater Model Boundary Conditions

Boundary conditions for groundwater flow models are mathematical statements or rules that specify head or groundwater flux around the margins and at locations within the model domain. The model uses specified head, specified flux, and no-flow boundary conditions.

3.4.1 No Flow

The topographic divides along the model domain were assigned as no-flow boundaries in Layer 1 (Figure 3-1). In Layers 2-16, the entire model domain boundary is a no-flow boundary, with the exception of constant head boundaries in Layer 14 (discussed in the following subsections). This is a simplifying assumption, as it is likely that there is non-zero subsurface flow crossing these boundaries. This component of the water budget was not simulated as it is deemed sufficiently distant from the main site to be of little consequence to the water budget at the site.

3.4.2 Specified Head

The creeks and streams within the model domain, except for the larger Rock Creek, are ephemeral, with no data on streamflow or duration (Figure 3-1). All streams were simulated as drains, with heads specified as land surface at the creeks. Drains only allow flow out of the model, and only when the elevation of groundwater in each cell is higher than the base of the stream in that cell. This is a slight simplification of the hydrologic system, as some small amounts of water may infiltrate from streams into groundwater along some reaches of the stream network.

The conductance term of the drain cells, which controls the rate of flux between the drain cells and adjacent regular model cells, was adjusted during calibration by altering the vertical hydraulic conductivity of the drain cells. The final value used in the drains was 10 ft/day (2.1E-03 cm/s).

The hydrogeology near Rock Creek is poorly characterized because of a lack of monitoring wells or borings. The previous version of the model specified a no flow boundary vertically beneath Rock Creek, forcing all groundwater in this area to move upward and ultimately discharge into Rock Creek. The revised model allows for the deep groundwater to bypass Rock Creek and continues moving toward the southwest by implementing a constant head boundary in model Layer 14 beneath Rock Creek. Layer 14 was chosen for the boundary condition as it has the highest hydraulic conductivity (2 ft/day) of the deep basalt. The head was specified to slope from 2,300 feet in southeast to 2280 feet in the northwest and to remain constant.

3.4.3 Specified Fluxes

Recharge from precipitation and irrigation, ET, school wastewater effluent, and groundwater extraction are specified flux boundary conditions in the model. Specified flux boundaries add or remove a specified volumetric flow to or from a model cell.

3.4.3.1 Groundwater Extraction

Groundwater withdrawals via pumping wells are also specified flux boundaries. Figure 3-3 shows pumping wells within the model domain. The Freeman School well (WS5) is the largest pumping well in the area and provides water for sports field and landscape irrigation and consumptive use. Pumping rate data were previously discussed in Section 2.2.3.

Domestic pumping rates for the 77 domestic wells were computed using the average per-person water use for Washington State (103 gallons per day) (USGS, 2015) and estimated household size. Household size was estimated by reviewing census data for nearby Rockport, as there are no census data for Freeman. In Rockport, the average household size was 2.45 people per household, for a household rate of 252 gallons per day (0.18 gpm). Return flow from septic systems was not simulated.

3.4.3.2 Precipitation, Evapotranspiration, and Groundwater Recharge

Precipitation data from two locations were evaluated for use in the model: Spokane International Airport is approximately 17 miles northwest of Freeman at an elevation of 2,370 feet, and Plummer, Washington is approximately 19 miles southeast of Freeman at an elevation of 2,750 feet (Freeman is at approximately 2,620 feet elevation, with elevations in the model domain ranging from 2,100 feet near Rock Creek to about 3,600 feet in the hills to the northeast) (NOAA, 2019). Daily average data for both locations were obtained for 2017 through June 2019, with the totals for this period 46.4 inches at Spokane and 73.3 inches at Plummer. Total snowfall for this time period at Spokane was 142 inches, and poorly or not recorded at Plummer. Assuming 10 percent water content, snowfall at Spokane represents approximately 14.2 inches of water, or approximately 23 percent of total precipitation.

Determining groundwater infiltration rates from precipitation is a complex process. The fate of precipitation includes interception, ET, and surface runoff, with the remainder as unsaturated flow that reaches the water table. Studies in nearby areas suggest that the percent of precipitation that results in groundwater infiltration is in the 1 to 5 percent range (Buchanan and Brown, 2003). Inherent in this process is a lag in the time of precipitation compared to the time of actual groundwater infiltration. For the model, these complex processes were simplified by scaling and lagging precipitation recharge to match observed water level trends in shallow wells. These simplifications serve to reduce model run times (compared to trial runs with full vadose zone simulations), eliminate the need for estimation of unknown vadose zone parameters (which tend to vary spatially and temporally), and streamline the modeling effort.

Ultimately, the precipitation rates from Plummer were rejected as being too high to represent the Freeman area. While the elevation at the town of Plummer is seemingly representative of elevations at Freeman, Plummer is surrounded by forested hills well over 3,000 feet elevation, and is likely subject to greater orographic effects than Freeman, which sits westward of the local forested mountains.

The Spokane-based precipitation data, when input directly into the model as groundwater recharge, also resulted in excessively high groundwater elevations that could not be mitigated by adjusting other model properties (hydraulic conductivity and storage) within reasonable ranges. Improved model performance was obtained by multiplying the precipitation data by a factor of 0.4 before input into the model, as well as lagging the input by 8 weeks (for better simulation of upper basalt and overburden well groundwater elevations). The 0.4 adjustment factor on precipitation rates accounts for surface runoff to streams and other drainage features, which is not explicitly simulated by the model.

Return flow rates for the Freeman School irrigated fields are directly related to the operation of the Freeman School well. The process for computing the return flow rate under the irrigated fields was as follows:

1. It was assumed that during times of high pumping rates, all but 10 gpm of the pumped school water went to irrigate the fields and landscaping.
2. The irrigated portion of the school grounds was estimated to be 11.5 acres, based on field sizes, which results in an application rate of 0.21 inches per day (6.3 feet per year on an annualized basis) when the school well is pumping at full rate. The rates were computed on a weekly basis. This results in a rate of approximately 1.5 inches per week during irrigation, within commonly recommended rates for turf grass irrigation of 1 to 2 inches per week (Cornell University, 2019)
3. The total rate applied to the school fields was the sum of this computed rate and the precipitation rate. The relationship between the computed school irrigation rate, precipitation, and the overall application rate for the school fields is shown on Figure 3-4.

Recharge rates for areas covered by Freeman School District buildings was set to 0, and parking lots at 1 percent of computed precipitation recharge. Runoff was assumed to route to surface water conduits (ditches and drains) to local streams and not enter the groundwater system,

Monthly average reference ET data are available from the USBR Agrimet weather network (USBR, 2019). The station nearest Freeman is Chamokane, Washington in northwest Spokane. The yearly average ET rate here is 3.3 inches per day, and was applied throughout the model domain with a

15-foot extinction depth (the depth below ground surface within which ET is active). A 15-foot extinction depth is within the range of extinction depths reported for grasslands in silty and clayey soils (14.1 to 23.4 feet) in the “Extinction Depth and Evapotranspiration from Ground Water under Selected Land Covers” (Shaw et. al., 2007) (ET rates are shown on Figures 1-2 and 3-4).

The school treats wastewater in a lined wastewater treatment pond and effluent is piped to a constructed wetland south of the school. Flow rate data into the wetlands were obtained for the period of 2008 through July 2011. Water was piped to the wetland primarily from November to April or May of this time period. The average monthly rate when water transfers occur is 6.7 gpm, and the average annual rate (200—to 2010) is 3.3 gpm. The wetlands drain into Little Cottonwood Creek, but rates are not routinely monitored. Because Little Cottonwood creek is simulated as a drain, and to address the possibility that water introduced into the wetland may infiltrate into the groundwater system, the wastewater flow rates were allowed to bypass the Little Cottonwood Creek drain boundary condition and enter the aquifer by using a single injection well.

3.5 Time Discretization

For model calibration, time was discretized in the following ways:

1. For the steady-state model, there is no time discretization.
2. For 2017 aquifer testing, the durations of the various pumping periods dictated model stress period durations.
3. For the evaluation of short-term well WS5 cycles, the on-off cycles of the school well dictated model stress period durations.
4. For the evaluation of longer term trends (the 2.5 year model), weekly (7-day) stress periods were used.
5. For remedial evaluations, two cycles per year were used to simulate well WS5 cycling and precipitation recharge. The high-pumping/low precipitation period was assumed to last 122 days, and the low-pumping/high precipitation period was assumed to last 243 days, based upon data from 2017 and 2018. This cycle was repeated for 15 years.

4. Numerical Model Calibration

Model calibration is a process of adjusting hydraulic properties in a numerical model to simulate observed subsurface head and flow conditions in the field (as described with measured data) within a reasonable degree of accuracy. This subsection discusses the calibration approach, targets, and results.

For the groundwater flow model, calibration was based upon three distinct conditions: (1) average steady-state hydrologic conditions, (2) short-term transient conditions imposed during the 2017 aquifer test and during short-term well WS5 cycling, and (3) seasonal conditions. As such, two separate calibration models were developed. The first, referred to as the aquifer test model, was a hybrid steady-state and transient model where the model runs under steady-state conditions initially, then switches to transient simulation over the duration of 2017 aquifer testing activities (step test, first constant rate test, second constant rate test, and recovery) followed by WS5 cycling evaluation. The second is the seasonal model, which evaluated seasonal changes from January 2017 through July 2019.

4.1 Groundwater Model Calibration Approach

The calibration approach relied solely on manual calibration, with relevant parameters adjusted to minimize the difference between measured and simulated values, known as model error. The objectives of calibration were to create a groundwater flow model that would sufficiently replicate steady-state groundwater conditions and drawdown observed during aquifer testing.

4.2 Groundwater Model Calibration Targets

Calibration targets are defined as the selected field-measured values that quantify site conditions of interest with consideration of data quality and reliability. Long-term groundwater elevation progress data and drawdown during aquifer testing were selected as calibration targets to evaluate the progress of calibration during the groundwater flow model development.

4.2.1 Head Targets

In general, steady-state groundwater models strive to simulate average hydrologic conditions. As such, average groundwater elevations at site wells from January 2017 through December 2018 were used as targets for steady-state model calibration (Table 4-1). Only manual measurements were used to compute the steady-state targets as the locations and duration of transducer-based data are inconsistent between wells.

Calibration summary statistics were computed to provide a measure of the steady-state model's ability to replicate the quantitative calibration-target head values. Head calibration was evaluated using the following summary statistics:

- Residual error, computed as the simulated head value minus the target head value at a single well
- Mean error, computed as the sum of all residual errors divided by the number of observations
- Coefficient of determination (R^2), computed as the square of the correlation coefficient between model simulated and measured heads
- Root mean squared error (RMSE), computed as the square root of the mean of all residual squared errors
- RMSE/Range, the RMSE divided by the range of target head values

4.2.2 Drawdown Targets

Drawdowns observed during the 2017 aquifer test (Jacobs, 2018) and short-term fluctuations because of pumping at well WS5 during early June 2019 pumping (Figure 2-14) were incorporated into the model

and used as targets during the transient portion of the model. Successful calibration of drawdown to aquifer test drawdown was primarily based on qualitative evaluation of the magnitude and timing of simulated drawdown.

4.3 Groundwater Model Calibration Results

Calibration of the groundwater flow model was an iterative process, alternating focus between the steady-state, short-term stresses, and seasonal stresses. The resultant model adequately satisfies calibration criteria for both sets of calibration data.

4.3.1 Calibration to Steady-state Heads

Figure 4-1 shows observed versus computed heads, and includes summary statistics. The residual mean was -2.58 feet, and the scaled residual mean error was 4.27 percent, with no notable biases. There are large ranges of observed head across some individual model layers. The residual errors were all within 10 percent of the total observed range.

Figures 4-2A and 4-2B show the distribution of wells and head calibration residuals with groundwater heads by layer. In general, the model realistically simulates the very steep hydraulic gradients, horizontal and vertical, across the site.

4.3.2 Calibration to Short-term Stresses

The entirety of the 2017 aquifer test, including step test, first constant rate test, and revised constant rate test, and the short-term stress response to well WS5 (data wells MW-4D, MW-6D, MW-15D, and MW-18D on Figure 2-14) were evaluated with the groundwater flow model. Figure 4-3 shows the observed and simulated drawdown at the monitoring wells. Figures 4-3A, 4-3B, and 4-3C correspond to the 2017 aquifer test, and Figure 4-3D corresponds to the WS5 response data.

In general, the model was able to simulate the large-magnitude drawdown observed at many wells, with a common theme of simulated recovery lagging behind observed recovery. Drawdown in the upper basalt overburden monitoring wells MW-8S and MW-9S was of similar magnitude to shallow wells screened only in the upper basalt (monitoring wells MW-7S and MW-10S). Monitoring well MW-9S dewatered during all pumping phases, so no drawdown is recorded beyond approximately 8 feet (the model continues to compute head during these times, although Layer 1 in this area does go dry during the simulations).

Most wells in granite or other tight materials exhibited a muted response to the pumping, which the model realistically simulated (for example, for wells MW-1D, MW-2D, and MW-14D). Some wells at relatively greater distances from the pumping well exhibited rather sharp responses to pumping stresses, which were challenging to replicate, and often the simulated drawdown was more muted than observed (for example, at wells MW-11S, W20, and to some extent, MW-19D).

For the June 2019 response to well WS5 pumping, four wells recorded drawdown (MW-15D, MW-18D, MW-4D, and MW-6D). Figure 4-4 shows the simulated and observed drawdown at these wells. In general, the model was able to replicate the sharp transitions associated with the pumping fluctuations, but overestimated the drawdown at the monitoring wells. Well MW-6D was particularly difficult to calibrate to, and any solution that achieved the approximate magnitude of drawdown here tended to create overly dampened responses at the other, more distant, monitoring wells. Well MW-6D is near well WS5 and responds rapidly to pumping fluctuations. Localized connecting fractures may play a role in the water level responses here.

In general, the groundwater flow model reasonably simulated drawdown at most observation wells, particularly wells in basalt with greater magnitudes of drawdown. The residual mean error for all short-term drawdown data was 0.2 foot, with a scaled RMSE of 11.3 percent.

4.3.3 Calibration to Long-term Stresses

The seasonal model simulates well WS5 and precipitation cycling from January 1, 2017 through July 2019. Figure 4-5 shows the simulated versus observed water level data for this time period as well as summary statistics. The residual mean error was -2.99 feet, and the scaled root mean squared error was 4.04 percent. Figures 4-6A, 4-6B, 4-6C, 4-6D, and 4-6E show the final simulated and observed water levels at wells across the site, organized by the layer of the monitoring wells. In general, the simulated water levels match the timing and amplitude of seasonal changes, with a slight bias toward higher than observed heads.

Water levels in Layers 1 and 2 (Figures 4-6A and 4-6B) are generally too high by about 5 feet, with better results to the south at well MW-6S. The timing and magnitude of seasonal fluctuations is well matched with the exception of MW-1S, where the observed cycles appear to have a greater amplitude, and a later seasonal low, than simulated. Water levels at MW-5D and MW-20D are closest to the Freeman School irrigated fields, and have low magnitude seasonal amplitudes, both observed and simulated.

Simulated water levels in the deep productive aquifer are monitored by wells MW-15D (Layer 5), MW-4D and MW-18D (Layer 6), and MW-6D (Layer 7) (Figures 4-6D and 4-6E). In general, the model was able to replicate the magnitude and timing of the seasonal fluctuations in this aquifer, although the simulated water levels were often more sensitive to changing well WS5 pumping rates than the daily average observed water levels suggest.

4.3.4 Sensitivity Analysis

A sensitivity analysis was performed to evaluate model input parameters on head distribution within the model. Two separate evaluations were performed, one on hydraulic conductivity (K_h and K_v) and one on storage parameters (specific storage and specific yield). The sensitivity evaluation was conducted on the steady-state model, aquifer test calibration model, and 2.5-year transient model.

The parameters evaluated were multiplied by factors of 0.5, 0.8, 0.9, 1.1, 1.2, and 1.5. Table 4-2 summarizes the results of the sensitivity evaluation. For the steady-state model, the minimum residual occurred using a factor of 1.1 for K values, indicating that results were slightly improved over the values used in the final model. For the aquifer test model, the minimum error was achieved with the 0.9 multiplier on storage properties and 0.8 multiplier on K values. For the seasonal model, the minimum error was achieved with the 1.1 multiplier on K values (as with the steady-state model), and storage was a relatively insensitive parameter, with the minimum using the 1.5 multiplier but only improving from 4.0 percent error to 3.9 percent.

The discrepancy of the effect of the K multiplier (better with higher values for steady state and seasonal, better with lower values for aquifer test model) points to the challenges of iteratively optimizing model parameters between the models. The final values used represent a compromise in calibration of the various target data sets.

4.3.5 Calibration Summary

Overall, the groundwater flow model successfully simulated the average sitewide head conditions and the aquifer test focused on conditions near the GHFF. A combination of steady-state, short-term, and seasonal targets give improved confidence in the performance of the model.

Model calibration was most challenging with respect to observations that exhibited sharp responses to pumping stresses at large distances from the origin of the pumping stress. This is likely because of the fractured and heterogeneous nature of the basalt aquifer. Columbia River basalts have been documented to have very wide ranges of permeabilities over short distances and include zones of hydraulic conductivity with magnitudes over 1,000 ft/day, which is much higher than the maximum 125 ft/day simulated here. Such zones could exist at the site, but the assignment of such high values did not prove advantageous during calibration.

4.3.5.1 Parameter Values

Simulating the very steep hydraulic gradients at the site required zones with very low vertical and/or horizontal hydraulic conductivity. From a vertical perspective, tight basalt layers could easily provide low enough K_v to generate the large head differences between upper and lower basalt. But for areas where the horizontal gradient is very steep, namely between wells screened in granite and those in lower basalt, low K_h was required along the basalt-granite interface.

Figures 4-7A, 4-7B, 4-7C, and 4-7D show the final K_h used in the model. There was generally wide range, over several orders of magnitude, for properties representing basalt and granite. Generally, hydraulic conductivity of the basalt aquifer ranges from 0.001 ft/day (3.5E-07 cm/s) in tight zones to 125 ft/day (4.4E-02 cm/s) in the more permeable zones. Granite K_h varied from 0.0001 (3.5E-08 cm/s) to 0.5 ft/day (1.8E-04 cm/s), generally decreasing with depth. The interface between granite and basalt, where the steep hydraulic gradients are present, had K values of 0.005 ft/day (1.8E-6 cm/s).

Figures 4-8A, 4-8B, 4-8C, and 4-8D show the K_v used in the model. K_v for basalt ranged from 0.002 ft/day (7.1E-07 cm/s) in tight basalt to 0.1 ft/day (3.5E-05 cm/s) in most of the fractured, productive basalt, with some areas as high as 1.25 ft/day (4.4E-04 cm/s). The lowest values were in portions of the granite upgradient of the GHFF and deeper zones at 0.0001 ft/day (3.5E-08 cm/s).

Storage properties specific yield and specific storage are generally regarded as time-sensitive, as water can be released from storage at different rates for different time scales (Neuman, 1979). Iterative calibration of the aquifer test and seasonal model suggested that the specific storage and specific yield values may be different for the different time scales. Table 4-3 summarizes layer-by-layer general geologic material and storage properties used in the final versions of the models at three locations between the source area (GHFF; MW-9D) and the Freeman School Well (WS5) shown in cross section on Figure 3-2. Table 4-3 also identifies where layer storage values used in the seasonal model deviate from those in the aquifer test model. Lower values of specific storage were used in the seasonal model in layers corresponding to the productive deeper basalt (Layers 5 through 7). Higher values of specific yield were used in the seasonal model in Layers 1 and 2, corresponding to the overburden and upper basalt. The storage values for other basalt layers and for granite were held consistent between the two versions of the model.

Table 4-4 summarizes the layer-by-layer horizontal and vertical hydraulic conductivity values at three points between the source area (GHFF; MW-9D) and the Freeman School Well (WS5) shown in cross section on Figure 3-2. As shown on Figures 4-7 and 4-8, the hydraulic conductivity values vary widely depending on location within each model layer.

4.3.5.2 Water Budget

The groundwater balance for the steady-state model is summarized in acre-feet per year (AF/yr) as follows:

- Inflow
 - Recharge from precipitation: 5,441 AF/yr
 - Constant Head: 1.1 AF/yr
 - Wells: 144 AF/yr
 - Total: 5,586 AF/yr
- Outflow
 - Wells: 193.4 AF/yr
 - Evapotranspiration: 2,706 AF/yr
 - Drains: 1,199 AF/yr
 - Constant Head: 309.2 AF/yr
 - River: 1,174 AF/yr
 - Total: 5,582 AF/yr
 - Error: 4.1 AF/yr, 0.07%

The constant head inflow term is an unintentional artifact of the constant head boundary condition beneath Rock Creek. The well portion of the water budget is slightly misleading, as it includes flow through domestic wells that span multiple layers across steep hydraulic gradients. Proscribed groundwater extraction was 54.7 AF/yr - 21.5 AF/yr from scattered domestic wells and 33.2 AF/yr (20.6 gpm) from well WS5, with simulated infiltration of 5.4 AF/yr (3.3 gpm) representing wetland effluent (see section 3.4.3.2). The remaining 138 AF/yr (83 gpm) in the water budget represents flow through well casings from areas of higher head to areas of lower head. Inter-well flow was observed in the ambient flow monitoring in borings RC-2 (0.07 gpm), RC-3 (0.09 gpm), and RC-4 (0.06 gpm) (Jacobs, 2019b), suggesting that this aspect of the water budget is real but possibly overestimated.

5. Model Application

The calibrated long-term stress model was modified to evaluate a potential remedial scenario involving groundwater recirculation (extraction, treatment [not simulated], and injection). The scenario uses two extraction wells located near the center of the carbon tetrachloride plume, with injection wells along the lateral and upgradient periphery (Figure 5-1). The remedial scenario involves two extraction wells and four injection wells. Extraction well EXT-1A is screened in model Layers 2 and 3 with a pumping rate of 15 gpm. Extraction well EXT-1B is screened in model Layers 4, 5, and 6, with a pumping rate of 35 gpm. Injection wells INJ-1 and INJ-2 inject 5 gpm each into model Layers 1 to 5. Injection well INJ-3 injects 15 gpm and INJ-4 25 gpm in Layers 2 to 5.

The remedial model was based on the long-term stress calibration model, with stress periods revised to 2 stress periods per year, with a total duration of 15 year run time. The biennial stress periods represent the seasonal alternation between low precipitation and high well WS5 pumping conditions and high precipitation and low WS5 pumping conditions. The duration for each was 243 and 122 days, respectively, based on 2017-2018 data.

Tracking the movement of water in the remedial scenario model was accomplished using MODPATH particle tracking software (Pollock, 1994). Reverse particle tracking was used to evaluate potential groundwater flow pathways leading to extraction wells EXT-1A and EXT-1B, and well WS5. The reverse particles originated in circular rings of 24 particles surrounding the cell center of the extraction well locations (Figure 5-2). To incorporate vertical variability within layers, nine vertically dispersed rings were started per layer per well, as shown on Figure 5-2.

Reverse particle tracks and groundwater elevations are presented for model Layers 2 through 6 on Figure 5-3. The groundwater elevations are from the final stress period of the model run, corresponding to low precipitation/high well WS5 pumping. Reverse particle tracks in Layers 2, 3, and 4 primarily originate from the remedial injection wells.

6. Summary and Conclusions

The Freeman groundwater flow model was updated to incorporate additional site data obtained since original model development. The additional data include lithologic information from borings RC-01, RC-02, RC-03, and RC-04; packer testing data from RC-02 and RC-04; slug testing from a variety of wells; and additional groundwater elevation data collected from site monitoring wells. Calibration targets were expanded from the 2017 aquifer test to include responses to short-term Freeman School well cycling and to seasonal changes over 2.5 years.

Iterative calibration between the steady-state targets, short-term drawdown aquifer testing and well WS5 operations, and seasonal effects of pumping and precipitation cycles illustrated the sensitive nature of the model. Small changes in hydraulic properties in one area of the model would have far reaching effects on heads in other areas of the model. For example, K-value adjustments focused on calibrating to drawdown at one well would often affect the steady-state calibration head at wells in different layers or far away from the area of change.

The calibrated groundwater flow model adequately represents site hydrogeologic conditions and can be used as a tool to assist in remedial efforts. The revised model was used to simulate one potential remedial scenario involving the use of a groundwater recirculation system (extraction, treatment, and reinjection of water at a rate of 50 gpm) in addition to the ongoing operation of well WS5. The simulation suggested that such a strategy may prevent portions of the plume core from migrating beyond the proposed new extraction wells located in the core of plume. The remedial option evaluated suggests that a recirculation system involving groundwater extraction and re-injection of 50 gpm in conjunction with the ongoing operation of well WS5 should hydraulically control the majority of the dissolved carbon tetrachloride plume at the site. The remedial option presented here represents a proof of concept of a remedial approach, and additional evaluation and optimization may be performed in the future.

7. References

- Bouwer, H. and R. C. Rice. 1976. "A Slug Test for Determining Hydraulic Conductivity of Unconfined Aquifers with Completely or Partially Penetrating Wells." *Water Resources Research*. Vol. 12. No. 3. June 1976. pp. 423-428.
- Butler, J.J., Jr., 2002. "A Simple Correction for Slug Tests in Small-Diameter Wells." *ground water*. Vol. 40. No. 3. pp. 303-307.
- Buchanan, John P. and Kevin Brown. 2003. *Hydrology of the Hangman Creek Watershed (WRIA 56), Washington and Idaho*. Prepared for the Spokane County Conservation District, Hangman (Latah) Creek Planning Unit (WRIA 56) and Washington State Department of Ecology. June.
- Cornell University. 2019. "Watering." Sports Field Management. <http://safesportsfields.cals.cornell.edu/watering>.
- Duffield, G.M., 2007. *AQTESOLV for Windows Version 4.5 User's Guide*. HydroSOLVE, Inc., Reston, Virginia.
- ECA Geophysics, 2019. *Geophysical Investigation Report, UPRR GHF and the FSD Complex, Freeman, Washington*. July 19.
- Harbaugh, A.W., E.R. Banta, M.C. Hill, and M.G. McDonald. 2000. *MODFLOW-2000, the U.S. Geological Survey modular ground-water model – the Ground-Water Flow Process*. U.S. Geological Survey, Reston, Virginia.
- Hvorslev, M.J. 1951. *Time Lag and Soil Permeability in Ground-Water Observations*. Bulletin No. 36, Waterways Experiment Station. Corps of Engineers, U.S. Army, Vicksburg.
- Interstate Technology and Regulatory Council (ITRC). 2017. *Characterization and Remediation of Fractured Rock*. December.
- Jacobs Engineering Group Inc. (Jacobs). 2018. *Aquifer Test and Groundwater Modeling Report, Grain Handling Facility at Freeman, Freeman, Washington*. June.
- Jacobs Engineering Group Inc. (Jacobs). 2019a. *Remedial Investigation/Feasibility Study Report, Grain Handling Facility at Freeman, Freeman, Washington*. In progress.
- Jacobs Engineering Group Inc. (Jacobs). 2019b. *Basalt Aquifer Characterization, Grain Handling Facility at Freeman, Freeman, Washington*. In progress.
- National Oceanic and Atmospheric Administration (NOAA). 2019. Daily Average Precipitation data. <https://www.ncdc.noaa.gov/cdo-web/>.
- Neuman, S.P. 1979. "Perspective on 'Delayed yield.'" *Water Resources Research*. Vol. 15. No. 4. August 1979. pp. 899-908.
- Niswonger, R.G., S. Panday, and M. Ibaraki. 2011. "MODFLOW-NWT, A Newton Formulation for MODFLOW-2005." *U.S. Geological Survey Techniques and Methods*, Book 6, Chapter A37. p. 44.
- Pollock, David W. 1994. *User's Guide for MODPATH/MODPATH-PLOT, Version: A particle tracking post-processing package for MODFLOW, the U.S. Geological Survey finite difference ground-water flow model*. U.S. Geological Survey Open File Report 94-464.

Shah, Nirjhar, Mahmood Nachabe, and Mark Ross. 2007. "Extinction Depth and Evapotranspiration from Ground Water under Selected Land Covers." *ground water*. Vol. 45. No. 3.

Springer, R.K. and L.W. Gelhar, 1991. *Characterization of large-scale aquifer heterogeneity in glacial outwash by analysis of slug tests with oscillatory response*. Cape Cod, Massachusetts, U.S. Geological Survey Water Resources Investigation Report 91-4034. pp. 36-40.

U.S. Bureau of Reclamation (USBR). 2017. *Monthly Average Reference Evapotranspiration*. Chamokane, Washington. Accessed October 2017. <https://www.usbr.gov/pn/agrimet/monthlyet.html>.

U.S. Geological Survey (USGS). 1969. *Clay Deposits of Spokane County, Washington*. Geological Survey Bulletin 1270.

U.S. Geological Survey (USGS). 2015. *Numerical Simulation of Groundwater Flow in the Columbia Plateau Regional Aquifer System, Idaho, Oregon and Washington*. Scientific Investigations Report 2014-5127.

U.S. Geological Survey (USGS). 2017. "Elevation." The National Map. <https://nationalmap.gov/elevation.html>.

Washington State Department of Ecology (Ecology). 2017. Washington State Well Report Viewer. <https://fortress.wa.gov/ecy/wellconstruction/Map/WCLSWebMap/default.aspx>.

Tables

Table 2-1. Packer Testing Results*2019 Groundwater Modeling Report, Grain Handling Facility at Freeman, Freeman, Washington*

Boring	Interval Tested	Depth to Top of Testing Interval (feet)	Depth to Bottom of Testing Interval (feet)	Approximate Elevation, Top of Testing Interval (feet)	Approximate Elevation, Bottom of Testing Interval (feet)	Hydraulic Conductivity (ft/day)	Hydraulic Conductivity (cm/s)
RC-02	1	57.1	142	2567	2482	0.03	9.9E-06
RC-02	2	145.5	156	2478.5	2468	1.9	6.8E-04
RC-02	3	156	225	2468	2399	0.43	1.5E-04
RC-02	4	192	225	2432	2399	0.49	1.7E-04
RC-04	1	120	148	2466	2438	0.12	4.2E-05
RC-04	2	254	264.5	2332	2322	78	2.8E-02
RC-04	3	265.5	276	2320.5	2310	4.5	1.6E-03
RC-04	4	282	292.5	2304	2294	50	1.8E-02

Notes:

ft/day = foot (feet) per day

cm/s = centimeter(s) per second

Table 2-2. Slug Test Results

2019 Groundwater Modeling Report, Grain Handling Facility at Freeman, Freeman, Washington

Testing Date	Well ID	Unit	Depth to Top of Screen (feet)	Depth to Bottom of Screen (feet)	Initial Depth To Water (feet bgs)	Depth of Transducer (feet bgs)	Depth of Slug (feet bgs)	Slug Test Type	Aquifer Type	Slug Test Curve-Fitting Method	Comments	Estimated Hydraulic Conductivity (ft/day)	Estimated Hydraulic Conductivity (cm/s)
9/13/2019	MW-26	Basalt / Palagonite	215	225	112.77	132	127	Rising-head	Unconfined	Bouwer-Rice ^a	good fit	4.8E+00	1.7E-03
9/12/2019	MW-27	Granitic	233	243	67.59	88	82	Rising-head	Unconfined	Bouwer-Rice ^a	good fit, but poor to later data	8.3E-02	2.9E-05
9/12/2019	MW-28	Basalt / Palagonite	180	190	59.13	79	74	Rising-head	Unconfined	Bouwer-Rice ^a	good fit, but poor to later data	4.0E+00	1.4E-03
9/12/2019	MW-29	Basalt	120	140	58.40	79	73	Rising-head	Unconfined	Bouwer-Rice ^a	good fit	4.2E-01	1.5E-04
9/12/2019	MW-30	Basalt	80	100	58.40	79	73	Rising-head	Unconfined	Bouwer-Rice ^a	poor fit	1.7E+00	6.1E-04
9/11/2019	MW-31	Granitic	380	385	99.54	120	115	Rising-head	Confined	Hvorslev ^b	excellent fit	2.3E-02	8.0E-06
9/10/2019	MW-32	Older Basalt	284	294	124.52	144	140	Rising-head	Confined	Hvorslev ^b	good fit	1.0E+01	3.6E-03
9/11/2019	MW-33	Basalt	254	274	125.03	145	140	Oscillatory	Confined	Butler ^c	good fit, oscillations	5.5E+01	1.9E-02
9/11/2019	MW-34	Basalt	165	185	124.88	145	140	Rising-head	Unconfined	Bouwer-Rice ^a	very poor fit	8.5E-02	3.0E-05
9/13/2019	MW-36	Basalt	60	75	20.51	41	35	Oscillatory	Unconfined	Springer-Gelhar ^d	good fit, oscillations	8.8E+01	3.1E-02

^aBouwer, H. and R. C. Rice. 1976. "A Slug Test for Determining Hydraulic Conductivity of Unconfined Aquifers with Completely or Partially Penetrating Wells." *Water Resources Research*. Vol. 12. No. 3. June 1976. pp. 423-428.

^bHvorslev, M.J. 1951. *Time Lag and Soil Permeability in Ground-Water Observations*. Bulletin No. 36, Waterways Experiment Station. Corps of Engineers, U.S. Army, Vicksburg.

^cButler, J.J., Jr., 2002. "A Simple Correction for Slug Tests in Small-Diameter Wells." *ground water*. Vol. 40. No. 3. pp. 303-307.

^dSpringer, R.K. and L.W. Gelhar, 1991. *Characterization of large-scale aquifer heterogeneity in glacial outwash by analysis of slug tests with oscillatory response*. Cape Cod, Massachusetts, U.S. Geological Survey Water Resources Investigation Report 91-4034. pp. 36-40.

Notes:

bgs = below ground surface

cm/s = centimeter per second

ft/day = foot (feet) per day

ft³ = cubic feet

Table 4-1. Well Details and Groundwater Elevations

2019 Groundwater Modeling Report, Grain Handling Facility at Freeman, Freeman, Washington

Well	Easting	Northing	Top of Casing (ft amsl)	Depth to Top Screen (ft)	Depth to Bottom Screen (ft)	Elevation Top Screen (ft amsl)	Elevation Bottom Screen (ft amsl)	Lithology of Screened Interval	Model Layer	Groundwater Elevation (ft amsl)											Average (Steady State Target)		
										8/1/16	12/1/16	2/23/17	3/30/17	5/25/17	8/31/17	12/7/17	3/3/18	6/22/18	10/3/18	1/16/19		3/11/19	6/12/19
MW-1D	2539524.6	211096.8	2598.5	88.0	98.0	2511	2501	Granite	5	2576.8	2574.9	2576.1	2577.9	2580.2	2576.3	2576.3	2579.2	2581.2	2577.9	2576.7	2577.9	2580.5	2577.8
MW-1S	2539516.9	211100.6	2598.6	15.0	25.0	2584	2574	Clay (saprolite)	1	2577.2	2575.4	2575.5	2576.9	2581.6	2580.0	2576.7	2579.0	2583.9	2578.9	2576.8	2577.6	2582.7	2578.6
MW-2D	2539795.1	210893.6	2597.7	135.0	145.0	2463	2453	Granite	7	2566.3	2566.0	2566.3	2567.4	2568.8	2567.9	2566.7	2568.4	2569.7	2567.9	2567.2	2568.1	2569.3	2567.7
MW-3D	2539415.0	210902.9	2604.9	168.0	178.0	2437	2427	Granite	8	2575.8	2572.1	2573.2	2575.0	2577.0	2574.5	2572.6	no data	2576.9	2573.9	2571.0	2574.6	2576.9	2574.5
MW-4D	2539671.0	209664.1	2576.1	182.5	187.5	2394	2389	Basalt	8	2461.1	2462.8	2465.1	2466.1	2467.8	2461.6	2464.7	2468.5	2467.5	2464.6	2469.0	2470.2	2470.0	2466.1
MW-5D	2538577.2	210981.2	2627.3	140.0	150.0	2488	2478	Granite	4	2563.9	2563.9	2564.2	2564.1	2564.7	2564.7	2564.0	2565.1	2565.2	2565.2	2565.2	2565.1	2565.3	2564.6
MW-6D	2539181.9	209427.9	2589.5	212.0	232.0	2378	2358	Basalt	8	2455.8	2461.3	2463.4	2464.3	2461.2	2454.6	2462.8	2461.5	2460.7	2462.9	2467.2	2463.0	2463.7	2461.7
MW-6S	2539171.0	209430.8	2589.9	35.0	45.0	2555	2545	Latah	1	2553.4	2553.9	2554.9	2556.5	2556.5	2554.8	2553.7	2556.6	2556.3	2554.3	2554.3	2554.4	2555.2	2555.0
MW-6U	2539140.5	209466.5	2590.8	50.0	60.0	2541	2531	Basalt	2	no data	no data	no data	no data	no data	no data	no data	2554.6	2555.0	2553.1	2553.5	2553.3	2554.1	Not Used
MW-7S	2539559.5	210943.1	2597.0	41.0	46.0	2556	2551	Basalt	2	2566.6	2566.8	2567.9	2569.8	2570.1	2567.6	2566.4	no data	2569.4	2567.3	2567.0	2570.3	2569.0	2568.2
MW-8S	2539492.2	210890.7	2603.4	47.0	52.0	2557	2552	Clay (saprolite)	1	2566.8	2566.9	2567.9	2569.5	2570.1	2567.7	2566.4	2569.3	2569.5	2567.3	2567.5	2568.2	2569.0	2568.2
MW-9D	2539617.8	210757.2	2599.0	85.0	95.0	2514	2504	Basalt	4	no data	no data	2567.5	2568.7	2569.5	2567.2	2566.1	2568.8	2569.0	2566.9	2567.1	2567.7	2568.5	2567.9
MW-9S	2539599.6	210768.1	2599.3	36.0	41.0	2564	2559	Clay (saprolite)	1	2566.5	2566.2	2567.3	2569.2	2569.7	2567.3	2566.3	2569.0	2569.1	2567.0	2567.3	2568.0	2568.7	2567.8
MW-9U	2539653.7	210729.1	2598.0	62.0	72.0	2536	2526	Basalt	3	no data	no data	no data	no data	no data	no data	no data	2668.7	2668.9	2666.9	2667.1	2667.7	2668.4	Not Used
MW-10S	2539516.7	210659.1	2615.3	66.0	76.0	2550	2540	Clay and basalt	2	2564.4	2565.8	2567.1	2568.2	2568.9	2567.0	2565.9	2567.8	2568.6	2566.8	2566.8	2567.3	2568.1	2567.1
MW-11S	2539510.0	210221.5	2623.5	65.0	80.0	2559	2544	Clay (saprolite)	1	2565.9	2565.5	2566.4	2567.5	2568.2	2566.6	2565.5	2567.9	2568.0	2566.5	2566.4	2566.8	2567.5	2566.8
MW-12S	2538995.3	211036.5	2622.0	46.0	56.0	2577	2567	Granite	2	2580.7	2577.4	2580.4	2581.9	2583.5	2583.2	2580.8	2581.2	2584.5	2582.9	2581.3	2581.9	2583.8	2581.8
MW-13S	2540408.5	210219.6	2580.1	16.0	36.0	2564	2544	Clay (saprolite)	1	no data	no data	2570.1	2571.4	2571.9	2570.0	2568.4	2570.7	2570.8	2569.8	2570.2	2570.6	2571.2	2570.5
MW-14D	2540106.3	210437.7	2579.9	122.0	132.0	2458	2448	Granite	7	no data	no data	2561.3	2563.5	2565.9	2564.9	2563.4	2565.7	2567.1	2565.2	2564.6	2565.2	2566.7	2564.9
MW-15D	2539322.0	208997.0	2551.3	116.0	136.0	2436	2416	Basalt	5	no data	no data	no data	no data	no data	2459.8	2462.7	no data	2465.5	2462.7	2467.0	2468.0	2467.8	2464.8
MW-16D	2536285.9	206442.5	2565.7	90.0	105.0	2476	2461	Basalt	2	no data	no data	2519.6	2521.3	2521.4	2518.8	2517.7	2520.7	2520.1	2518.3	2518.6	2519.1	2520.2	2519.6
MW-17D	2539046.3	210296.5	2613.6	209.0	219.0	2405	2395	Granite	8	no data	no data	no data	no data	2550.2	2550.3	2550.3	2549.7	2551.0	2550.6	2550.3	2550.7	2551.1	2550.5
MW-18D	2538417.7	206366.1	2513.0	144.0	164.0	2369	2349	Basalt	5	no data	no data	2462.8	2463.8	2465.4	2460.0	2462.3	2466.1	2465.7	2462.4	2466.5	2467.7	2467.9	2464.6
MW-19D	2539718.5	210343.4	2624.0	155.0	175.0	2469	2449	Basalt	6	no data	no data	no data	no data	2568.4	2566.4	2565.5	2567.8	2568.0	2566.2	2566.4	2566.9	2567.4	2567.0
MW-20D	2538304.0	209885.7	2616.2	130.0	150.0	2486	2466	Basalt	3	no data	no data	no data	no data	no data	2523.8	2522.5	2523.7	2523.9	2523.6	2523.5	2523.8	2523.7	2523.6
MW-21D	2535814.0	208089.0	2526.2	110.0	130.0	2413	2393	Basalt	4	no data	no data	no data	no data	no data	2460.2	2462.0	no data	2465.7	2462.3	2466.4	2467.6	2467.8	2464.6
W20	2539985.1	209819.7	#N/A	81.0	100.0	2498	2479	Basalt	3	no data	2559.2	2560.2	no data	2561.5	2559.1	2561.9	2564.2	2564.1	2562.2	2562.6	2563.0	2563.3	2561.9

Notes:

The Top of Casing, Northing, and Easting are estimated for EW-9U and MW-6U.

The Top of Casing is estimated for W20

amsl = above mean sea level

ft = foot (feet)

Table 4-2. Sensitivity Evaluation Results*2019 Groundwater Modeling Report, Grain Handling Facility at Freeman, Freeman, Washington*

Multiplier on Final Values	50%	80%	90%	Final	110%	120%	150%
Steady State Model, Variation in Hydraulic Conductivity							
Residual Mean	-11.4	-6.3	-4.5	-2.6	-0.6	1.6	10.0
Absolute Residual Mean	11.5	6.6	5.4	4.5	4.0	4.0	10.2
Residual Std. Deviation	4.7	4.3	4.3	4.4	4.6	4.8	5.9
Sum of Squares	3831	1431	976	657	536	638	3404
RMS Error	12.4	7.6	6.2	5.1	4.6	5.0	11.7
Min. Residual	-19.0	-14.1	-12.7	-11.2	-9.6	-8.0	-1.8
Max. Residual	0.03	3.5	4.8	6.2	7.6	9.8	21.7
Number of Observations	25	25	25	25	25	25	25
Range in Observations	120.1	120.1	120.1	120.1	120.1	120.1	120.1
Scaled Residual Std. Deviation	0.039	0.035	0.036	0.037	0.038	0.040	0.049
Scaled Absolute Residual Mean	0.095	0.055	0.045	0.038	0.033	0.033	0.085
Scaled RMS Error	0.103	0.063	0.052	0.043	0.039	0.042	0.097
Scaled Residual Mean	-0.095	-0.052	-0.038	-0.021	-0.005	0.014	0.084
Aquifer Test Model, Variations in Hydraulic Conductivity							
Residual Mean	-0.3	0.1	0.1	0.2	0.3	0.3	0.3
Absolute Residual Mean	1.2	1.0	1.0	1.0	1.0	1.0	1.0
Residual Std. Deviation	2.1	1.8	1.8	1.8	1.8	1.8	1.8
Sum of Squares	8083	6046	5736	5718	5698	5668	5860
RMS Error	2.1	1.8	1.8	1.8	1.8	1.8	1.8
Min. Residual	-13.2	-9.2	-8.1	-7.6	-7.0	-6.6	-5.8
Max. Residual	7.08	7.3	7.5	7.7	7.9	8.1	8.3
Number of Observations	1780	1780	1780	1780	1780	1780	1780
Range in Observations	15.72	15.72	15.72	15.72	15.72	15.72	15.72
Scaled Residual Std. Deviation	0.134	0.117	0.114	0.113	0.112	0.112	0.114
Scaled Absolute Residual Mean	0.075	0.065	0.063	0.062	0.061	0.061	0.062
Scaled RMS Error	0.136	0.117	0.114	0.114	0.114	0.114	0.115
Scaled Residual Mean	-0.018	0.003	0.008	0.013	0.017	0.018	0.019
Aquifer Test Model, Variations in Storage Properties							
Residual Mean	-0.4	0.0	0.1	0.2	0.3	0.4	0.5
Absolute Residual Mean	1.2	1.0	1.0	1.0	1.0	1.0	1.0
Residual Std. Deviation	2.0	1.8	1.8	1.8	1.8	1.8	1.8
Sum of Squares	7627	5862	5794	5718	5768	5861	6292
RMS Error	2.1	1.8	1.8	1.8	1.8	1.8	1.9
Min. Residual	-10.7	-8.6	-8.4	-7.6	-7.2	-6.9	-6.0
Max. Residual	6.29	7.1	7.5	7.7	8.0	8.2	8.7
Number of Observations	1780	1780	1780	1780	1780	1780	1780
Range in Observations	15.72	15.72	15.72	15.72	15.72	15.72	15.72
Scaled Residual Std. Deviation	0.129	0.115	0.114	0.113	0.113	0.113	0.115
Scaled Absolute Residual Mean	0.079	0.065	0.063	0.062	0.061	0.061	0.061
Scaled RMS Error	0.132	0.115	0.115	0.114	0.115	0.115	0.120
Scaled Residual Mean	-0.026	0.002	0.008	0.013	0.018	0.022	0.033

Table 4-2. Sensitivity Evaluation Results*2019 Groundwater Modeling Report, Grain Handling Facility at Freeman, Freeman, Washington*

Multiplier on Final Values	50%	80%	90%	Final	110%	120%	150%
Seasonal Model, Variations in Hydraulic Conductivity							
Residual Mean	-11.5	-6.6	-4.8	-3.0	-1.0	1.2	9.1
Absolute Residual Mean	11.5	7.0	5.7	4.4	3.7	4.0	9.6
Residual Std. Deviation	5.4	4.4	4.3	4.3	4.4	4.5	6.0
Sum of Squares	175200	67876	46017	30115	22104	23885	128972
RMS Error	12.7	7.9	6.5	5.3	4.5	4.7	10.9
Min. Residual	-23.4	-16.4	-15.0	-13.6	-12.1	-10.5	-17.2
Max. Residual	1.35	4.5	5.6	6.8	8.3	10.9	23.8
Number of Observations	1088	1088	1088	1088	1088	1088	1088
Range in Observations	130.2	130.2	130.2	130.2	130.2	130.2	130.2
Scaled Residual Std. Deviation	0.042	0.034	0.033	0.033	0.034	0.035	0.046
Scaled Absolute Residual Mean	0.089	0.054	0.043	0.034	0.028	0.031	0.074
Scaled RMS Error	0.097	0.061	0.050	0.040	0.035	0.036	0.084
Scaled Residual Mean	-0.088	-0.050	-0.037	-0.023	-0.008	0.009	0.070
Seasonal Model, Variations in Storage Properties							
Residual Mean	-3.4	-3.2	-3.1	-3.0	-2.9	-2.9	-2.7
Absolute Residual Mean	4.8	4.5	4.5	4.4	4.4	4.3	4.2
Residual Std. Deviation	4.5	4.4	4.4	4.3	4.3	4.3	4.3
Sum of Squares	34995	31669	30844	30115	29495	28947	27658
RMS Error	5.7	5.4	5.3	5.3	5.2	5.2	5.0
Min. Residual	-15.5	-14.1	-13.8	-13.6	-13.5	-13.4	-13.2
Max. Residual	7.88	7.0	6.9	6.8	6.7	6.7	6.9
Number of Observations	1088	1088	1088	1088	1088	1088	1088
Range in Observations	130.2	130.2	130.2	130.2	130.2	130.2	130.2
Scaled Residual Std. Deviation	0.035	0.034	0.033	0.033	0.033	0.033	0.033
Scaled Absolute Residual Mean	0.037	0.035	0.034	0.034	0.034	0.033	0.032
Scaled RMS Error	0.044	0.041	0.041	0.040	0.040	0.040	0.039
Scaled Residual Mean	-0.026	-0.024	-0.024	-0.023	-0.022	-0.022	-0.021

Table 4-3. Storage Properties of Basalt

2019 Groundwater Modeling Report, Grain Handling Facility at Freeman, Freeman, Washington

Model Layer	General Descriptions			Aquifer Test Model		Changes to Seasonal Model		Deviations	
	WS-5	RC-3	Source Area	Specific Storage	Specific Yield	Specific Storage	Specific Yield	Specific Storage	Notes
Layer 1	Overburden / Loess	Overburden / Loess	Overburden / Clays	5.0E-05	5.0E-05		7.0E-02		
Layer 2	Tight basalt	Moderately fractured basalt	Fractured, productive basalt	5.0E-05	5.0E-05		3.0E-02		
Layer 3	Tight basalt	Tight basalt	Fractured, productive basalt	1.0E-06	5.0E-05				
Layer 4	Tight basalt	Tight basalt	Tight basalt	5.0E-06	5.0E-05				
Layer 5	Fractured, productive basalt	Tight basalt	Tight basalt	5.0E-05	5.0E-05	5.0E-07		1.0E-08	Basalt near MW-19D, both models
Layer 6	Fractured, productive basalt	Palagonite	Granite	5.0E-05	5.0E-05	5.0E-08			
Layer 7	Fractured, productive basalt	Palagonite	Granite	5.0E-06	5.0E-05	5.0E-08		1.0E-08	Basalt near MW-6D, both models
Layer 8	Tight basalt	Granite	Granite	1.0E-07	5.0E-05				
Layer 9	Moderately fractured basalt	Granite	Granite	1.0E-07	5.0E-05				
Layer 10	Moderately fractured basalt	Granite	Granite	1.0E-07	5.0E-05				
Layer 11	Granite	Granite	Granite	1.0E-07	5.0E-05				
Layers 12-14	Granite	Granite	Granite	1.0E-07	5.0E-05				

Table 4-4. Hydraulic Conductivities in Representative Areas

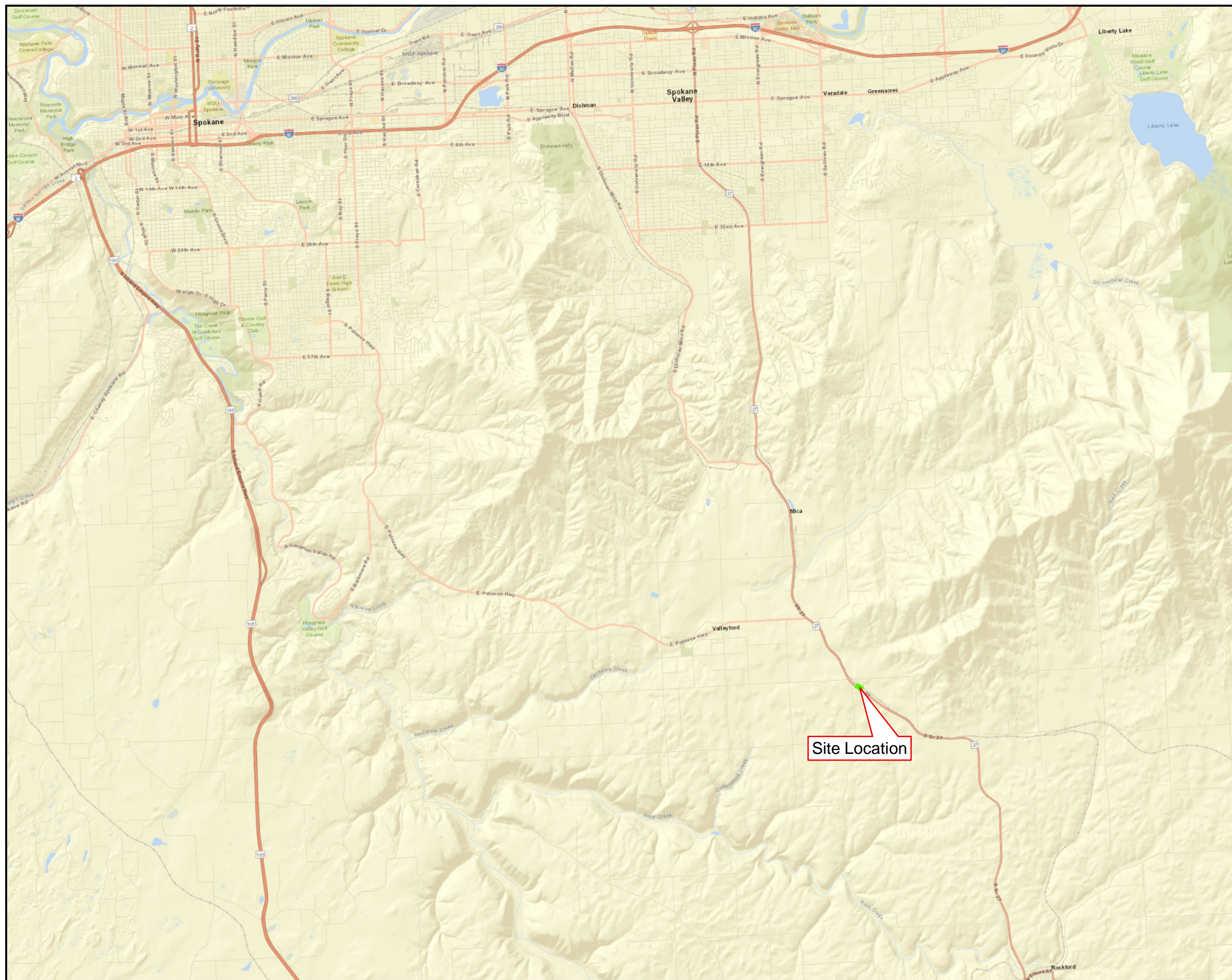
2019 Groundwater Modeling Report, Grain Handling Facility at Freeman, Freeman, Washington

Model Layer	WS-5			RC-3			Source Area (MW-9D)		
	General Description	Hydraulic Conductivity (Kh, ft/d)	Hydraulic Conductivity (Kv, ft/d)	General Description	Hydraulic Conductivity (Kh, ft/d)	Hydraulic Conductivity (Kv, ft/d)	General Description	Hydraulic Conductivity (Kh, ft/d)	Hydraulic Conductivity (Kv, ft/d)
Layer 1	Overburden / Loess	0.5	0.02	Overburden / Loess	0.5	0.02	Overburden / Clays	0.5	0.02
Layer 2	Tight basalt	0.1	0.001	Moderately fractured basalt	1	0.01	Fractured, productive basalt	50	5
Layer 3	Tight basalt	0.05	0.005	Tight basalt	0.05	0.005	Fractured, productive basalt	2	0.02
Layer 4	Tight basalt	0.05	0.005	Tight basalt	0.05	0.005	Low permeability granite	0.005	0.05
Layer 5	Fractured, productive basalt	25	1.25	Tight basalt	0.05	0.005	Low permeability granite	0.005	0.05
Layer 6	Moderately fractured basalt	2	0.01	Tight basalt	0.05	0.005	Low permeability granite	0.005	0.05
Layer 7	Tight basalt	0.1	0.1	Tight basalt	0.1	0.1	Granite	0.5	0.05
Layer 8	Tight basalt	0.05	0.005	Palagonite / Altered basalt	0.005	0.05	Granite	0.1	0.05
Layer 9	Moderately fractured basalt	2	0.01	Palagonite / Altered basalt	0.005	0.05	Granite	0.1	0.05
Layer 10	Moderately fractured basalt	20	0.2	Palagonite / Altered basalt	0.005	0.05	Granite	0.1	0.05
Layer 11	Moderately fractured basalt	2	0.02	Granite	0.1	0.05	Granite	0.1	0.05
Layer 12	Low permeability granite	0.005	0.05	Granite	0.1	0.05	Granite	0.1	0.05
Layer 13-14	Granite	0.1	0.05	Granite	0.1	0.05	Granite	0.1	0.05


Notes:

Kh = Horizontal hydraulic conductivity Kv = Vertical hydraulic conductivity ft/d = foot (feet) per day

Figures



LEGEND

 Grain Handling Facility at Freeman

Service Layer Credits: Sources: Esri, HERE, Garmin, USGS, Intermap, INCREMENT P, NRCan, Esri Japan, METI, Esri China (Hong Kong), Esri Korea, Esri (Thailand), NGCC, © OpenStreetMap contributors, and the GIS User Community

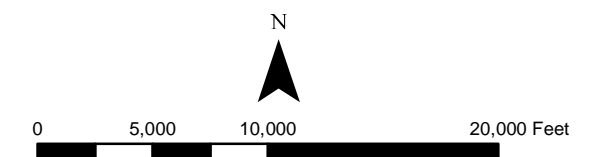
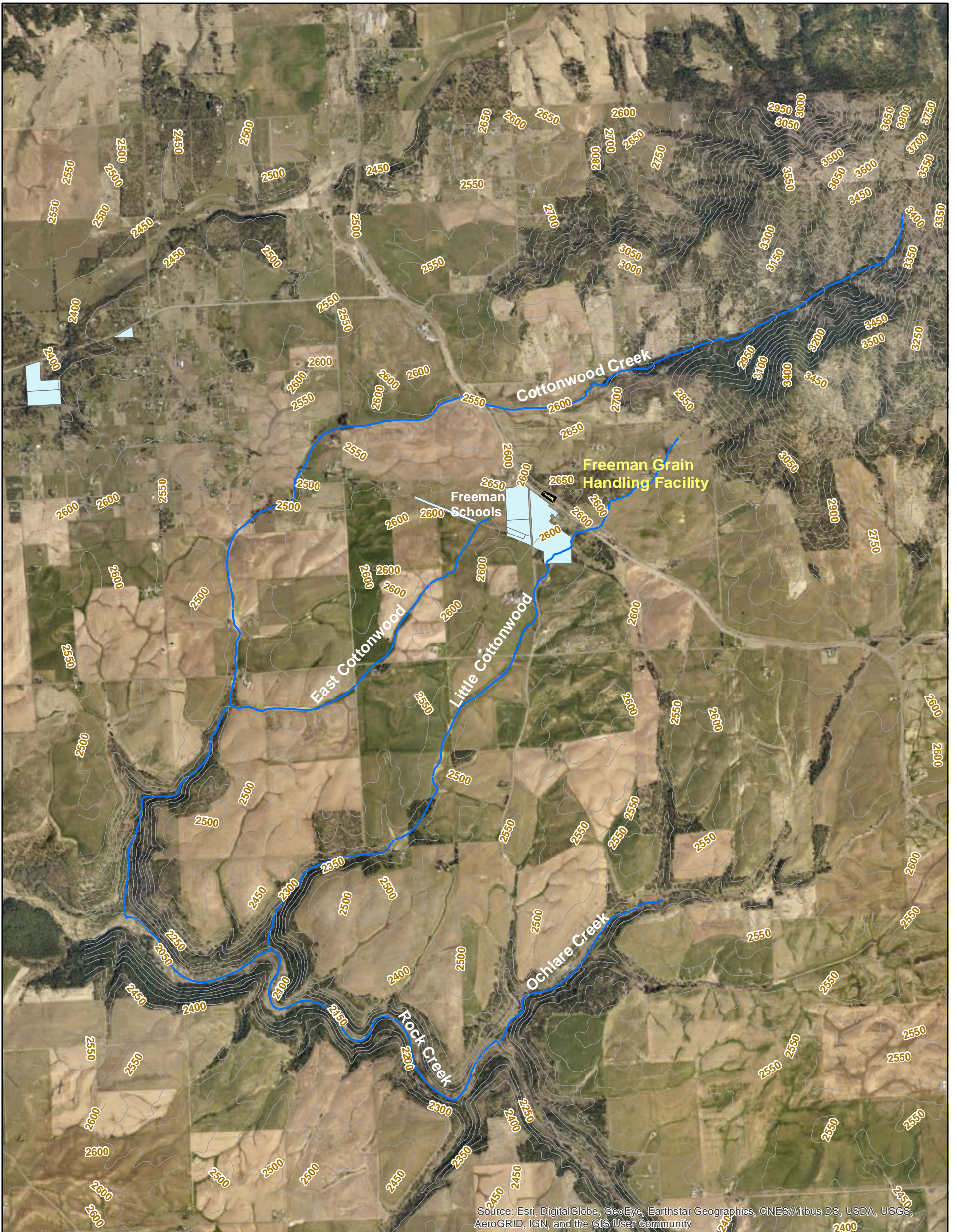


Figure 1-1
Site Location
 2019 Groundwater Modeling
 Report
*Grain Handling Facility at
 Freeman, Freeman, Washington*



Legend

- Streams
- Grain Handling Facility, Freeman
- Freeman School District Properties
- Land Surface (50 ft contour)

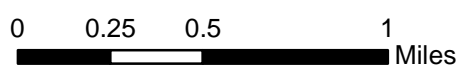


Figure 1-2
Site Details
 2019 Groundwater
 Modeling Report
*Grain Handling Facility at Freeman
 Freeman, Washington*



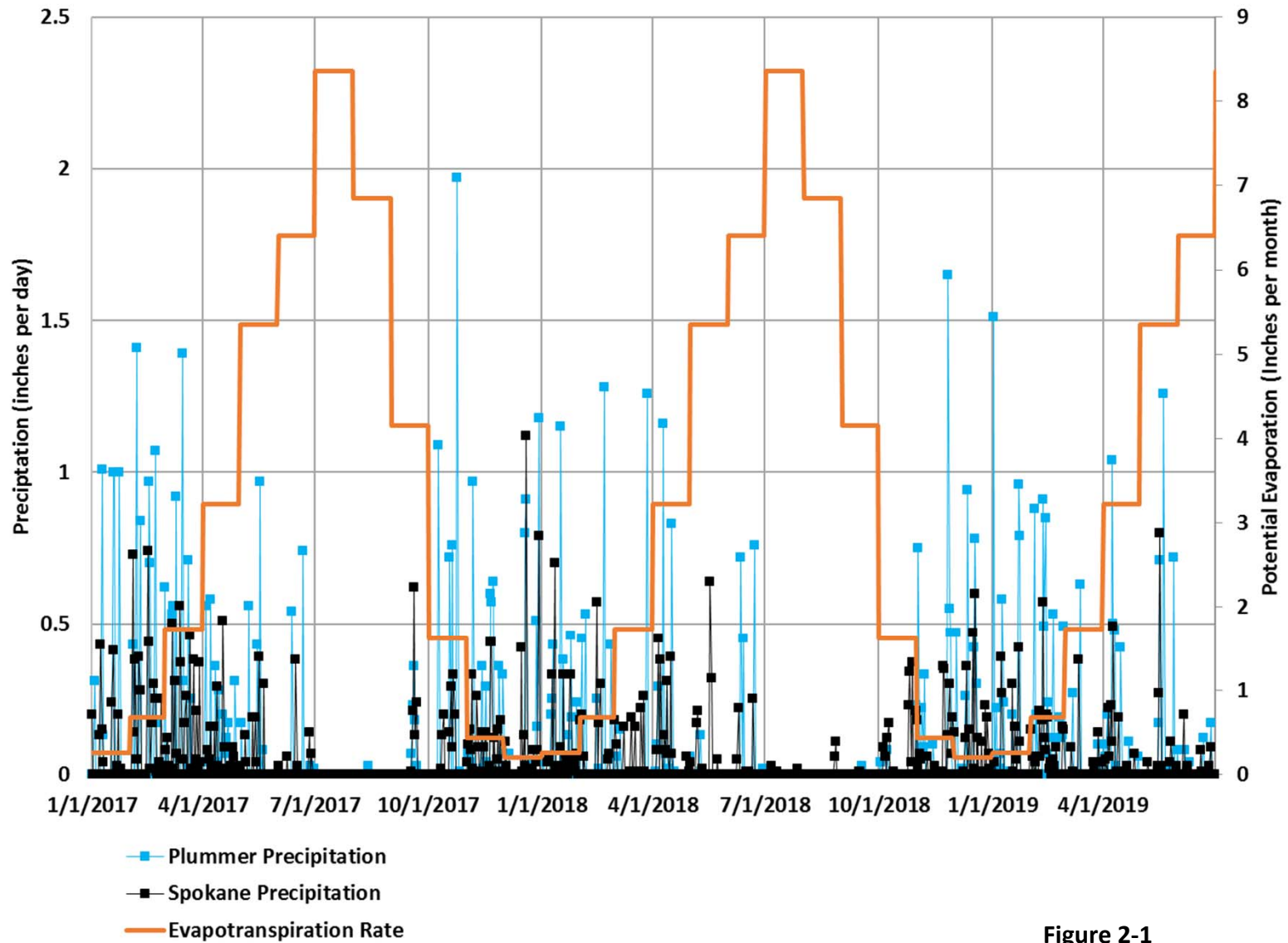
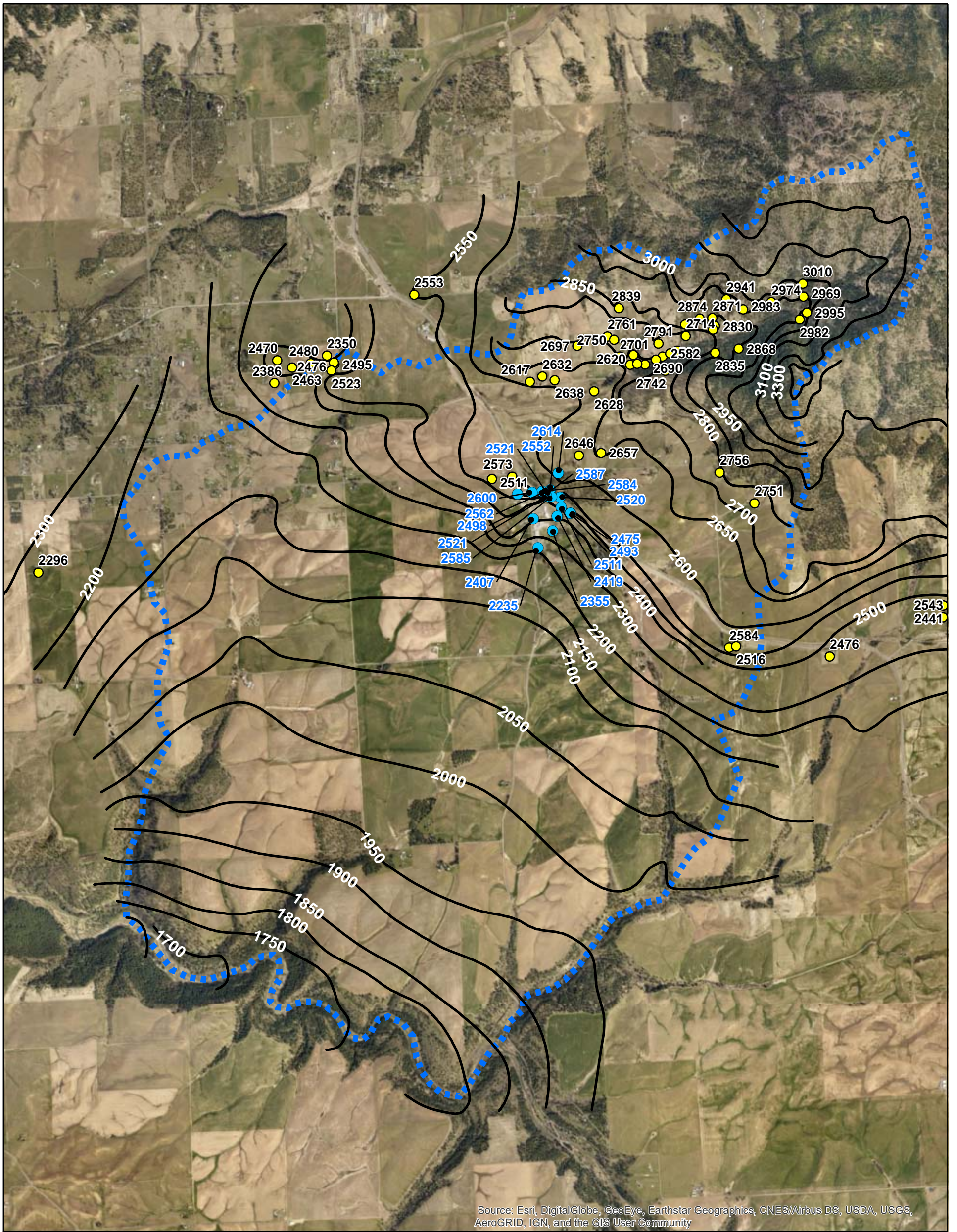


Figure 2-1
Precipitation and
Evapotranspiration Rates
 2019 Groundwater
 Modeling Report
Grain Handling Facility at Freeman
Freeman, Washington



Source: Esri, DigitalGlobe, GeoEye, Earthstar Geographics, CNES/Airbus DS, USDA, USGS, AeroGRID, IGN, and the GIS User Community

Legend

- Elevation Granite (ft), Site Wells or Borings
- Elevation Granite (ft), WA State Well Logs
- Granite Surface Contours (feet amsl)
- ■ ■ Model Boundary

Note: The granite surface is interpreted and based on information from wells and borings where possible.

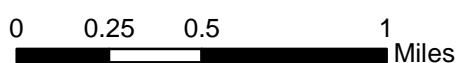
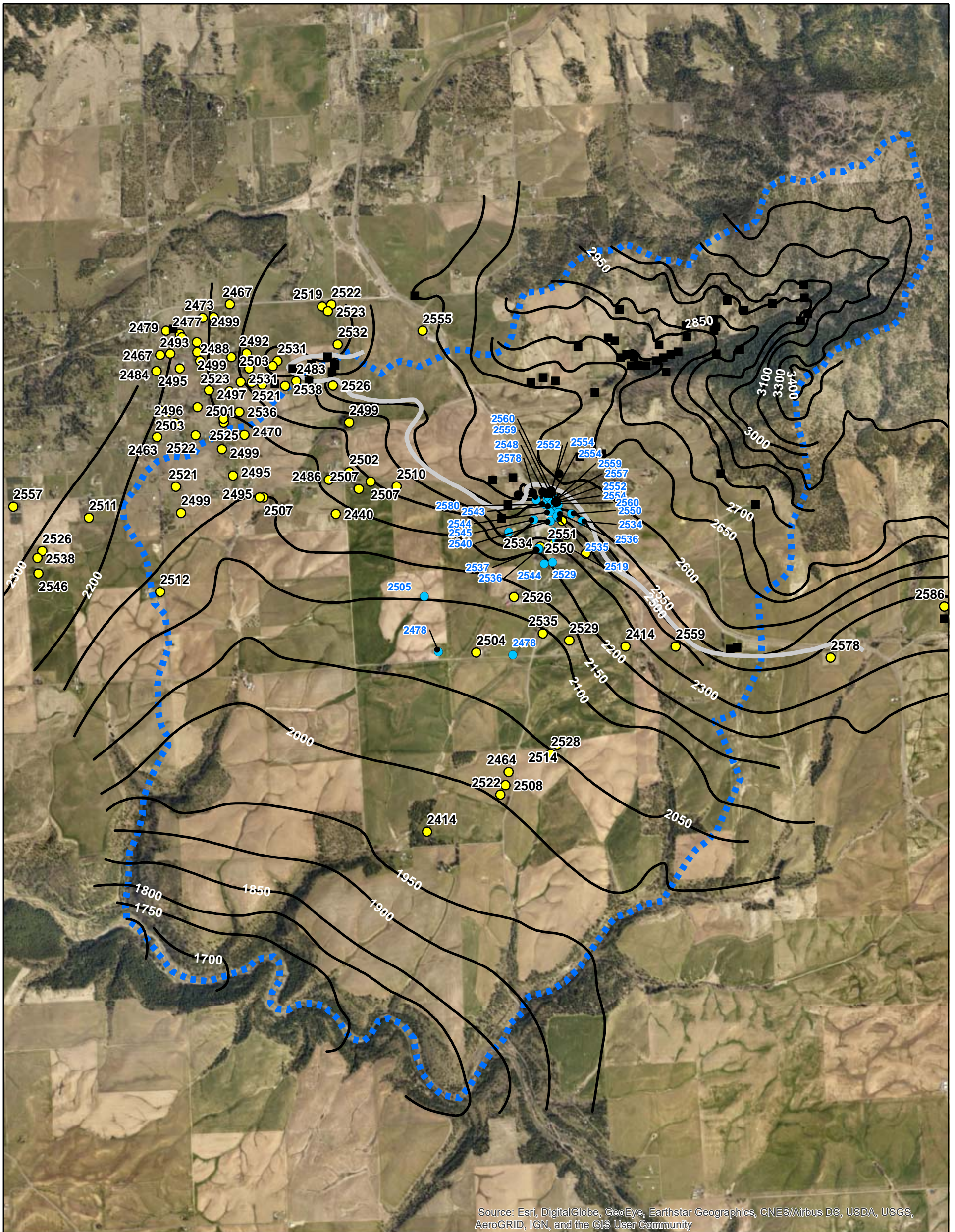


Figure 2-2
Wells and Borings with
Elevation Top of Granite
 2019 Groundwater
 Modeling Report
Grain Handling Facility at Freeman
Freeman, Washington



Legend

- No Basalt (ft), WA State Well Logs
- Elevation Basalt (ft), Site Wells or Borings
- No Basalt (ft), Site Wells or Borings
- Elevation Basalt (ft), WA State Well Logs
- Approximate Extent Basalt
- Interpreted Granite Surface (ft)
- ■ Model Boundary

Note: The posted basalt elevations represent the first contact of competent or weathered basalt, but not basalt saprolite. Generally, basalt, where present, extends to the granite surface, and the granite contours are shown in order to give a sense of the basalt thickness.

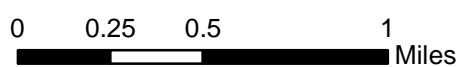


Figure 2-3
Wells and Borings with
Elevation Top of Basalt
 2019 Groundwater
 Modeling Report
 Grain Handling Facility at Freeman
 Freeman, Washington



Legend

- ▲ 2019 Borings
- ⊕ Monitoring Wells
- ⊕ Monitoring Wells, With Transducers
- ⊕ Aquifer Test Monitoring Wells, Manual Measurements
- ⊕ Aquifer Test Monitoring Wells, With Transducers
- ⊕ Aquifer Test Pumping Wells
- ⊕ Freeman School Well (WS5)

Note: Locations of 2019 borings are approximate.

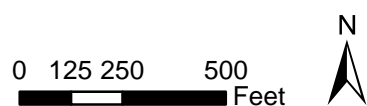


Figure 2-4
Aquifer Test and Monitoring
Well Locations

2019 Groundwater
 Modeling Report
 Grain Handling Facility at Freeman
 Freeman, Washington

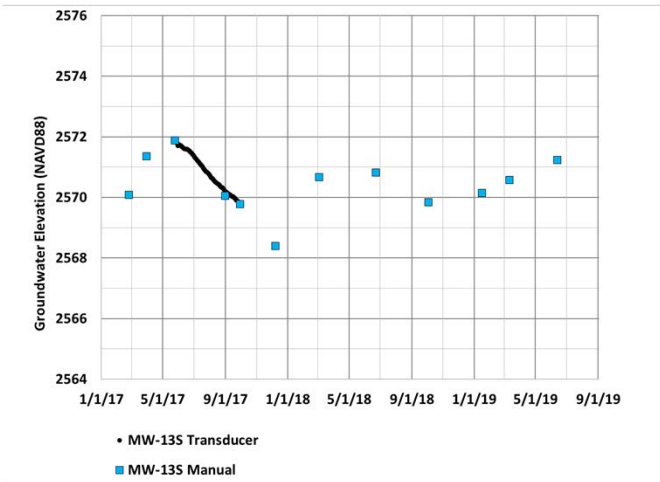
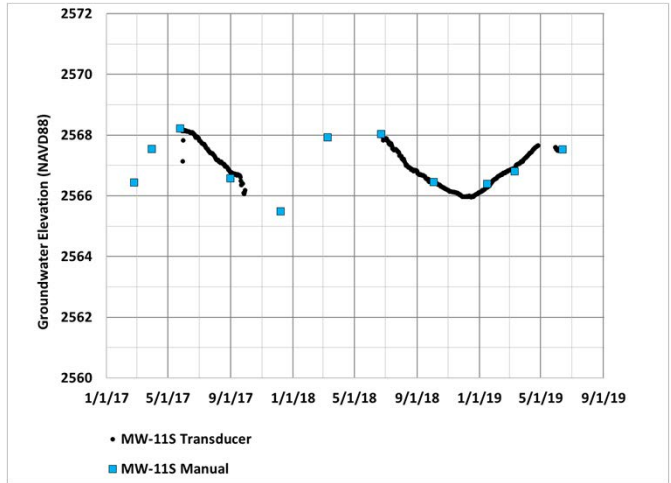
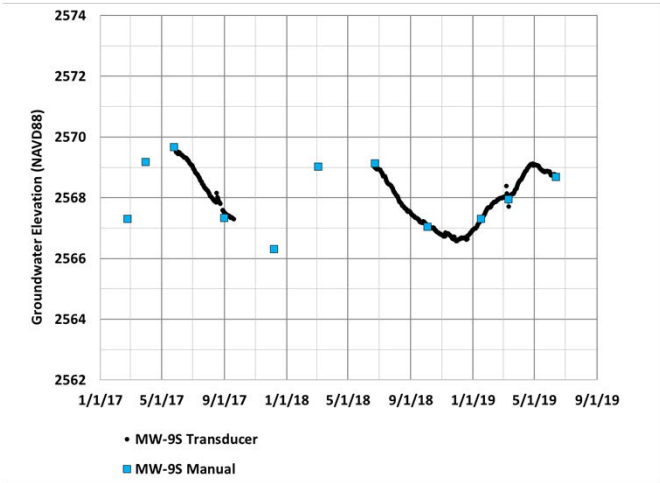
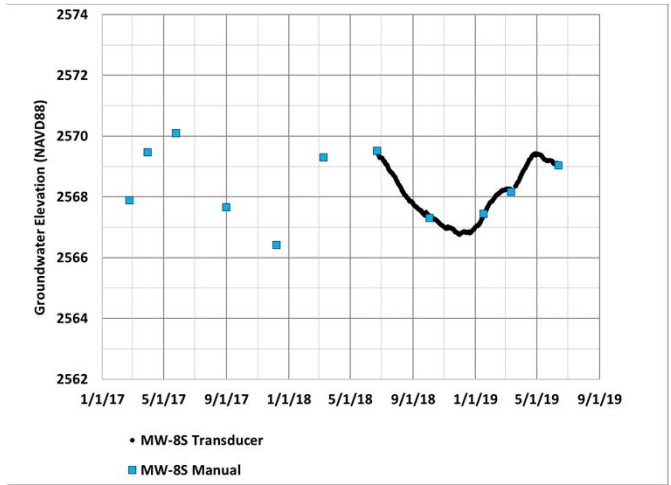
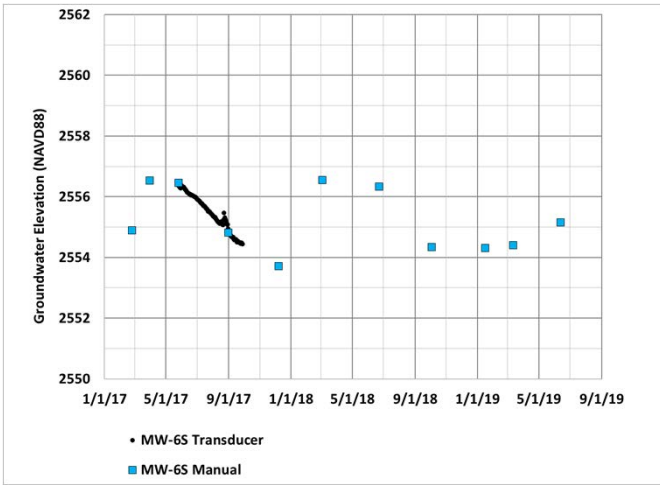


Figure 2-5
Hydrographs, Overburden
Wells
 2019 Groundwater Modeling
 Report
Grain Handling Facility at Freeman
Freeman, Washington

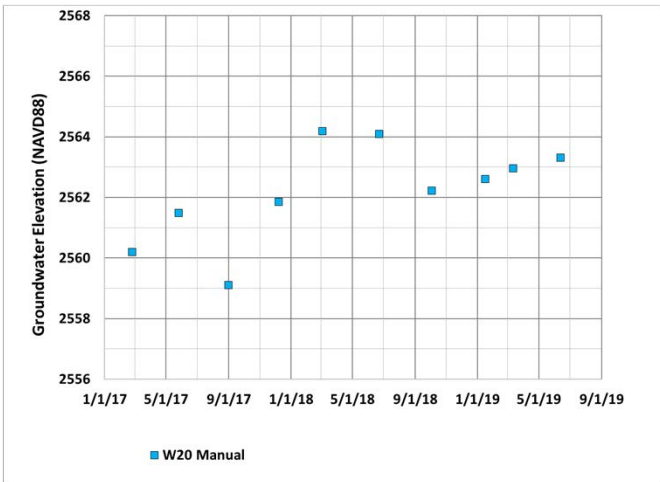
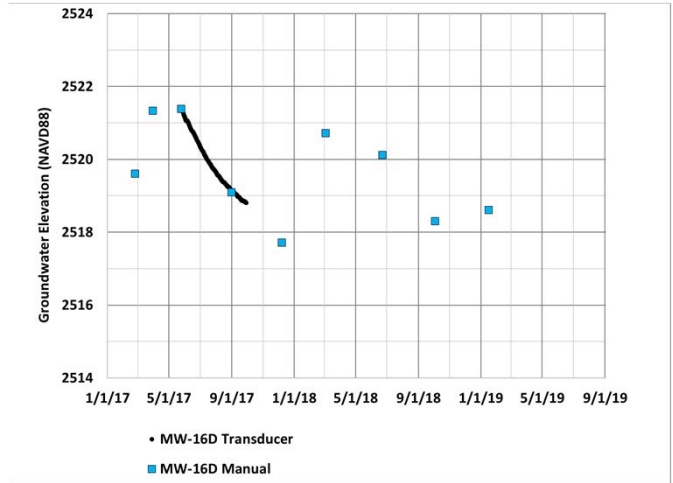
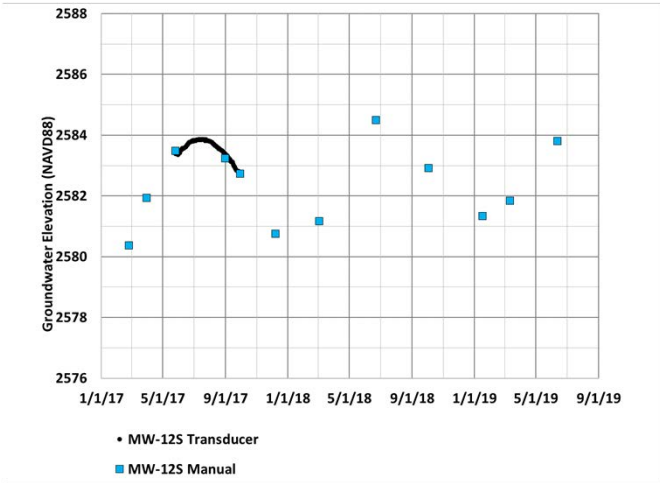
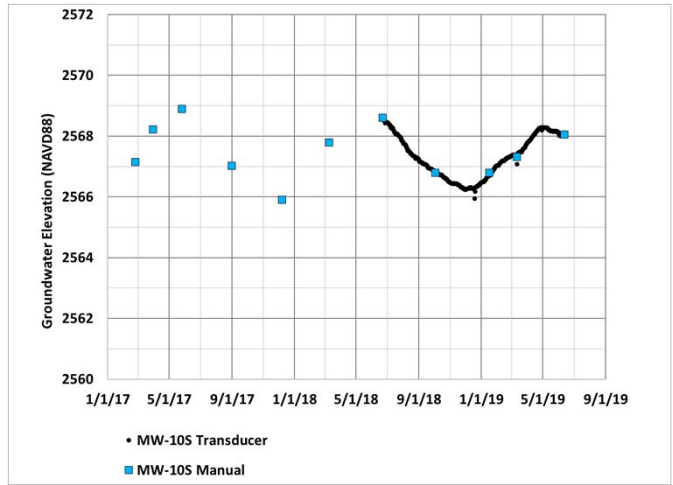
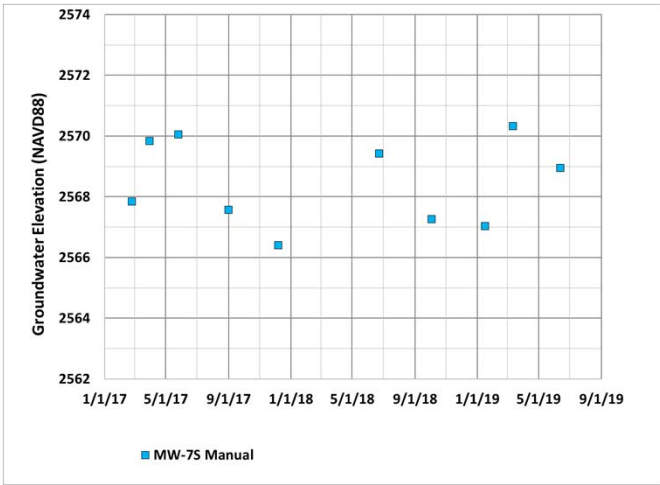


Figure 2-6
Hydrographs, Upper Basalt
Wells
 2019 Groundwater Modeling
 Report
Grain Handling Facility at Freeman
Freeman, Washington

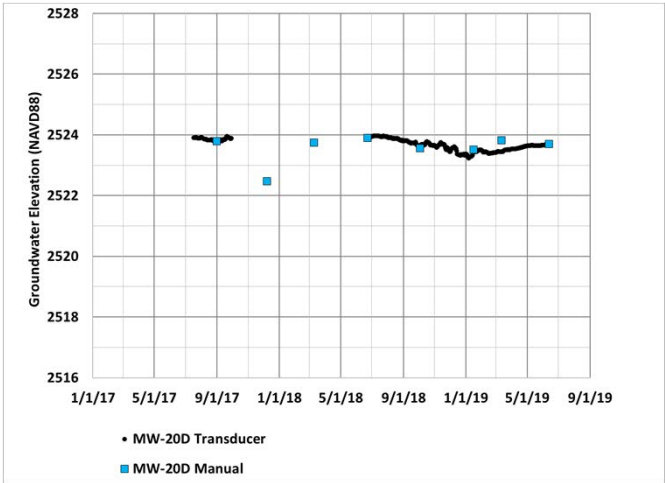
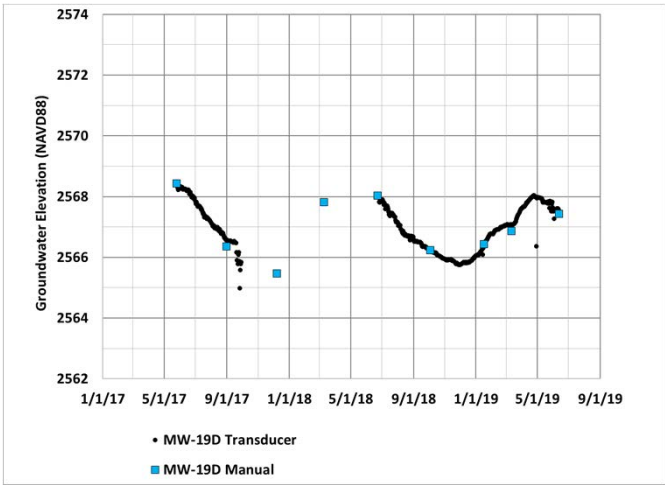
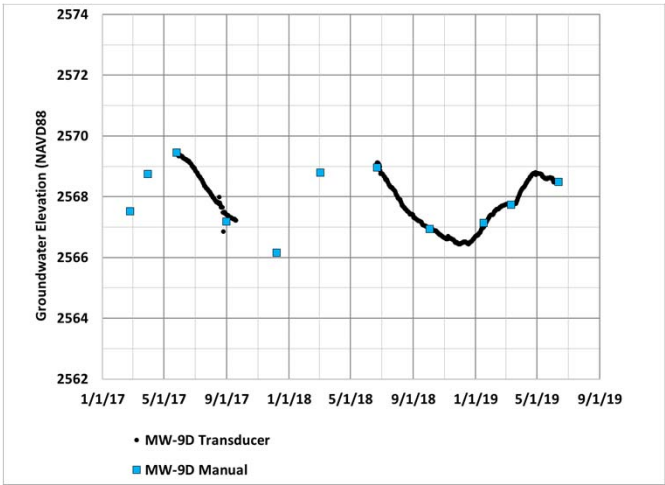


Figure 2-7
Hydrographs, Basalt Wells
 2019 Groundwater Modeling
 Report
*Grain Handling Facility at Freeman
 Freeman, Washington*

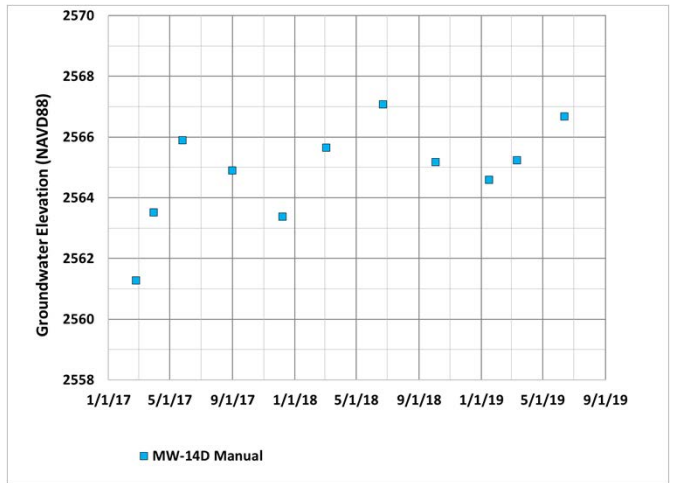
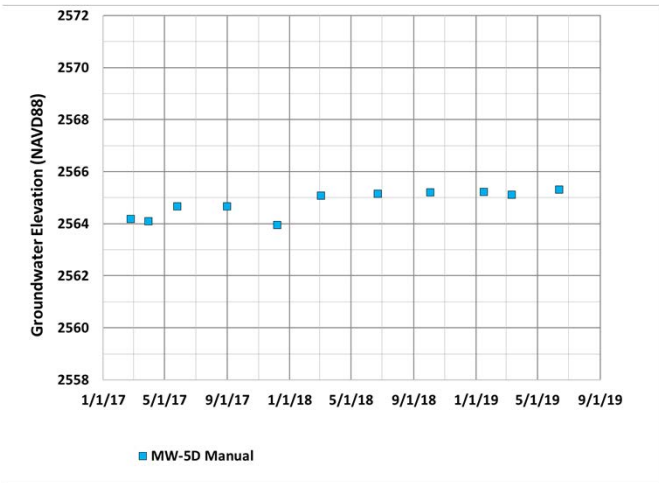
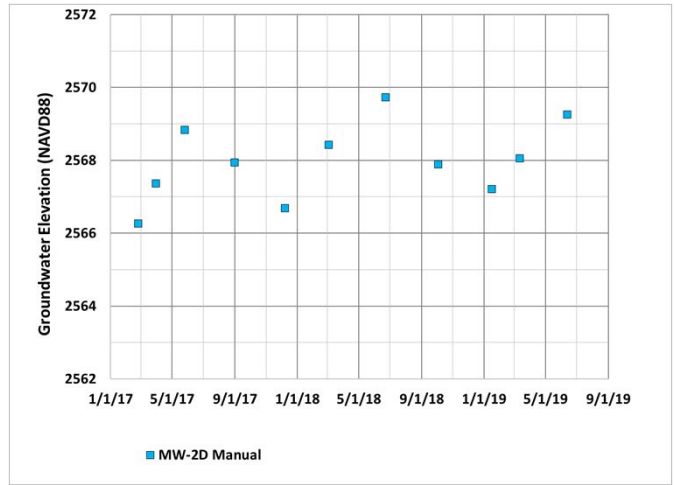
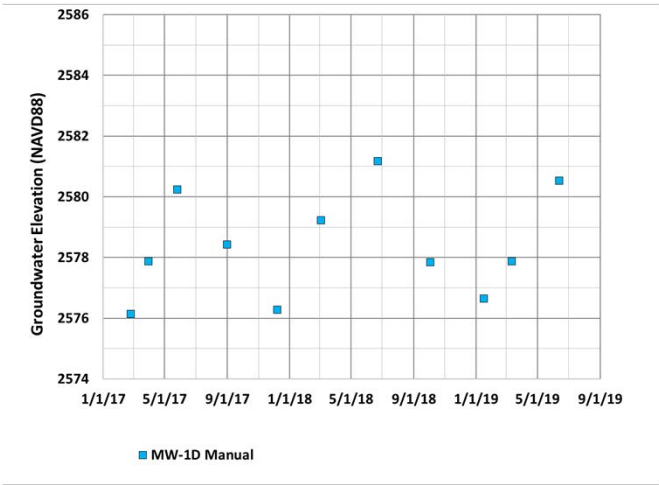


Figure 2-8
Hydrographs, Deep Granite
Wells
 2019 Groundwater Modeling
 Report
Grain Handling Facility at Freeman
Freeman, Washington

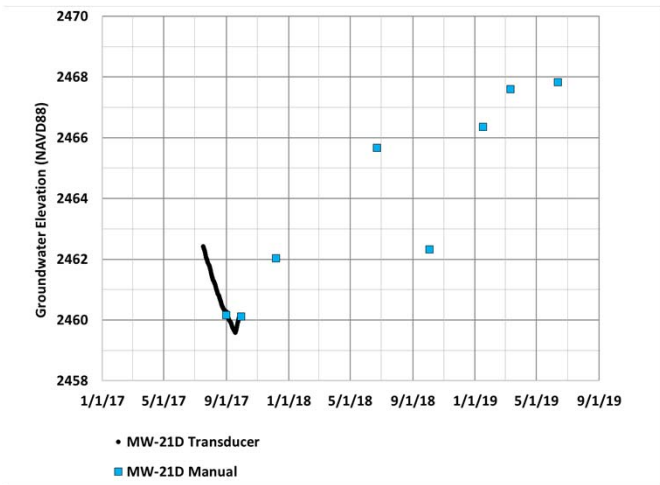
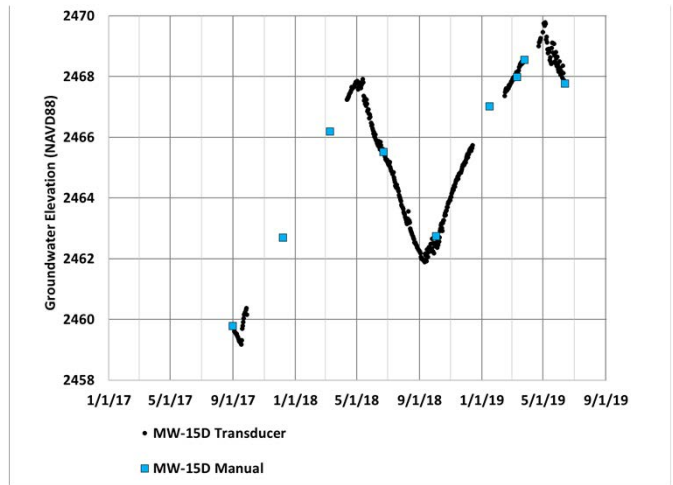
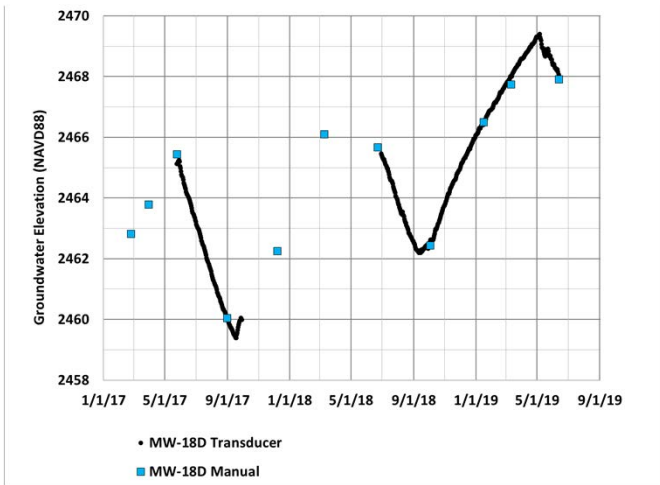
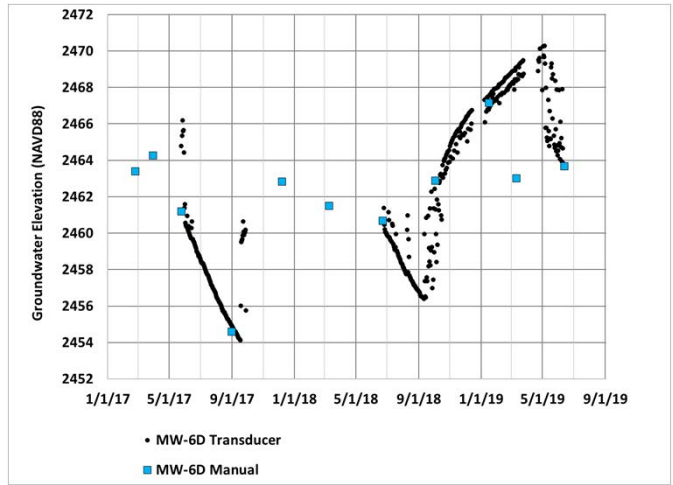
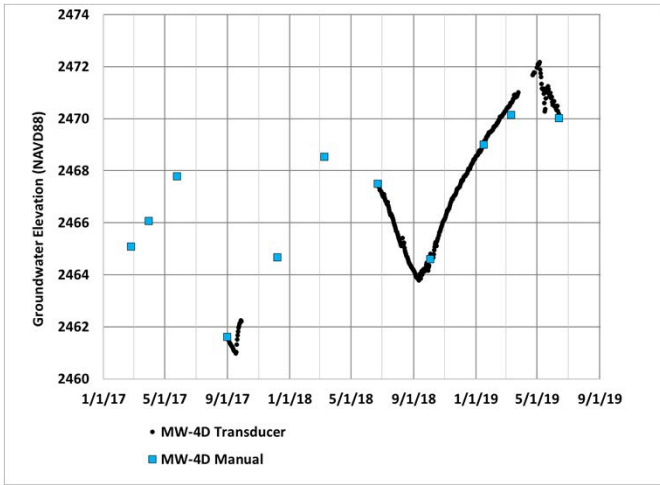
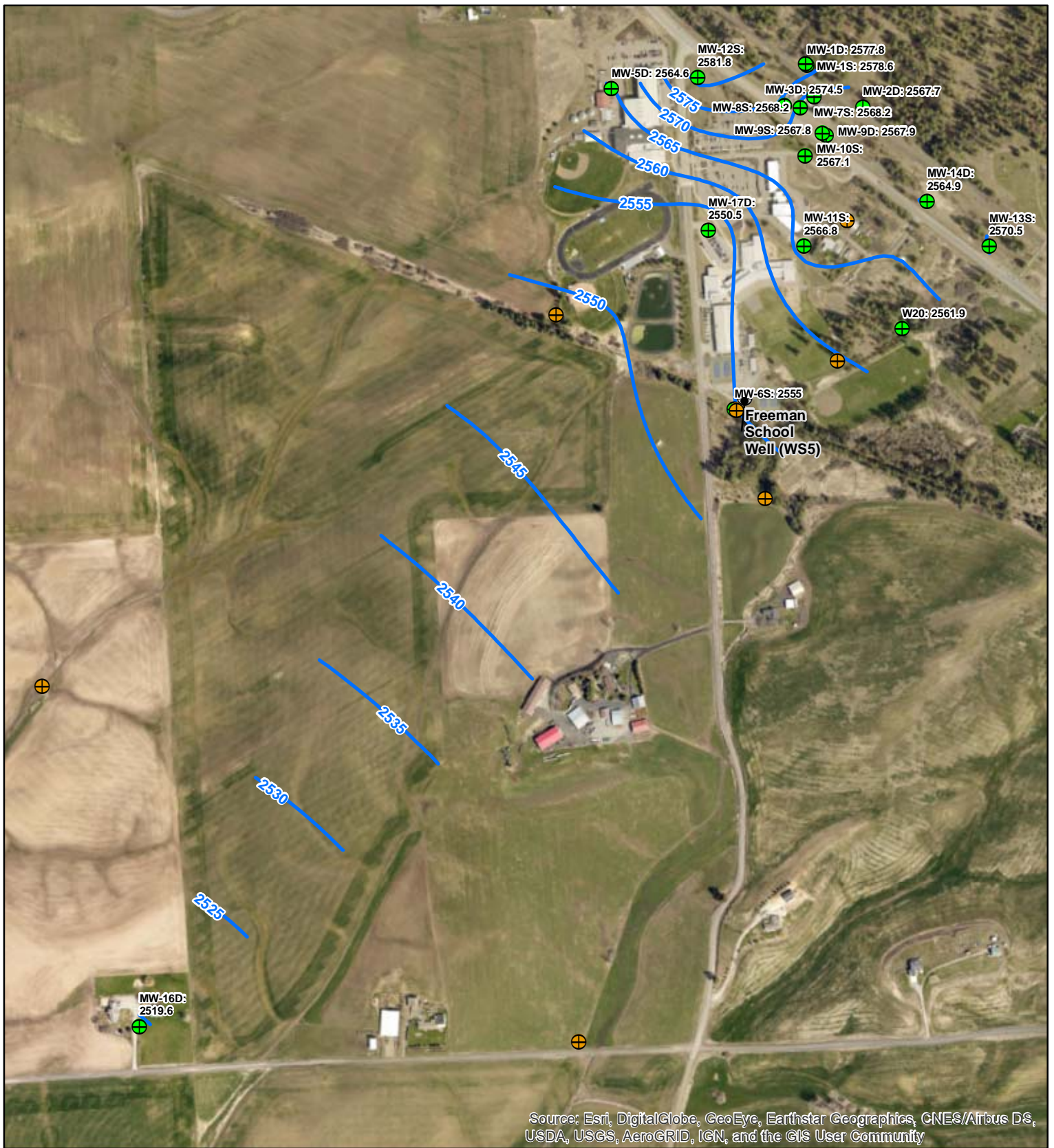


Figure 2-9
Hydrographs, Lower Basalt
Wells
 2019 Groundwater Modeling
 Report
Grain Handling Facility at Freeman
Freeman, Washington



Legend

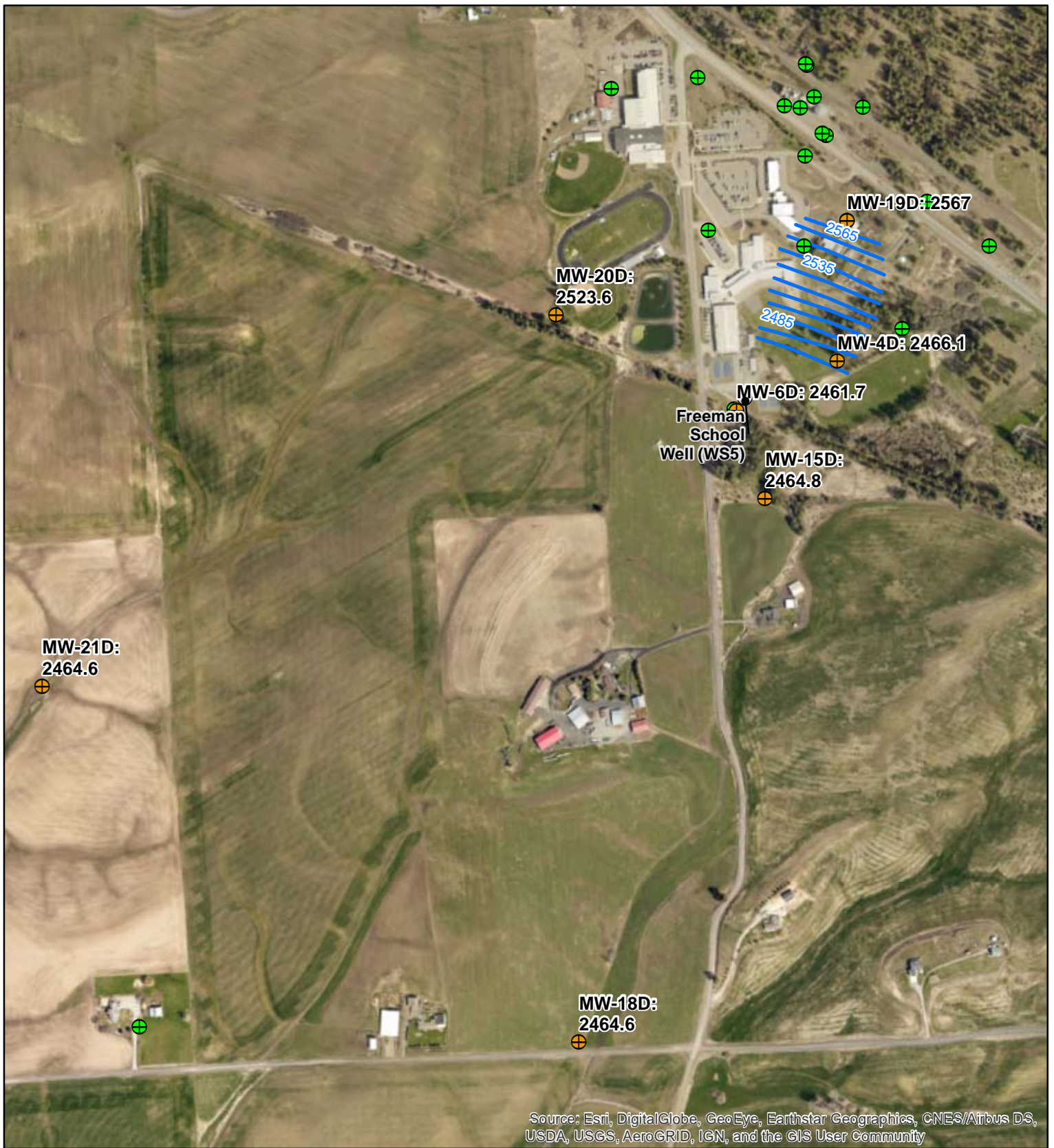
- Groundwater Contours (ft amsl)
- Shallow and Granite Wells
- ⊕ Deep Basalt Wells
- ⊕ Freeman School Well (WS5)

0 0.125 0.25 Miles



Figure 2-10
Groundwater Elevations,
Shallow and Granite Wells
 2019 Groundwater
 Modeling Report
Grain Handling Facility at Freeman
Freeman, Washington

JACOBS



Source: Esri, DigitalGlobe, GeoEye, Earthstar Geographics, CNES/Airbus DS, USDA, USGS, AeroGRID, IGN, and the GIS User Community

Legend

- Groundwater Contours (ft amsl)
- ⊕ Shallow and Granite Wells
- ⊕ Deep Basalt Wells
- ⊕ Freeman School Well (WS5)

Note: MW-20D not used for contouring

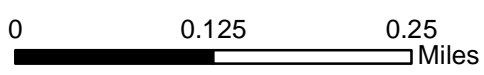


Figure 2-11
Groundwater Elevations,
Deep Basalt Wells
 2019 Groundwater
 Modeling Report
 Grain Handling Facility at Freeman
 Freeman, Washington



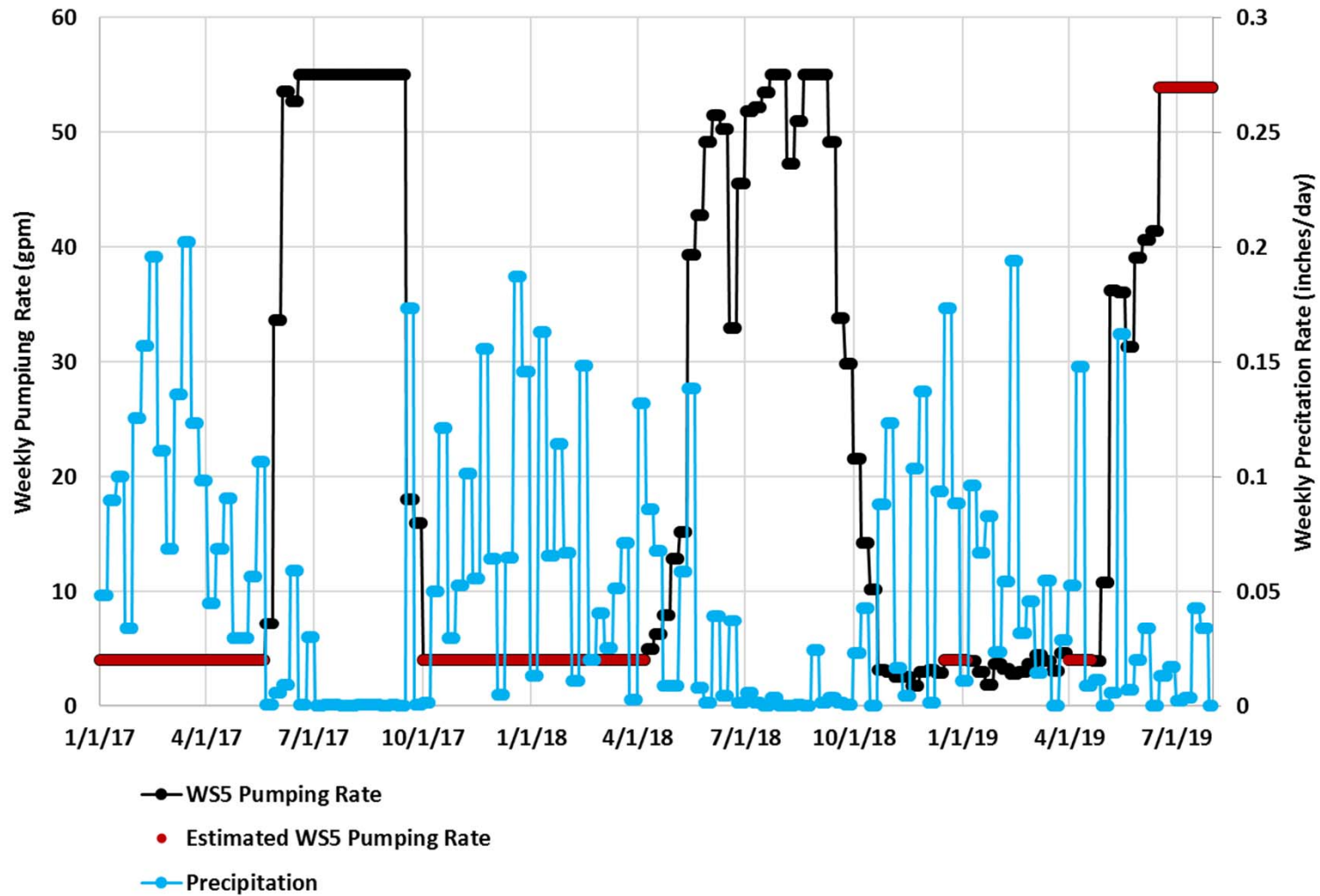


Figure 2-12
Freeman School Well (WS5)
Pumping Rates
 2019 Groundwater
 Modeling Report
Grain Handling Facility at Freeman
Freeman, Washington

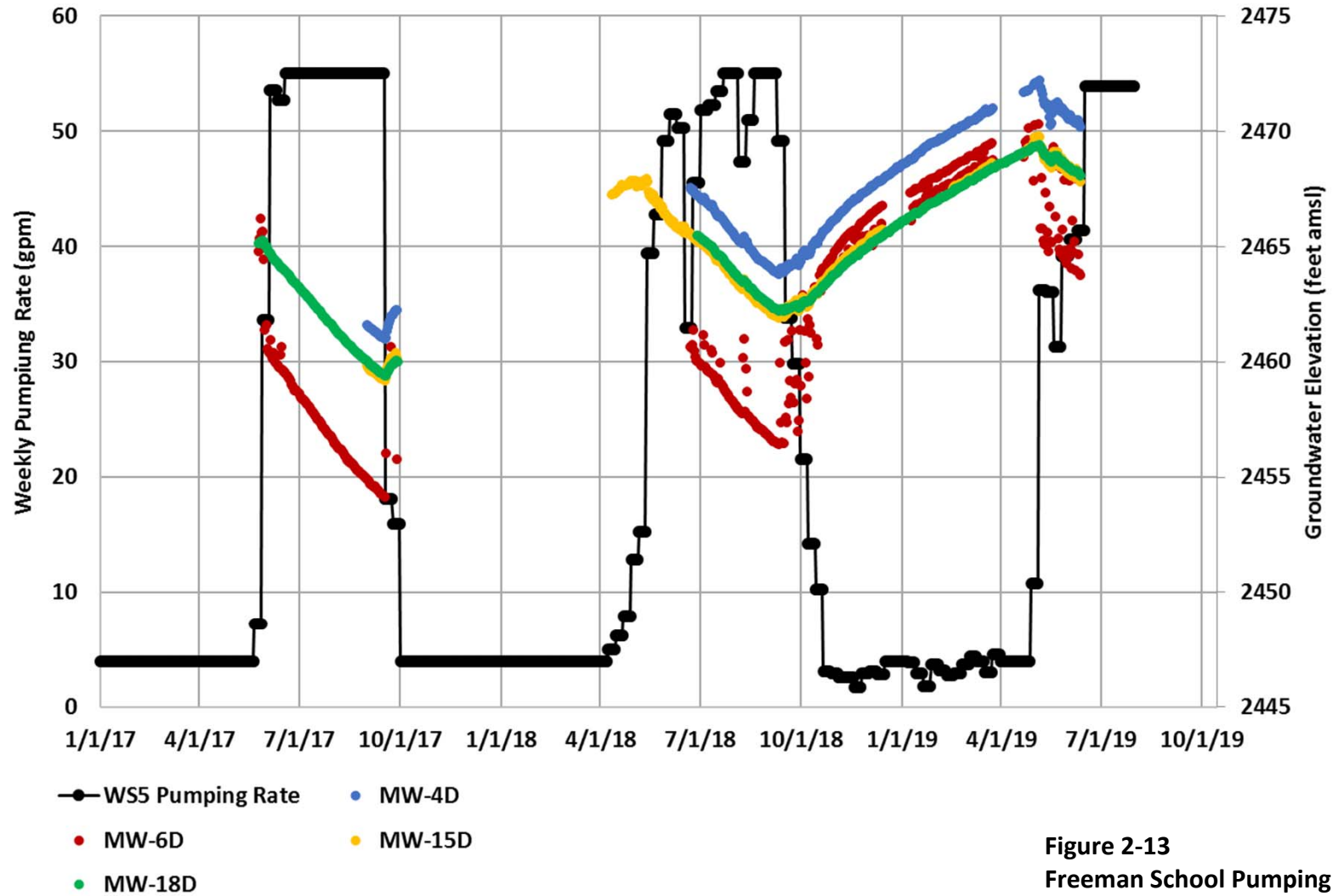


Figure 2-13
Freeman School Pumping Rates
And Deep Basalt Groundwater
Elevations
 2019 Groundwater
 Modeling Report
Grain Handling Facility at Freeman
Freeman, Washington

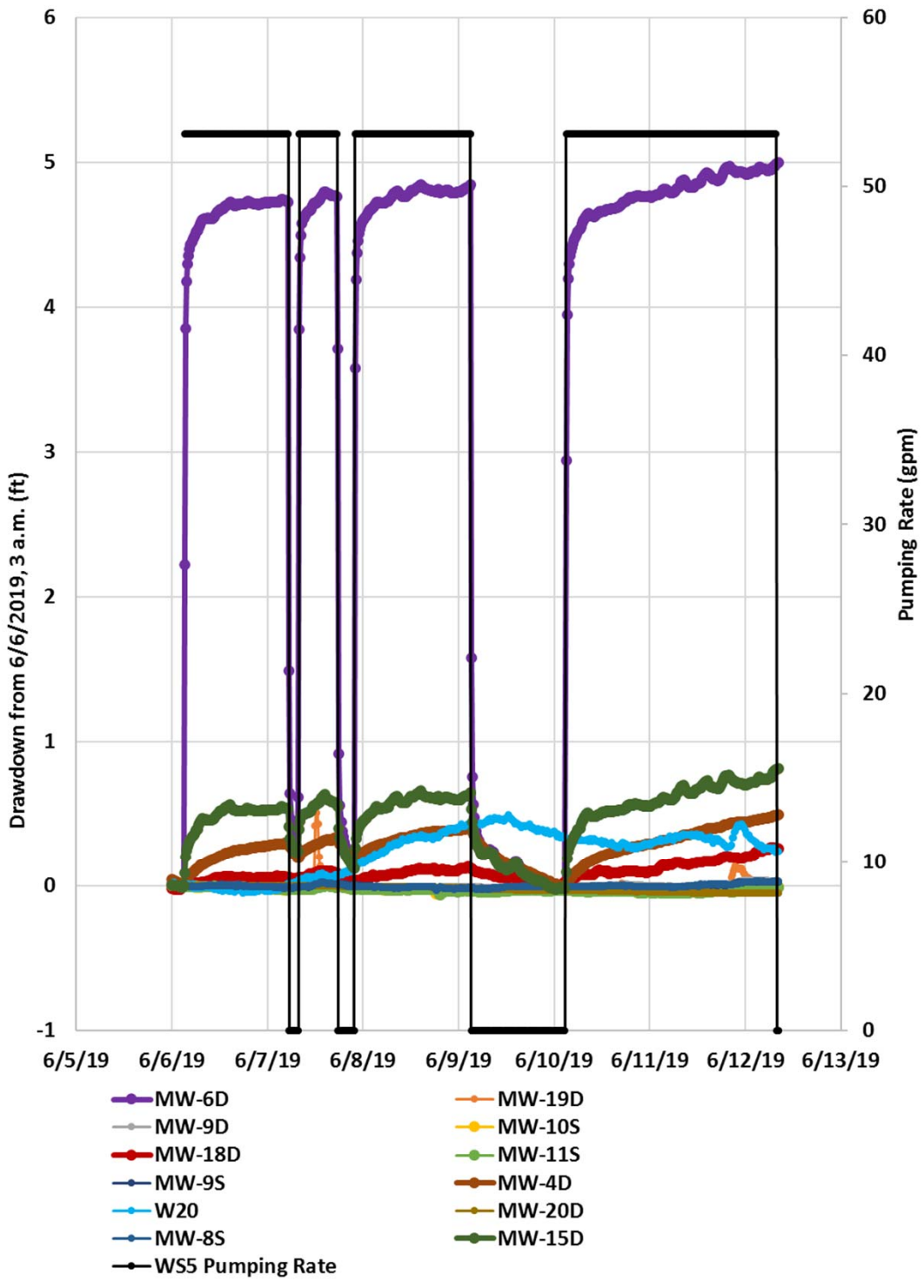
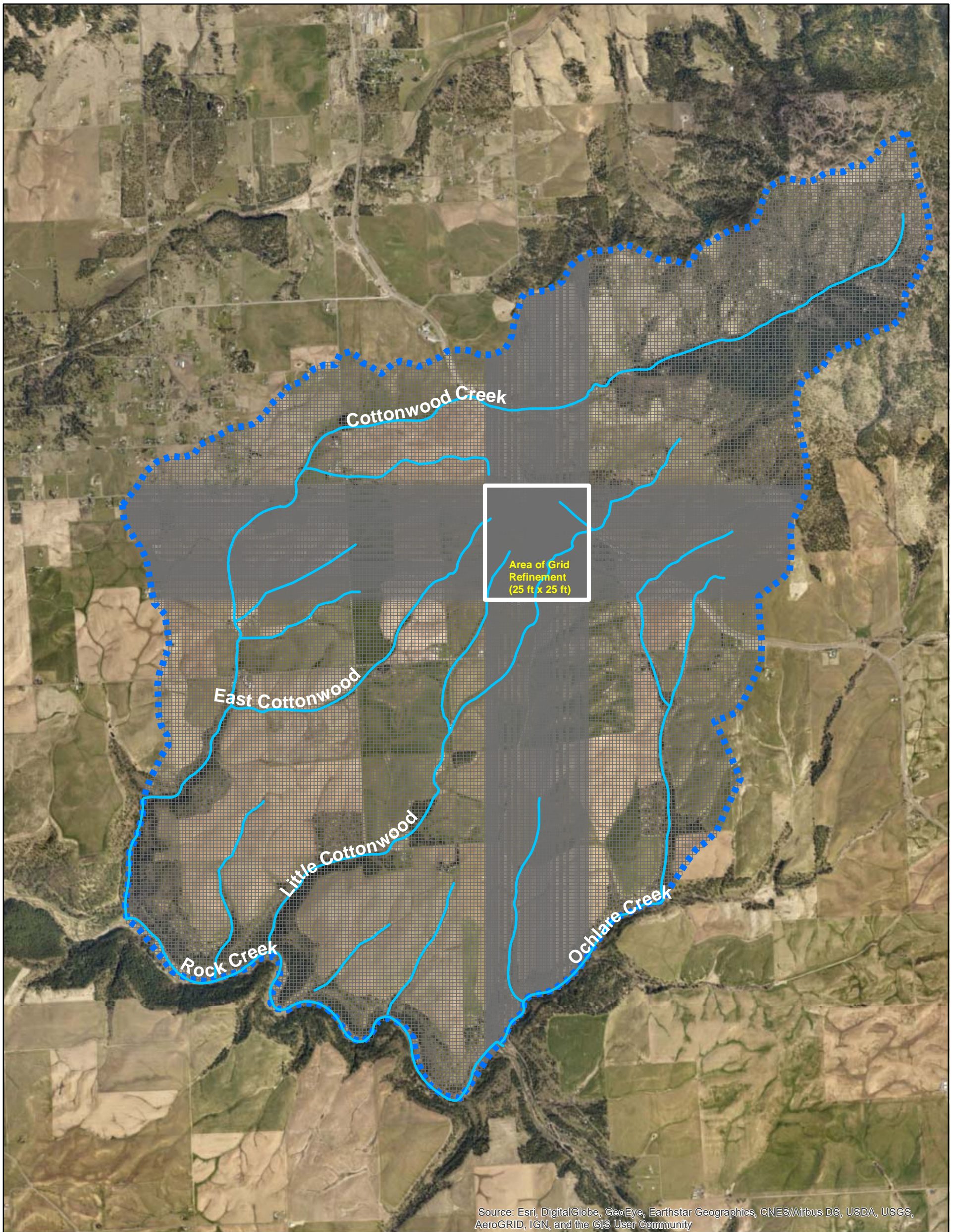


Figure 2-14
Example Short-Term
Groundwater Elevations
Fluctuations
 2019 Groundwater Modeling
 Report
Grain Handling Facility at Freeman
Freeman, Washington



Legend

- ■ ■ Model Boundary
- Streams
- Model Grid

Note:

The extent of the No Flow boundary shown applies to model layer one only. In model layers 2-16, the entire model boundary is No Flow with the exception of the southwest boundary in layer 14, specified as constant head to simulate deep groundwater flux to the south.

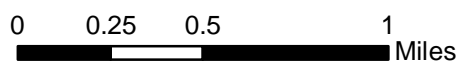
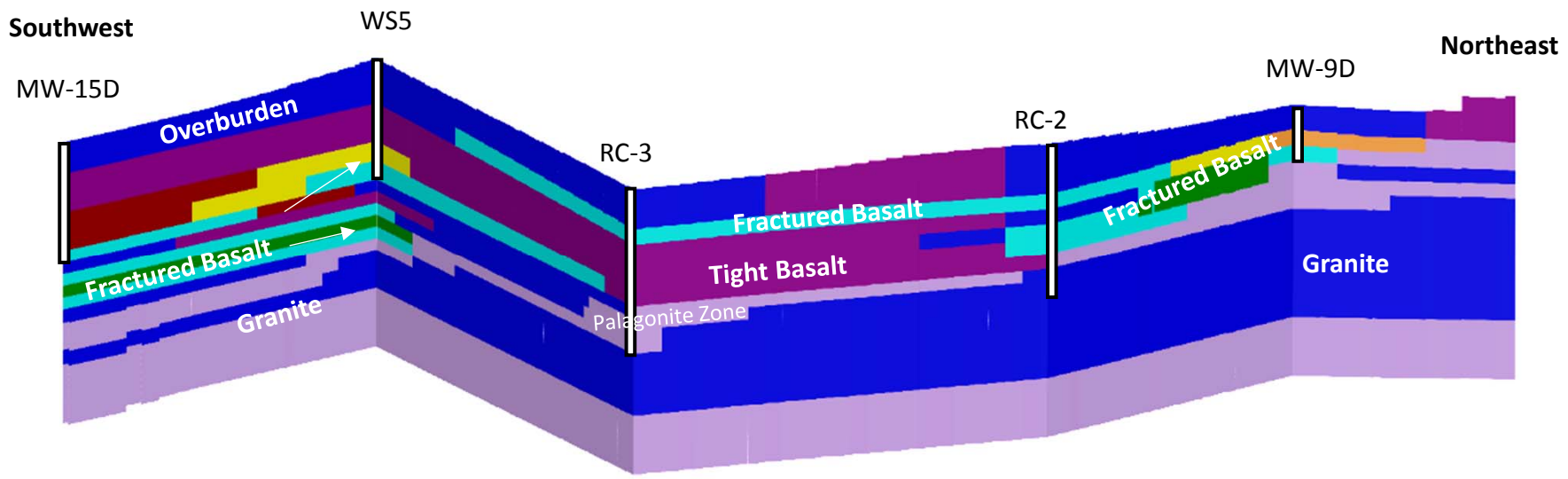


**Figure 3-1
Model Domain
and Streams**

2019 Groundwater
Modeling Report
Grain Handling Facility at Freeman
Freeman, Washington





Horizontal Hydraulic Conductivity (ft/d)

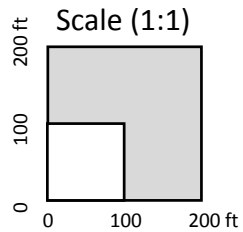
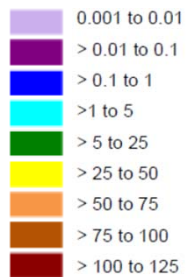
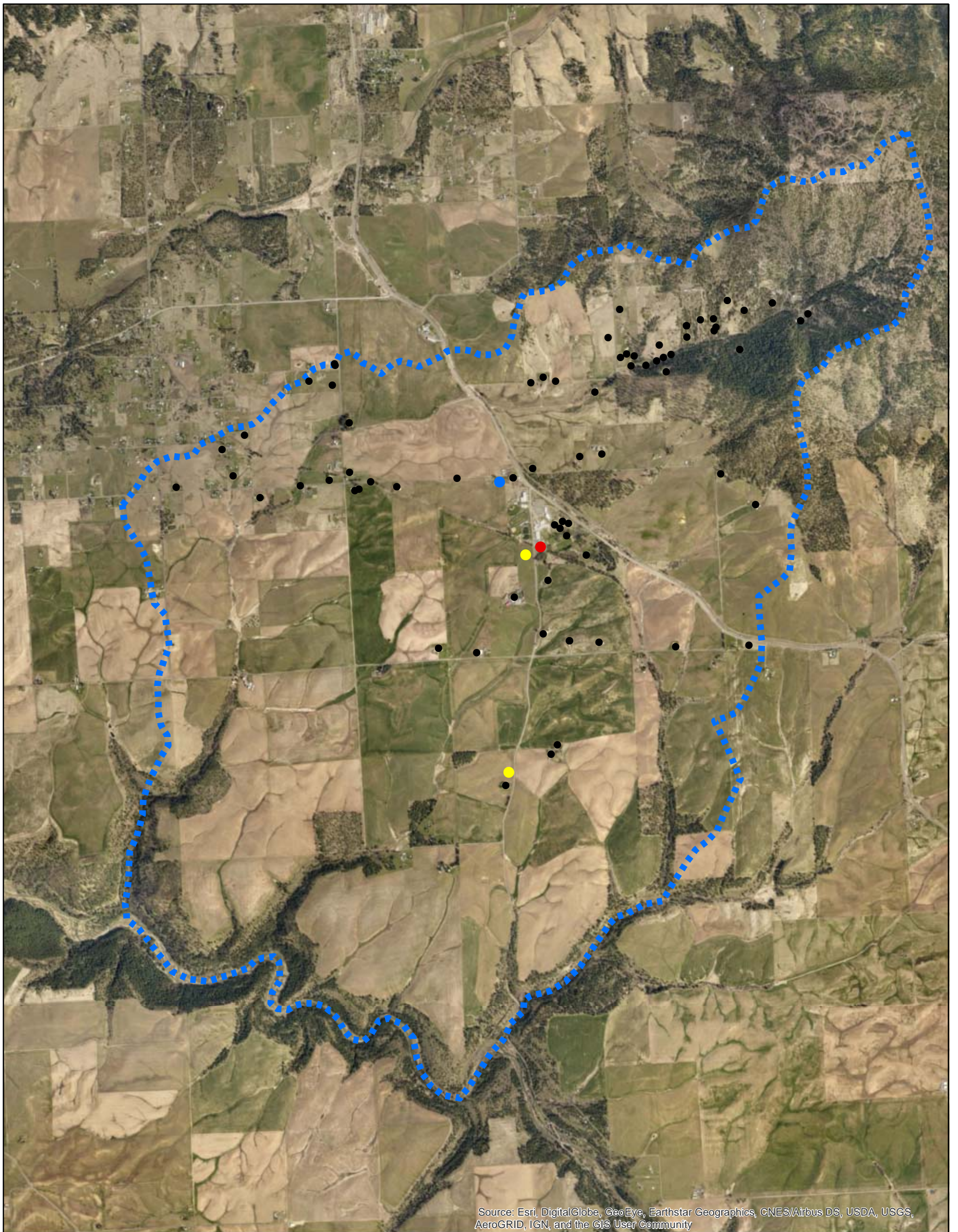


Figure 3-2
Model Cross Section
 2019 Groundwater
 Modeling Report
Grain Handling Facility at Freeman
Freeman, Washington



Legend

- ■ ■ Model Boundary
- Domestic Wells
- Freeman Store Well
- Minor Agricultural Wells
- Freeman School Well

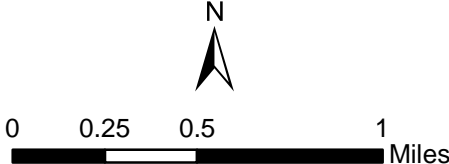


Figure 3-3
Simulated Pumping Wells
 2019 Groundwater
 Modeling Report
Grain Handling Facility at Freeman
Freeman, Washington

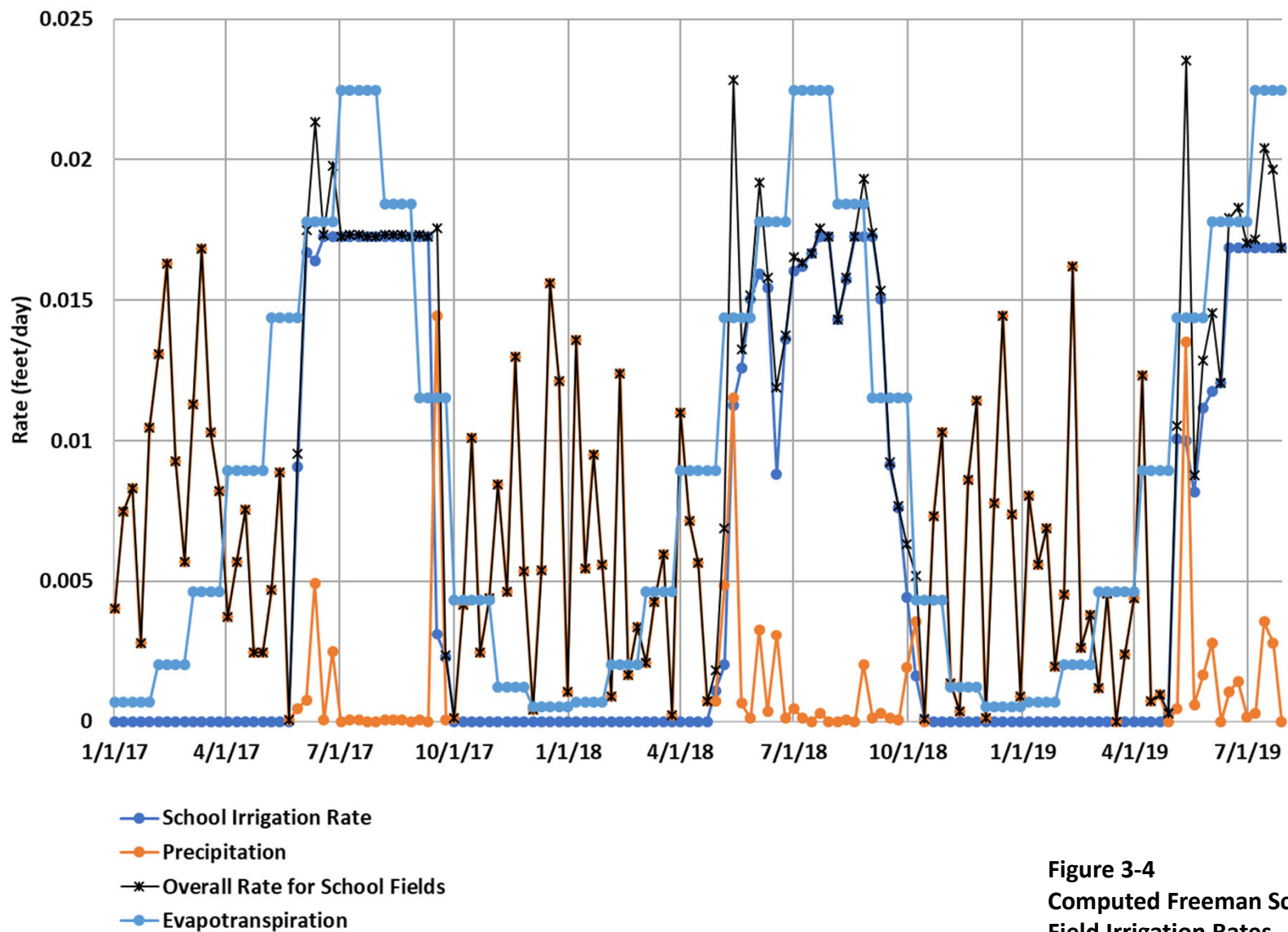
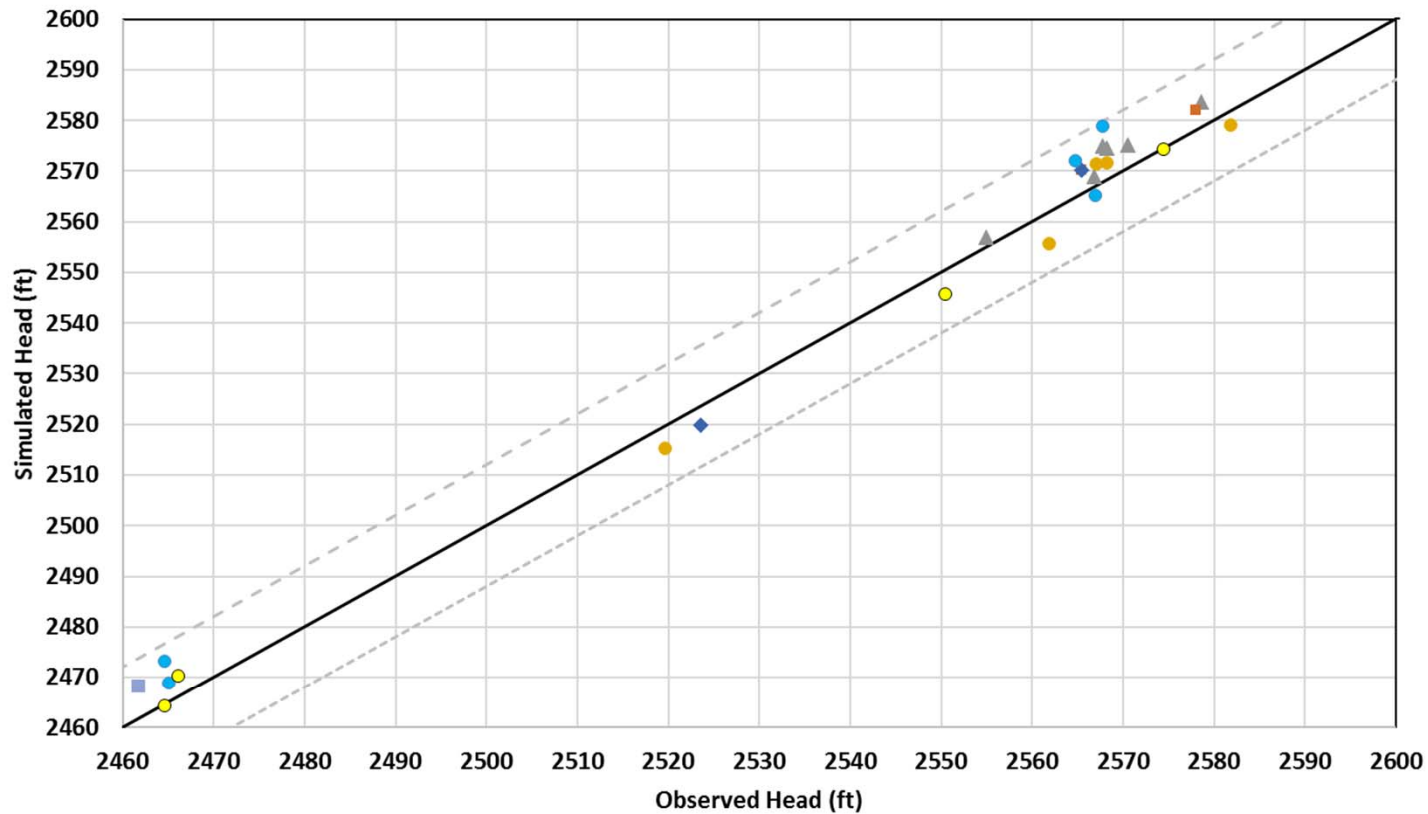


Figure 3-4
Computed Freeman School
Field Irrigation Rates
 2019 Groundwater
 Modeling Report
Grain Handling Facility at Freeman
Freeman, Washington

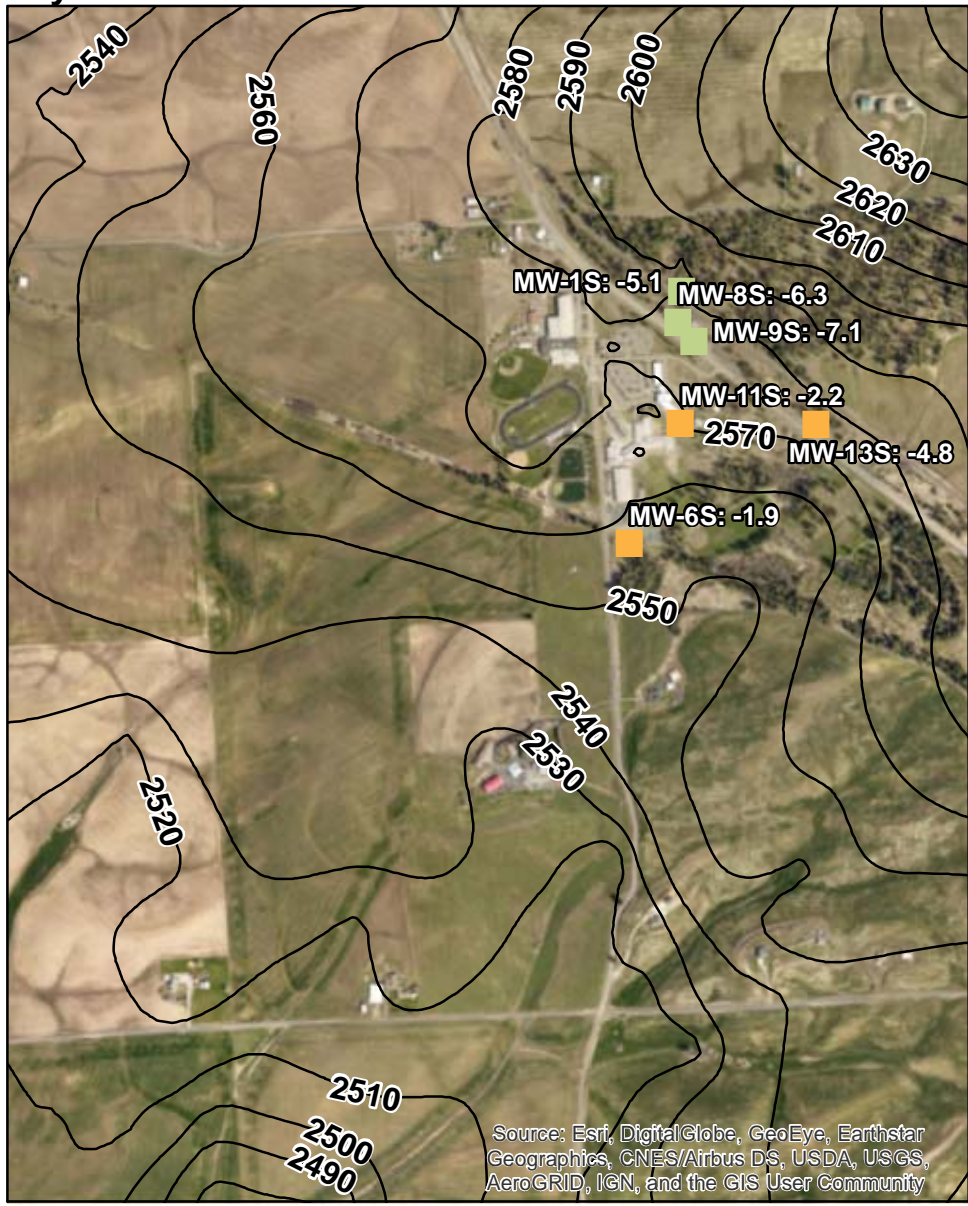


- ▲ Layer 1
- Layer 3
- Layer 5
- Layer 7
- Layer 2
- ◆ Layer 4
- Layer 6
- 1:1
- - - minus 10%
- - - plus 10%

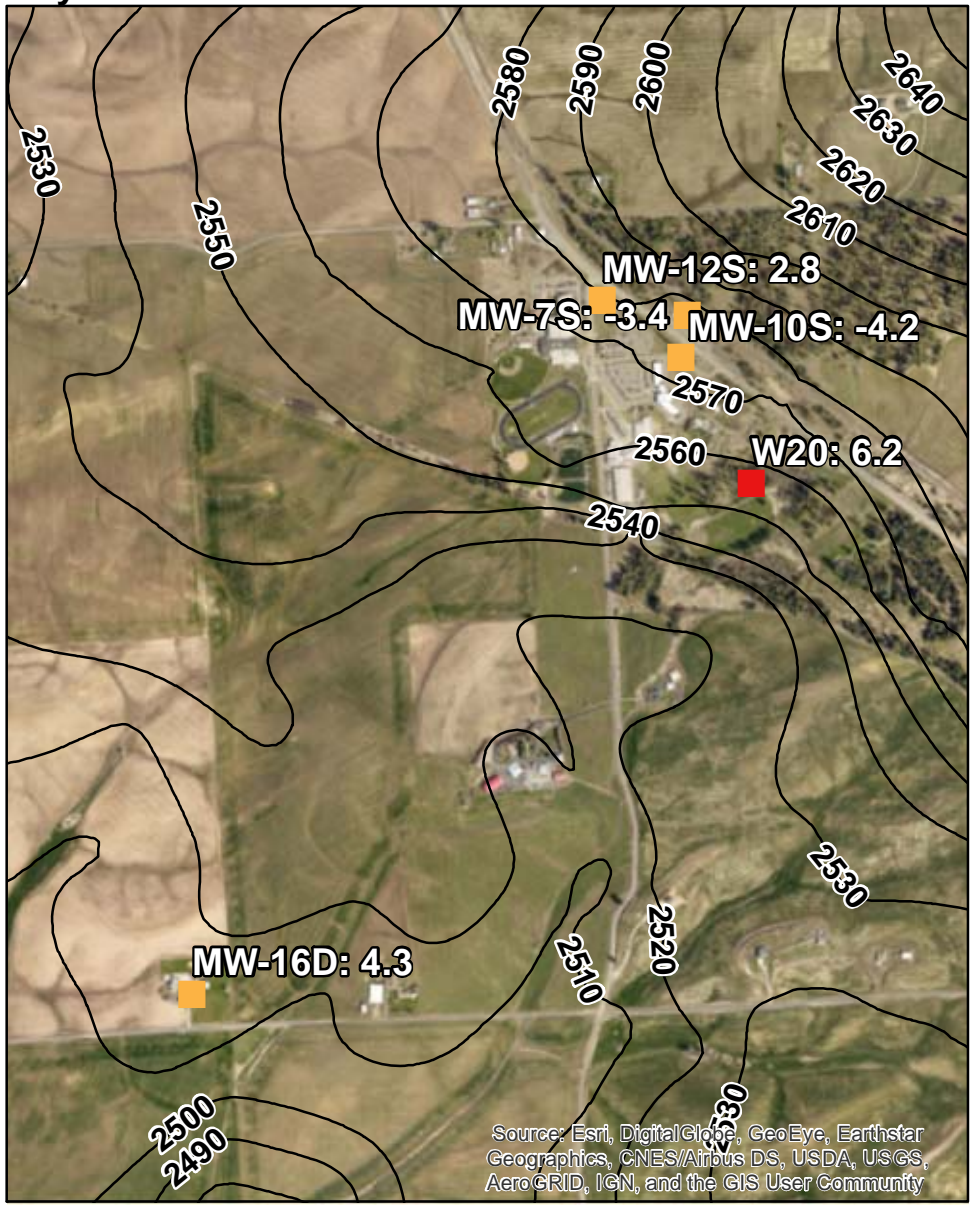
<u>Summary Statistics</u>		(feet)
Residual Mean	-2.58	
Absolute Residual Mean	4.51	
Residual Std. Deviation	4.43	
Sum of Squares	657	
RMS Error	5.13	
Min. Residual	-11.18	
Max. Residual	6.16	
Number of Observations	25	
Range in Observations	120.1	
Scaled Residual Std. Deviation	0.037	
Scaled Absolute Residual Mean	0.038	
Scaled RMS Error	4.27%	
Scaled Residual Mean	-0.021	

Figure 4-1
Simulated vs Observed
Steady State Groundwater
Elevations
 2019 Groundwater
 Modeling Report
Grain Handling Facility at Freeman
Freeman, Washington

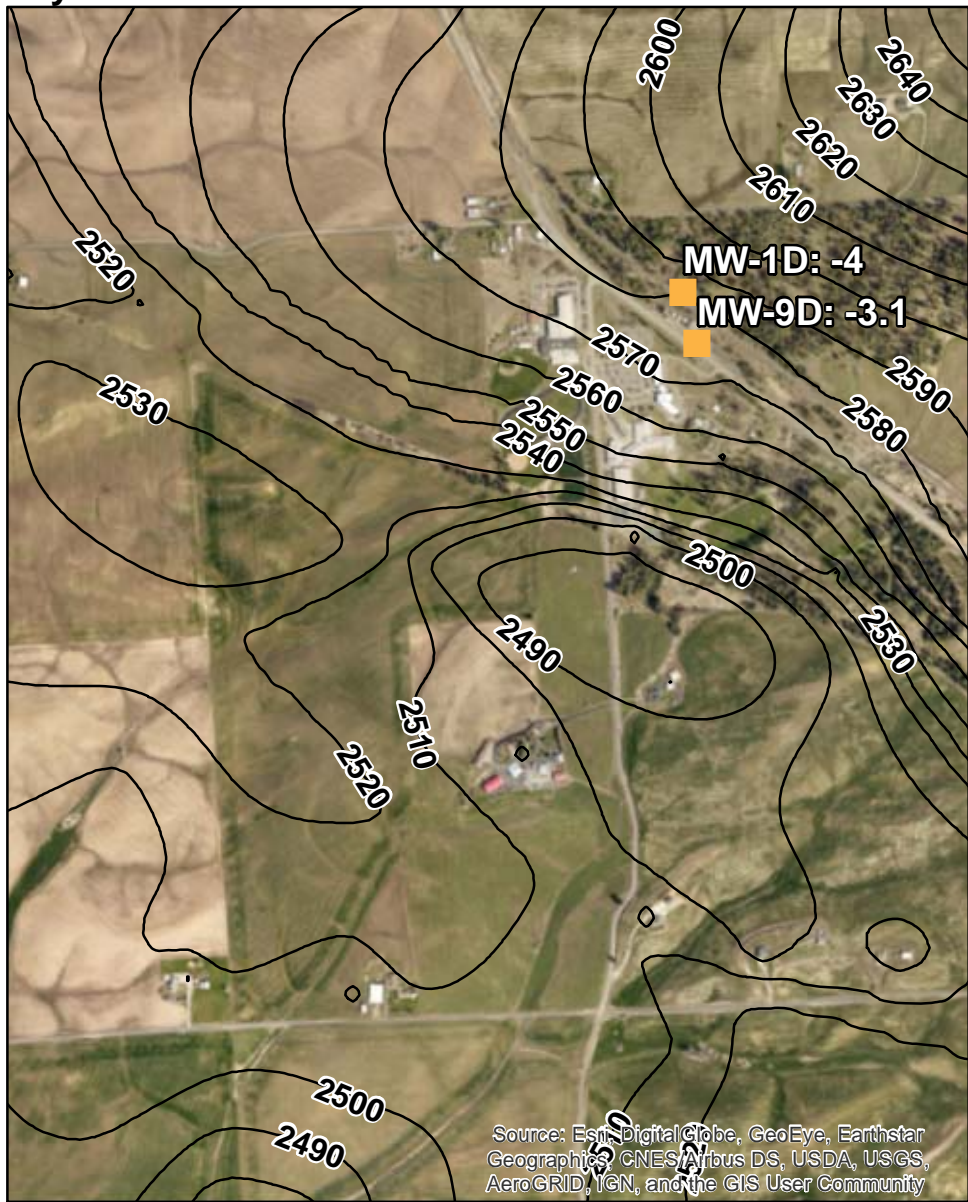
Layer 1



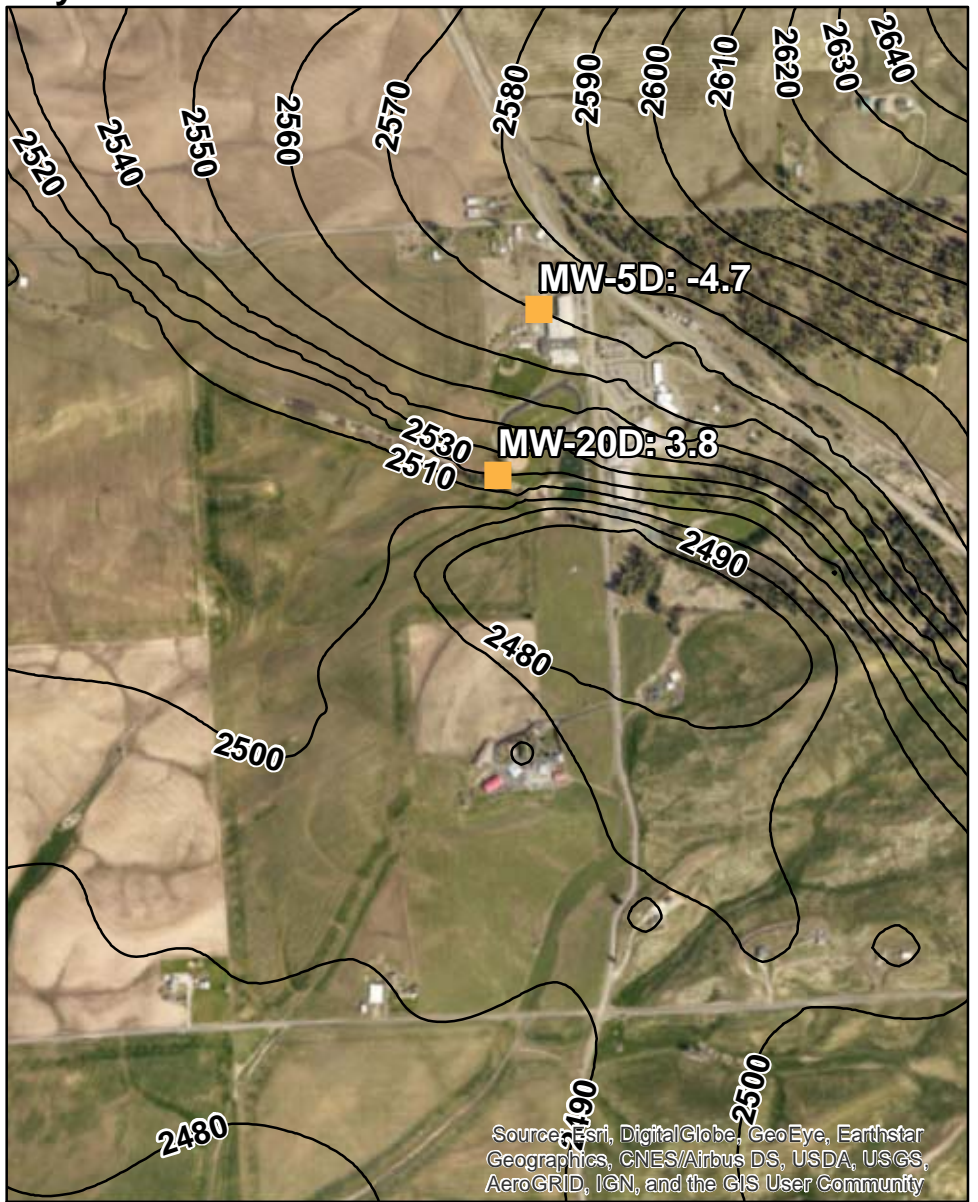
Layer 2



Layer 3



Layer 4



Legend

Target Residuals

Residual

- < -10
- -10 to -5
- -5 to 5
- 5 to 10

— Simulated Groundwater Elevation (ft)

Note:

Residual is computed as observed groundwater elevations minus simulated groundwater elevation. Negative values indicate model heads too high.

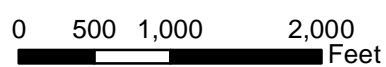
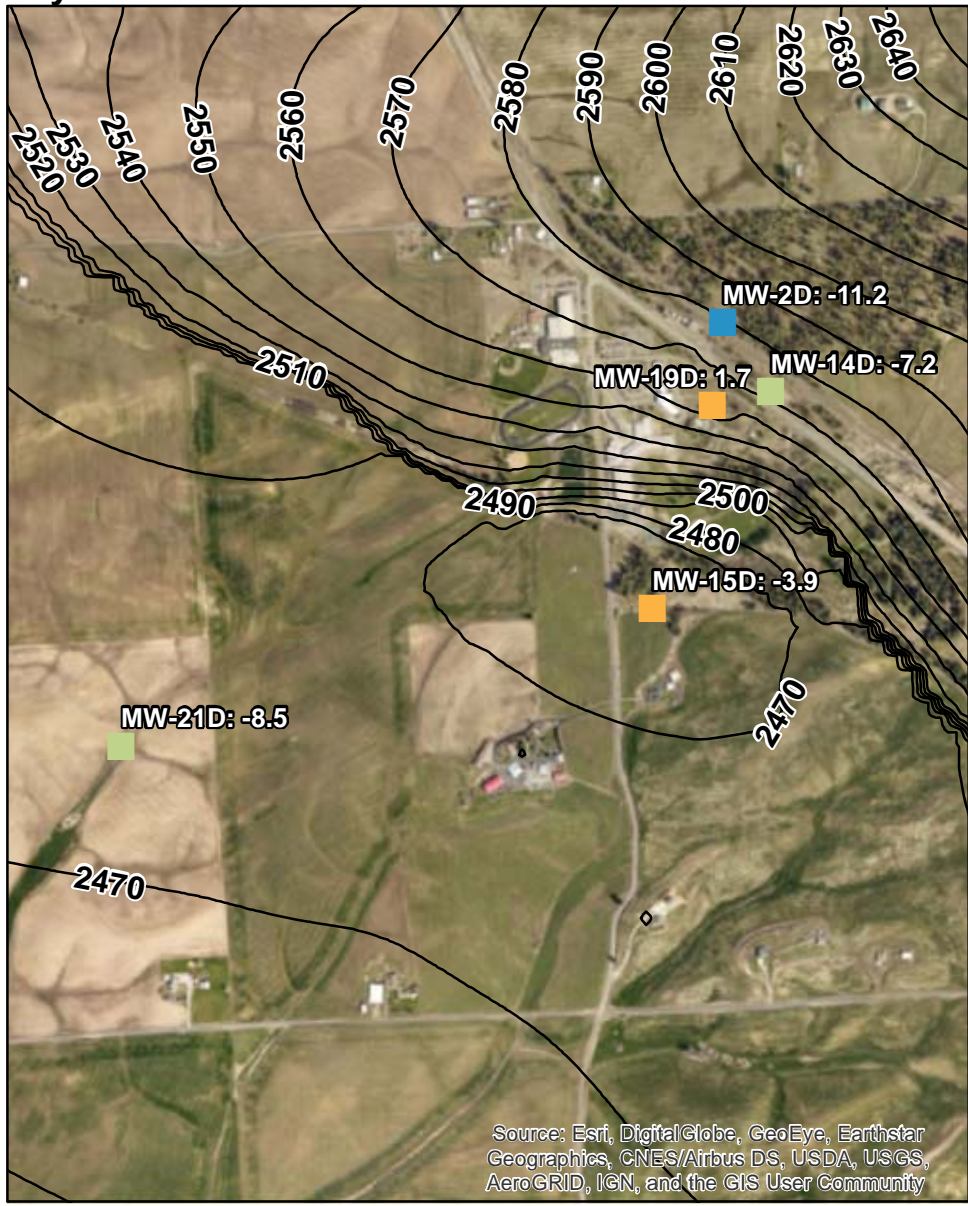


Figure 4-2A
Steady State Groundwater Elevations and Residuals
Layers 1-4

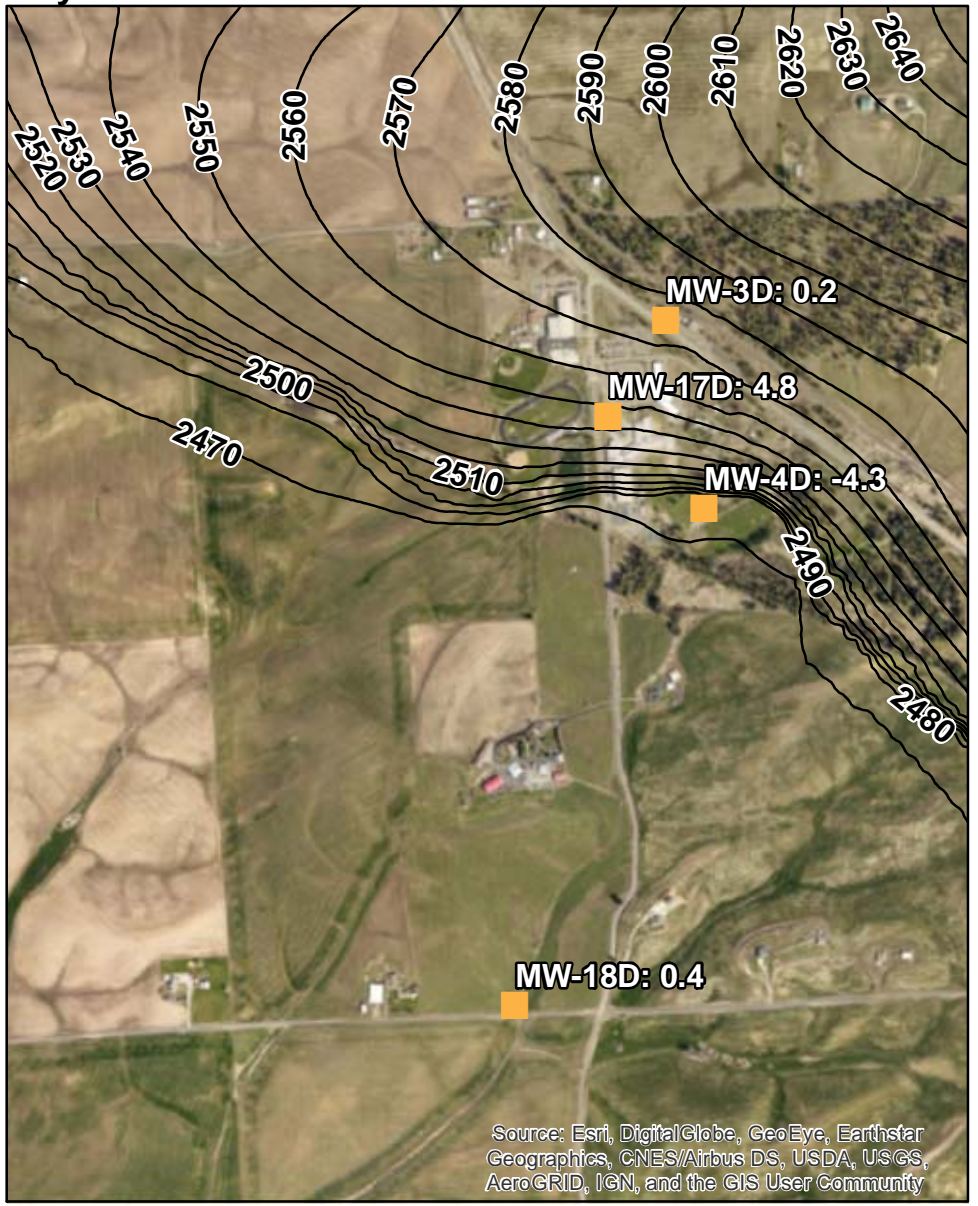
2019 Groundwater Modeling Report
Grain Handling Facility at Freeman
Freeman, Washington



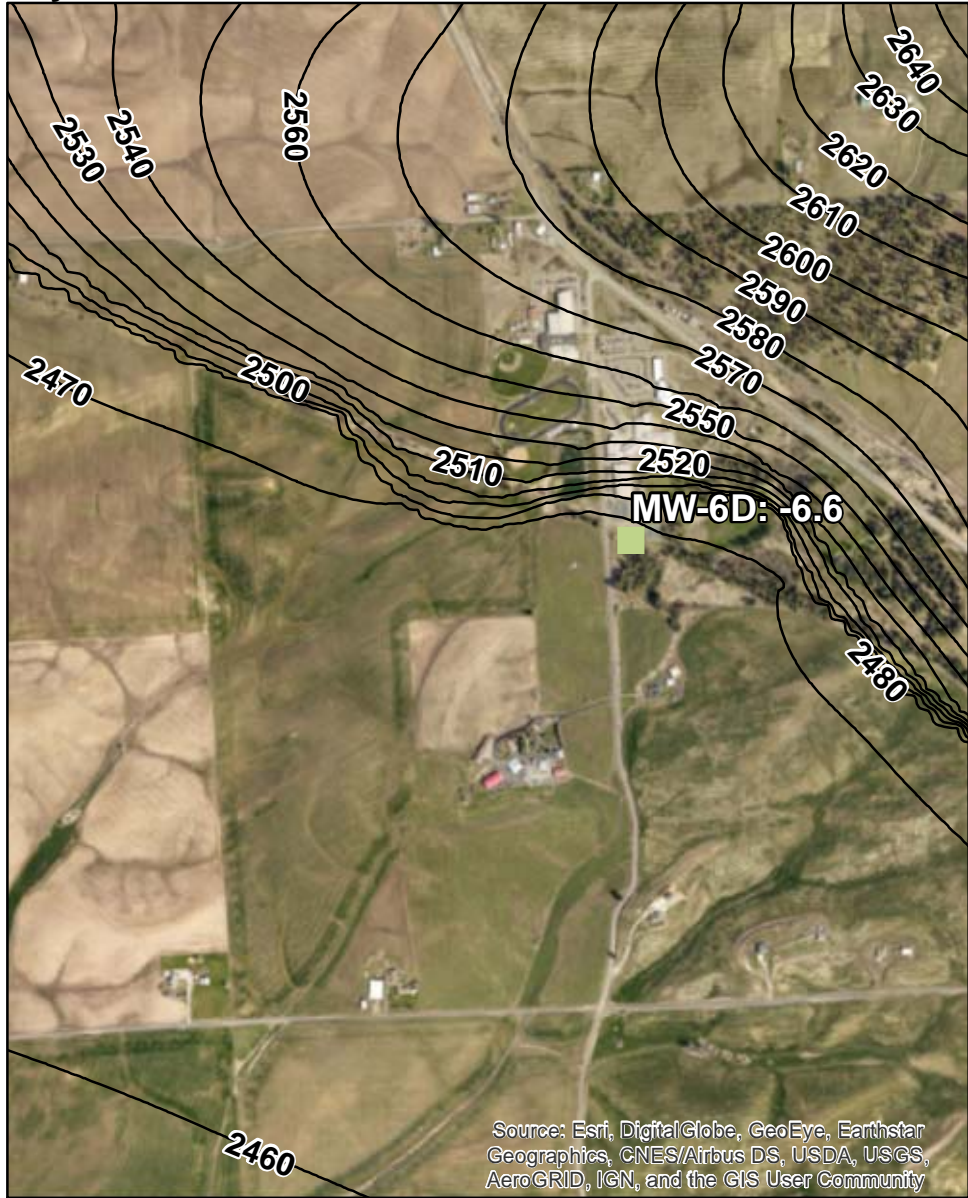
Layer 5



Layer 6



Layer 7



Legend

Target Residuals

Residual

- < -10
- -10 to -5
- -5 to 5
- 5 to 10

— Simulated Groundwater Elevation (ft)

Note:

Residual is computed as observed groundwater elevations minus simulated groundwater elevation. Negative values indicate model heads too high.



Figure 4-2B
Steady State Groundwater Elevations and Residuals
Layers 5-7

2019 Groundwater Modeling Report
Grain Handling Facility at Freeman
Freeman, Washington



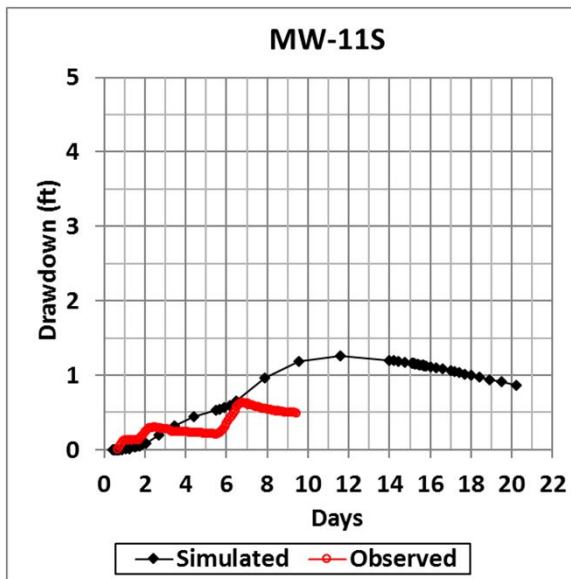
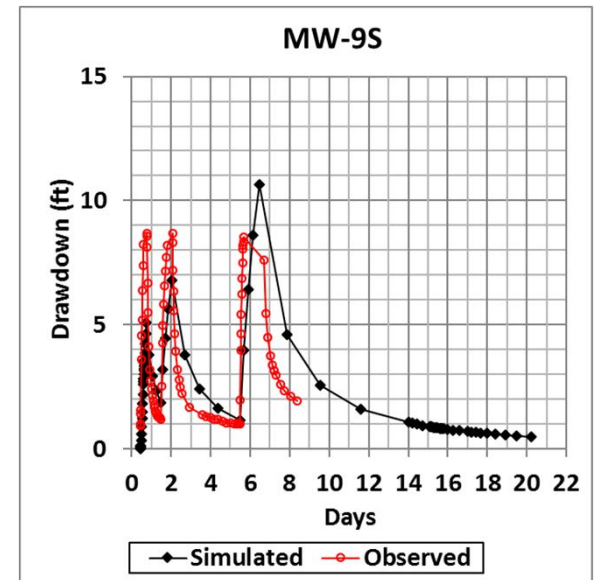
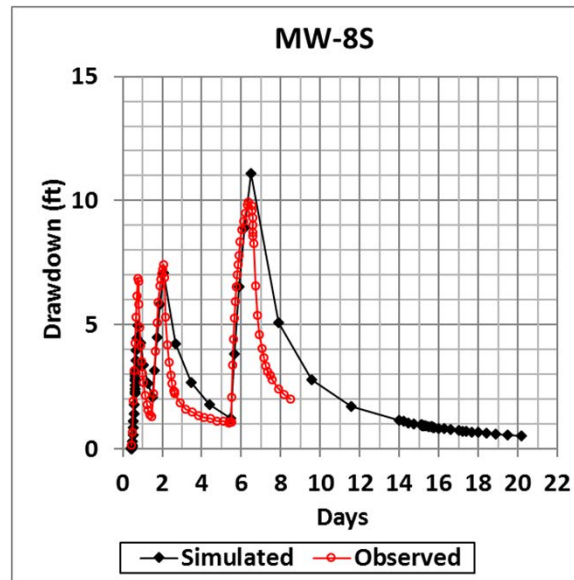
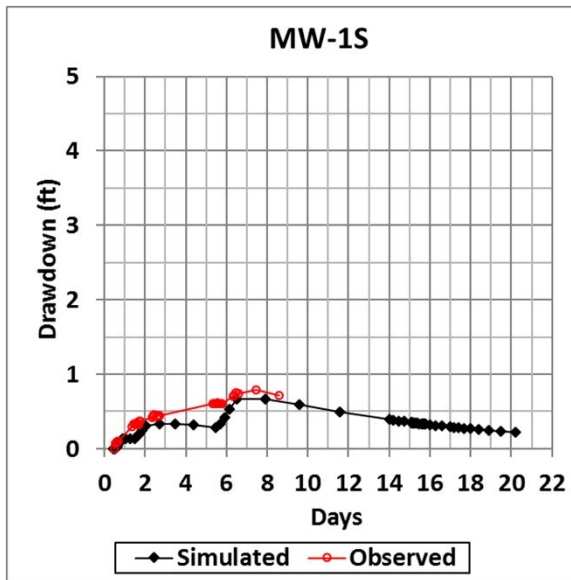


Figure 4-3A
Observed and Simulated
Drawdown, 2017 Aquifer Test
Model Layer 1
 2019 Groundwater
 Modeling Report
Grain Handling Facility at Freeman
Freeman, Washington

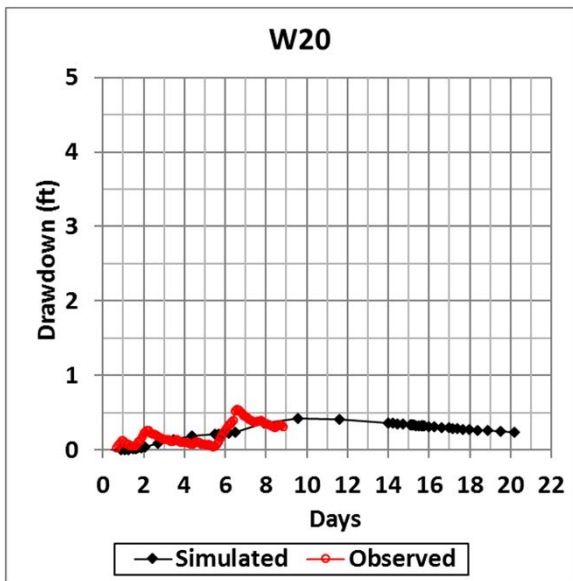
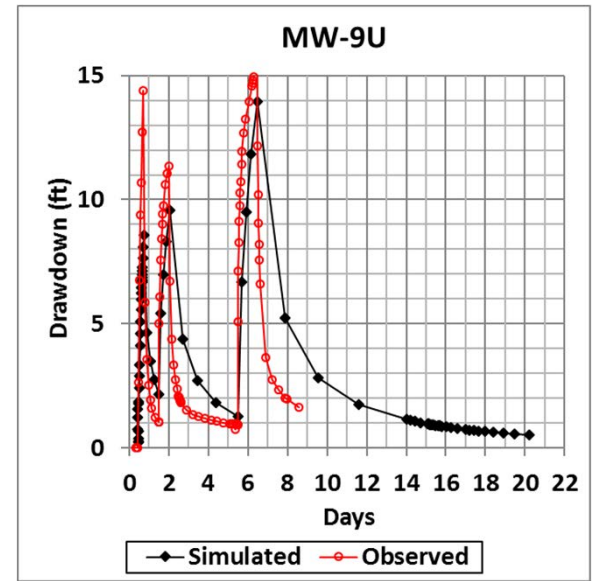
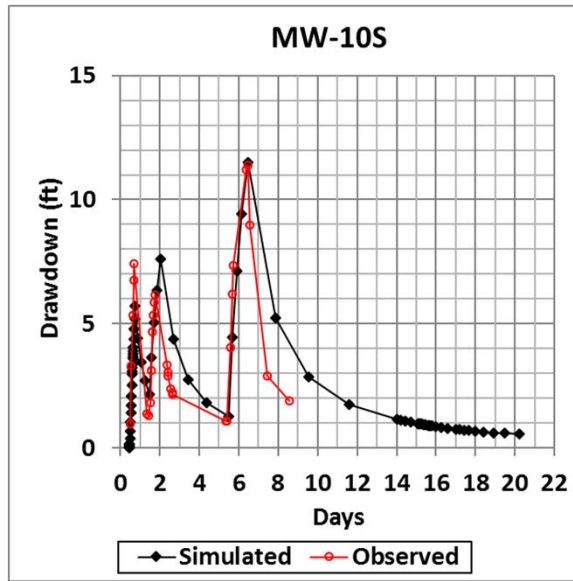
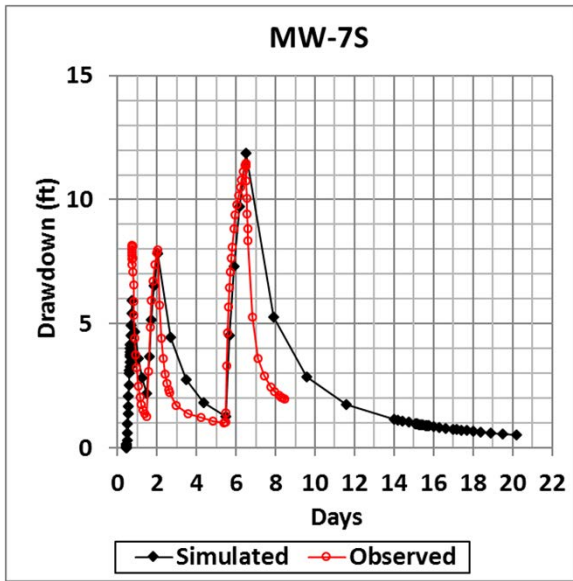


Figure 4-3B
 Observed and Simulated
 Drawdown, 2017 Aquifer Test
 Model Layer 2
 2019 Groundwater
 Modeling Report
 Grain Handling Facility at Freeman
 Freeman, Washington

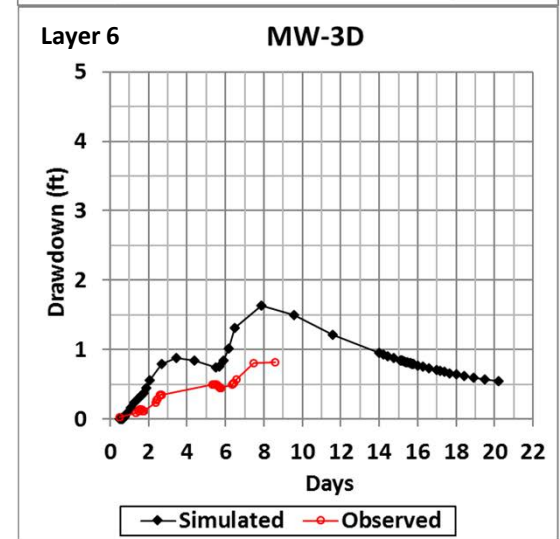
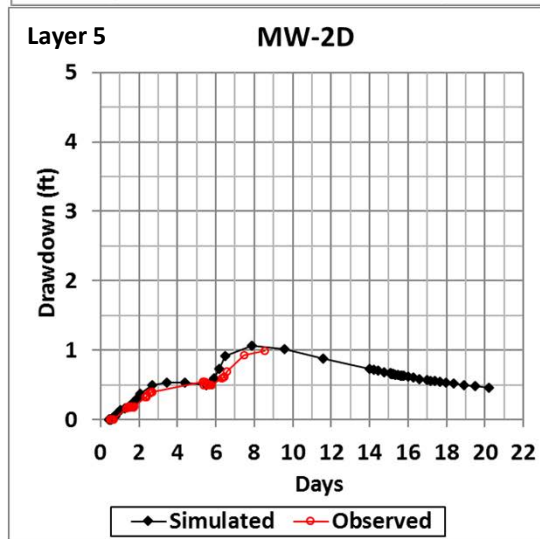
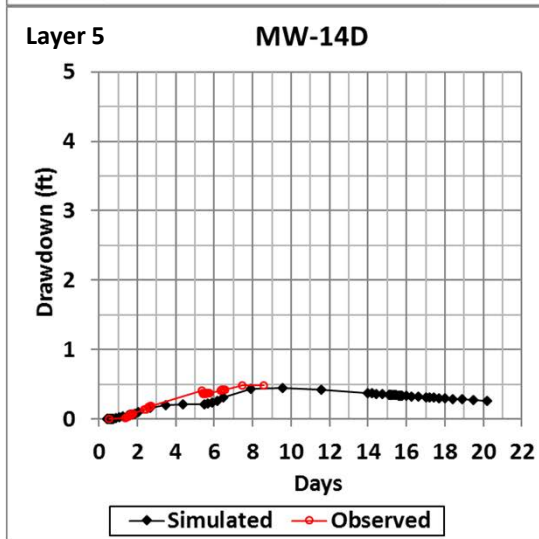
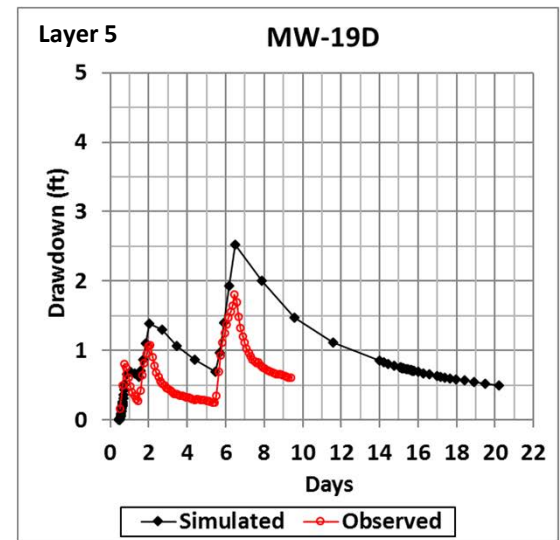
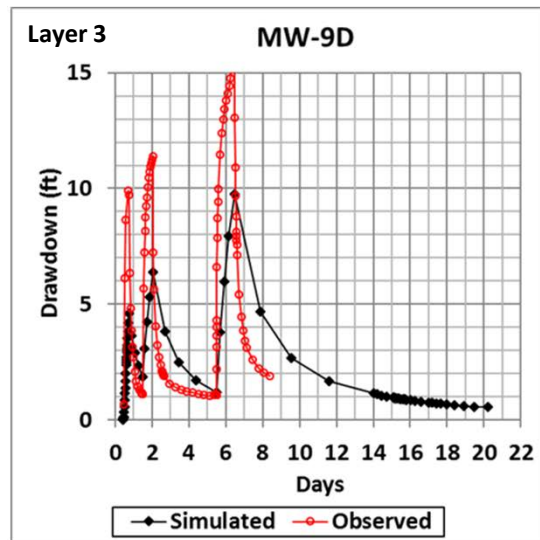
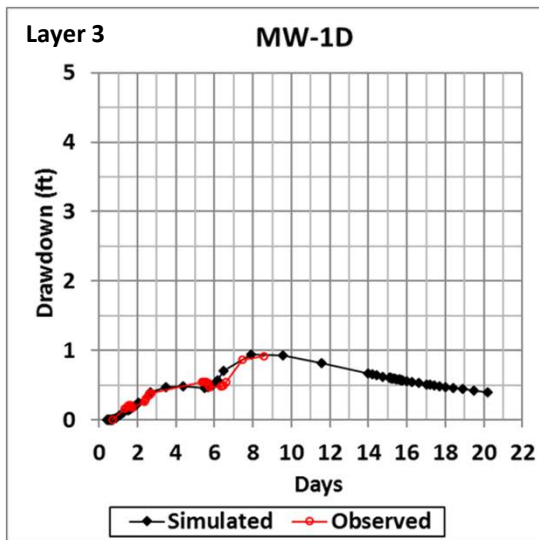
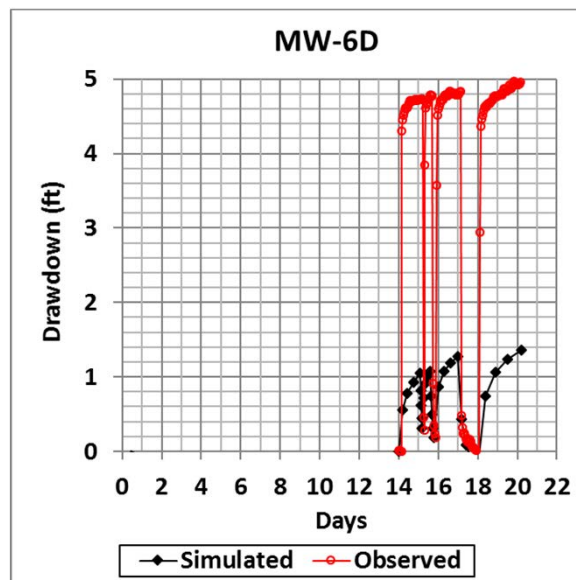
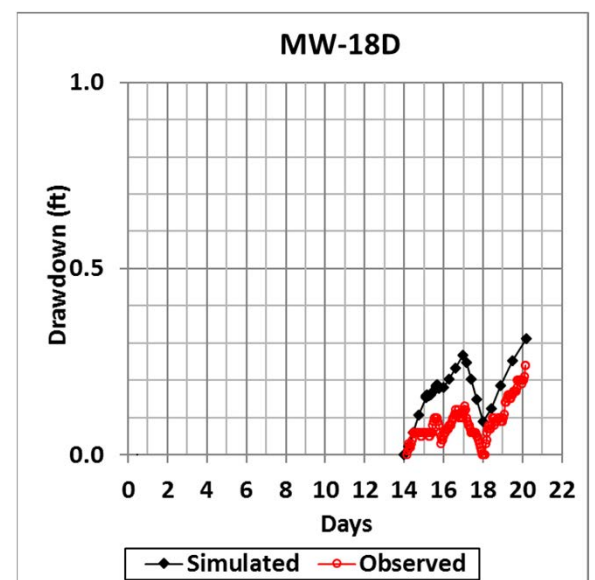
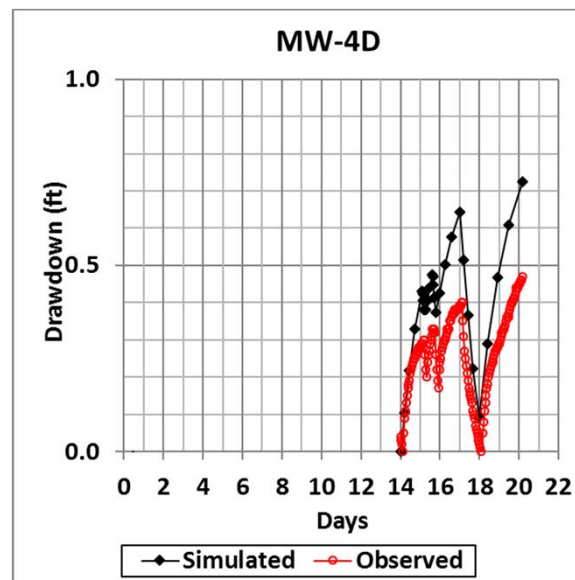
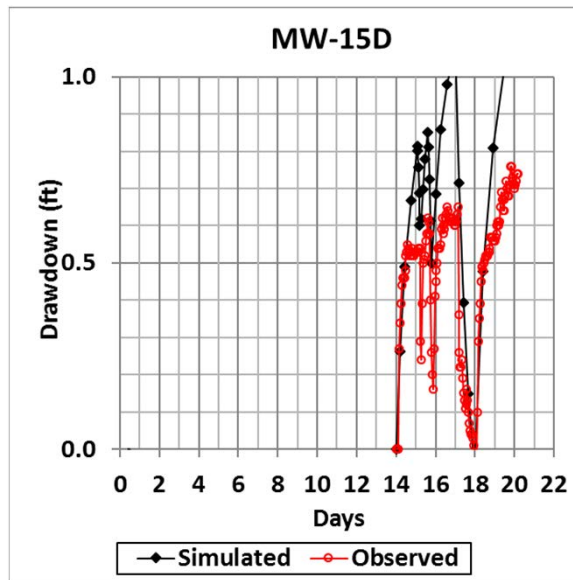
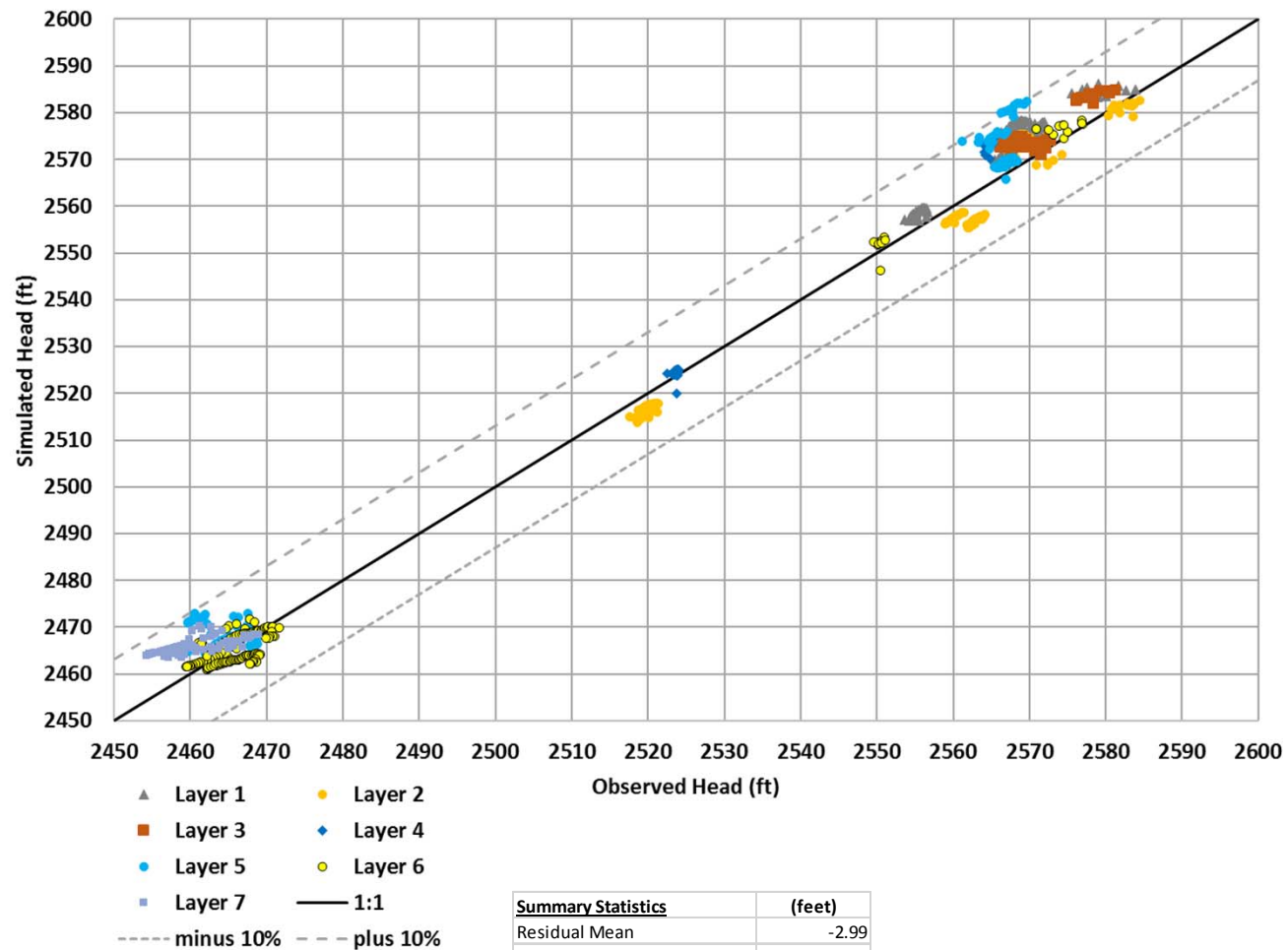


Figure 4-3C
Observed and Simulated
Drawdown, 2017 Aquifer Test
Model Layers 3, 5, and 6
 2019 Groundwater
 Modeling Report
Grain Handling Facility at Freeman
Freeman, Washington



Note: The model initiated the WS5 stress evaluation starting on model day 14.

Figure 4-4
Observed and Simulated
Drawdown, Response to WS5
 2019 Groundwater
 Modeling Report
Grain Handling Facility at Freeman
Freeman, Washington



Summary Statistics	(feet)
Residual Mean	-2.99
Absolute Residual Mean	4.42
Residual Std. Deviation	4.33
Sum of Squares	30115
RMS Error	5.26
Min. Residual	-13.57
Max. Residual	6.80
Number of Observations	1088
Range in Observations	130.2
Scaled Residual Std. Deviation	0.033
Scaled Absolute Residual Mea	0.034
Scaled RMS Error	4.04%
Scaled Residual Mean	-0.023

Figure 4-5
Simulated vs Observed
Transient Groundwater
Elevations
 2019 Groundwater
 Modeling Report
 Grain Handling Facility at Freeman
 Freeman, Washington

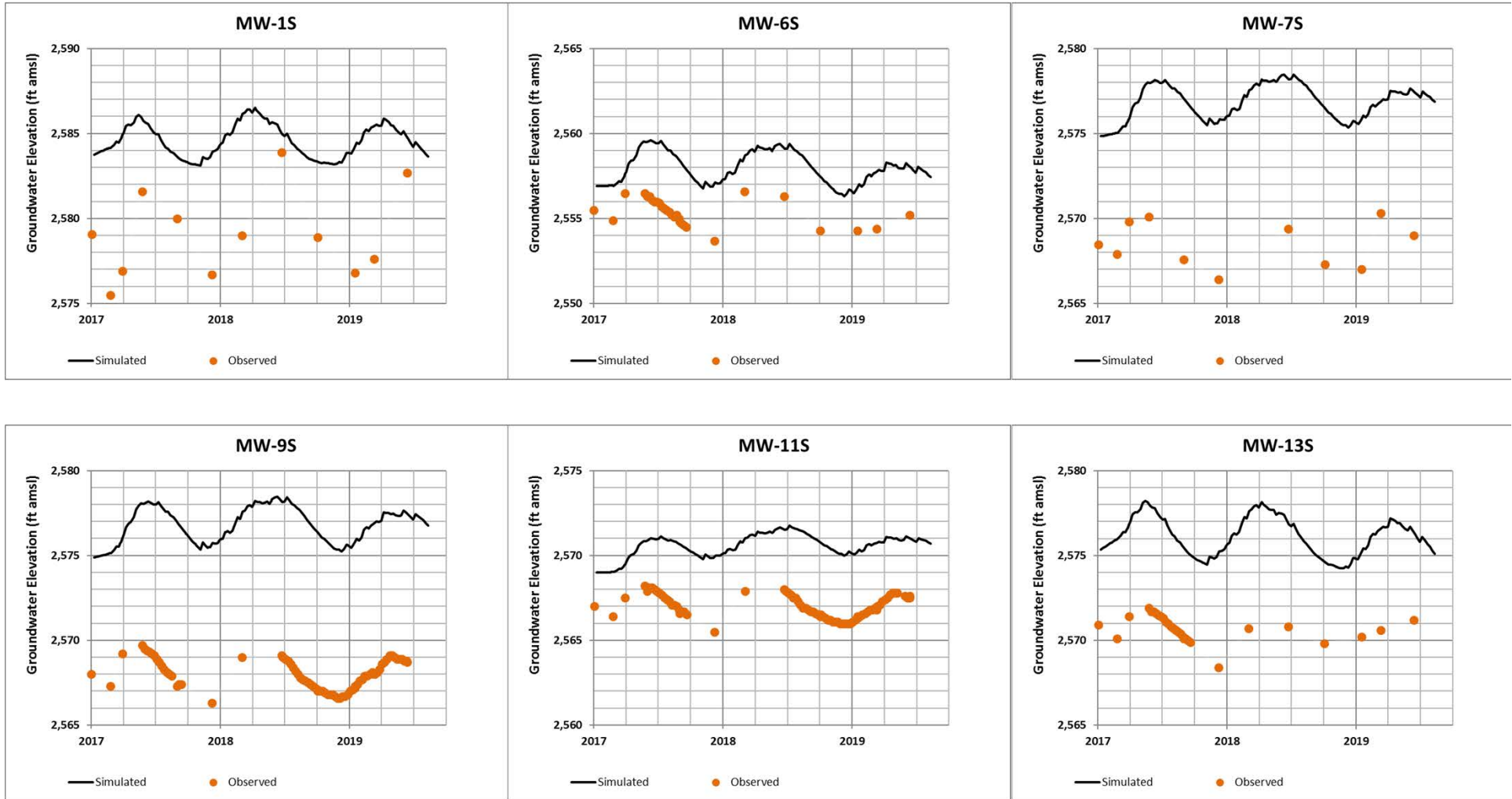


Figure 4-6A
Observed and Simulated
Groundwater Elevations
Model Layer 1
 2019 Groundwater
 Modeling Report
Grain Handling Facility at Freeman
Freeman, Washington

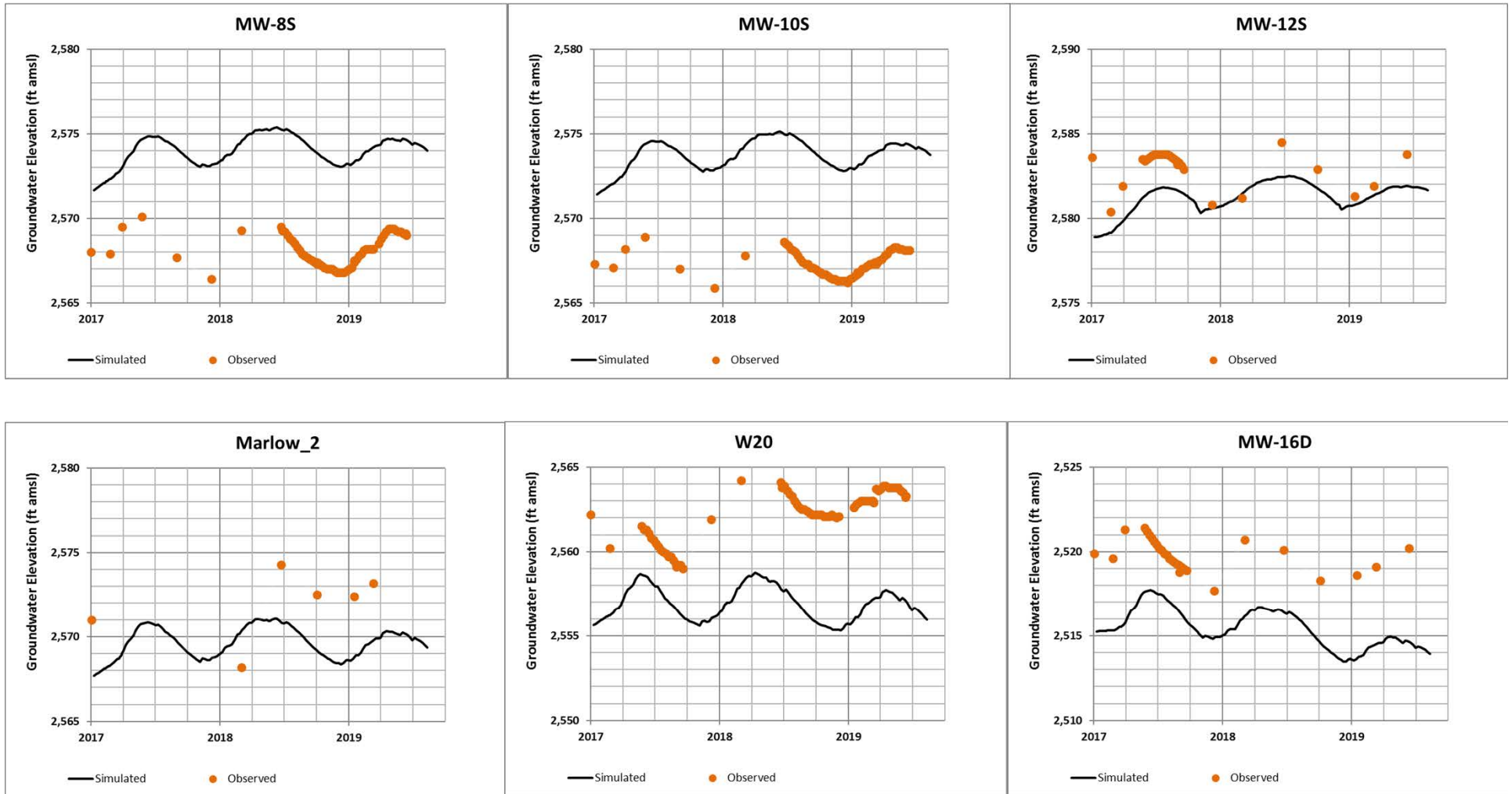
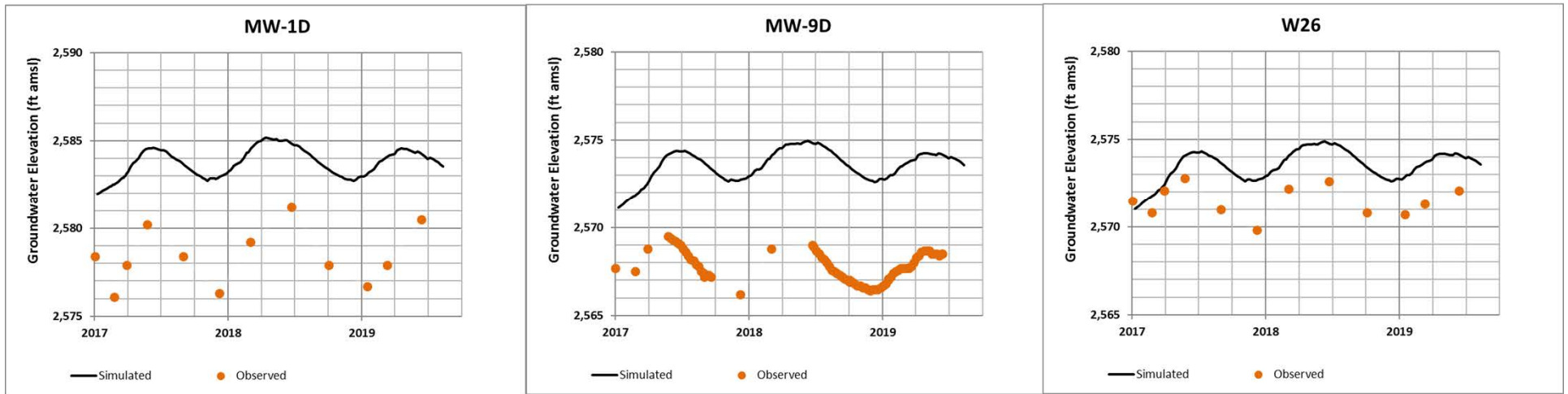
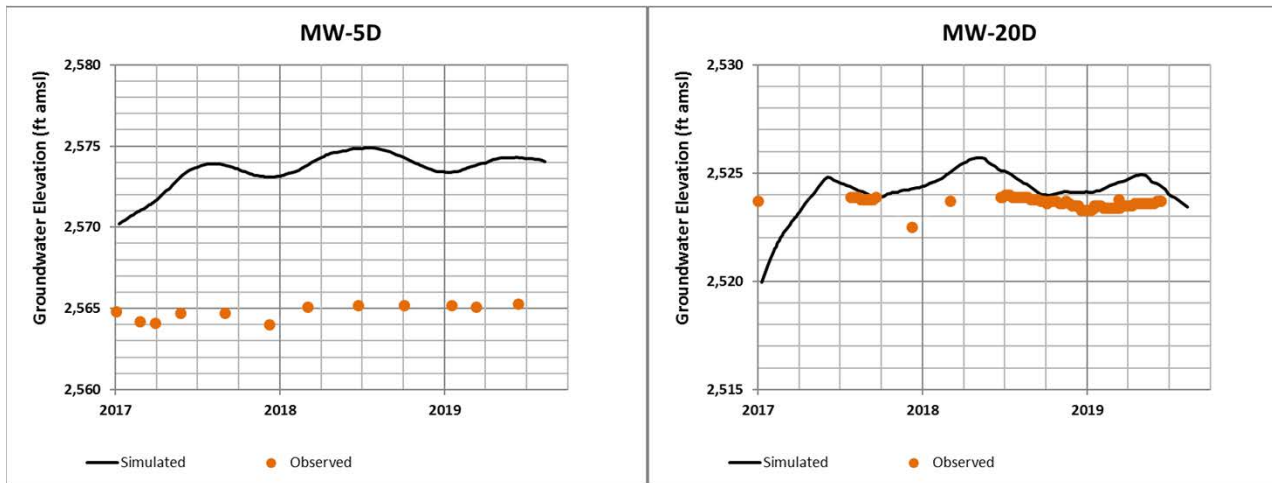


Figure 4-6B
Observed and Simulated
Groundwater Elevations
Model Layer 2
 2019 Groundwater
 Modeling Report
 Grain Handling Facility at Freeman
 Freeman, Washington



Layer 3 wells



Layer 4 wells

Figure 4-6C
Observed and Simulated
Groundwater Elevations
Models Layer 3 and 4
 2019 Groundwater
 Modeling Report
Grain Handling Facility at Freeman
Freeman, Washington

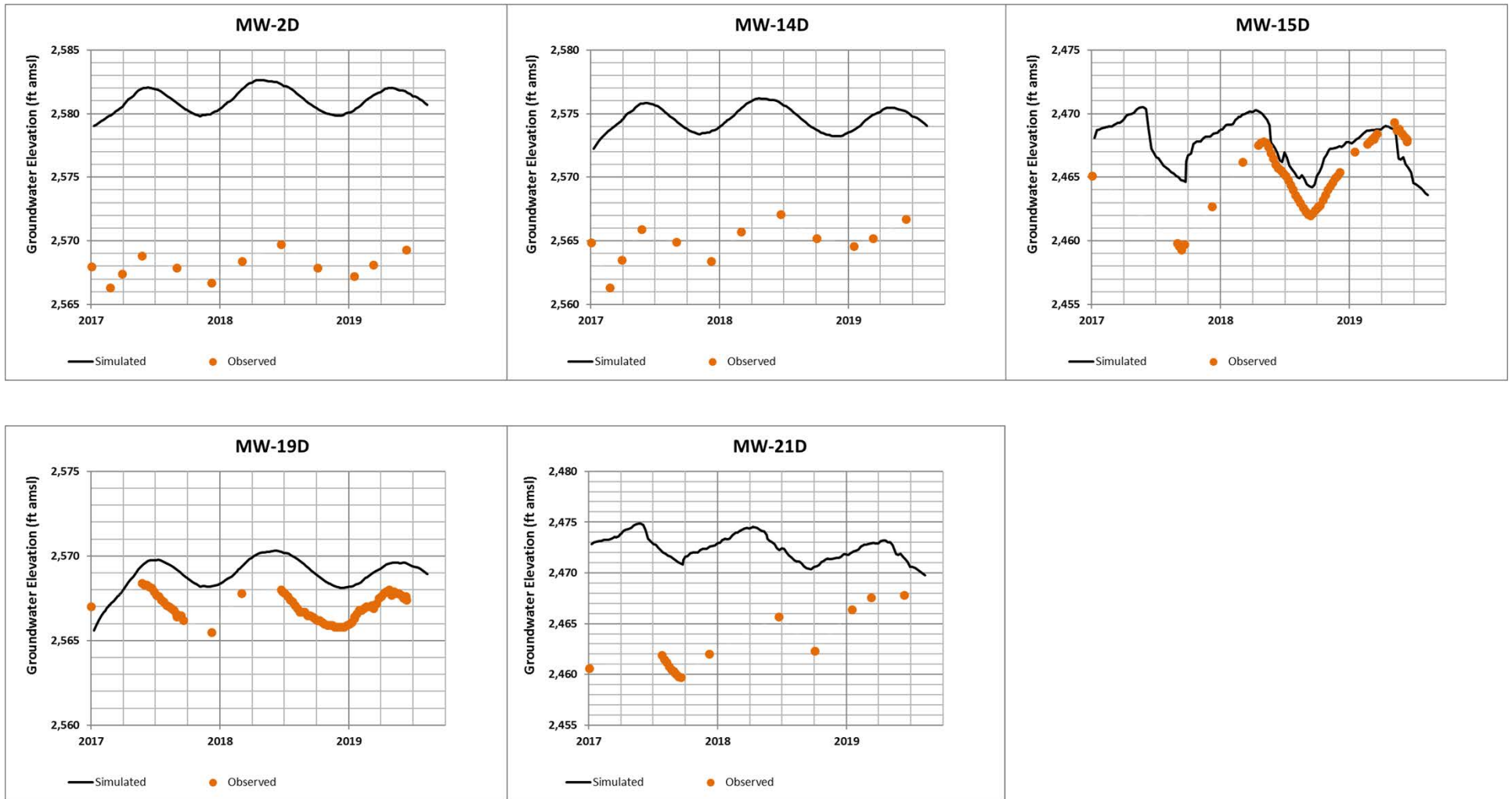
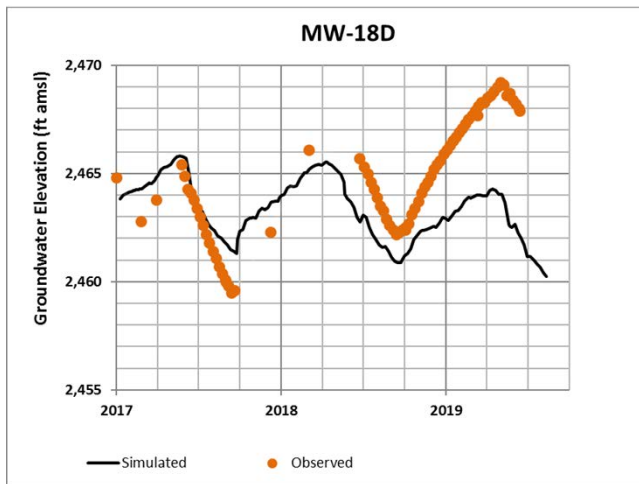
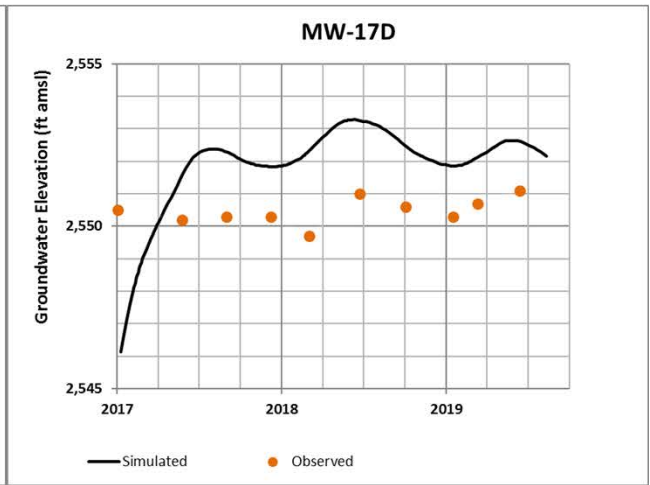
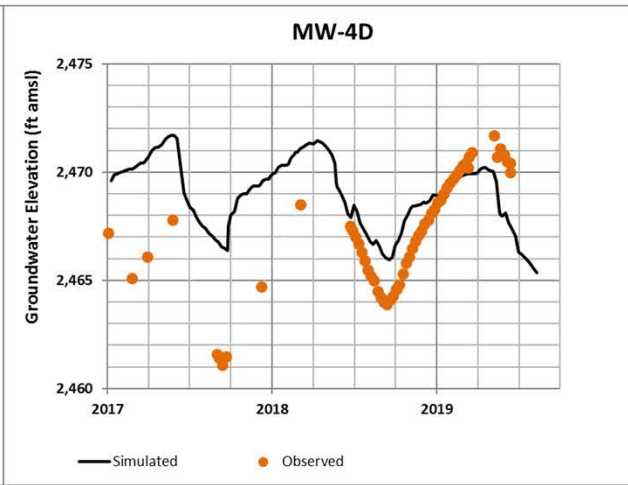
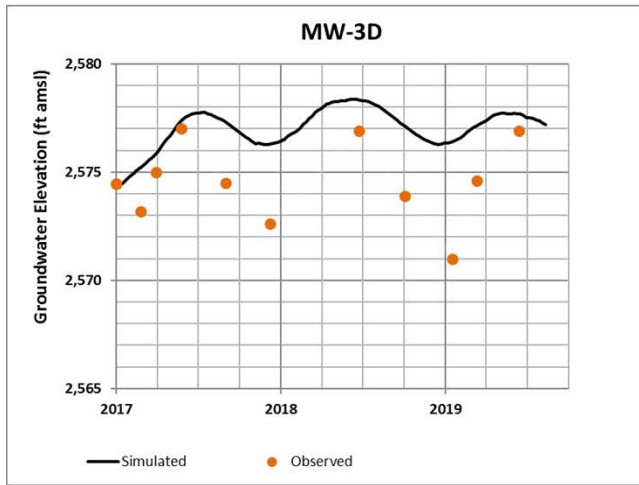
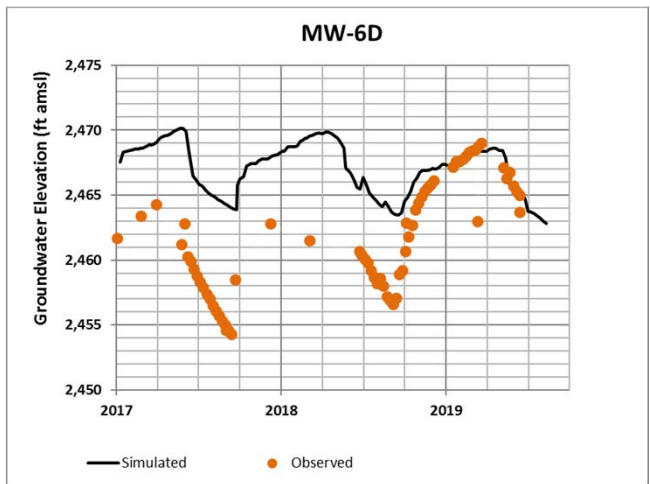


Figure 4-6D
Observed and Simulated
Groundwater Elevations
Model Layer 5
 2019 Groundwater
 Modeling Report
Grain Handling Facility at Freeman
Freeman, Washington

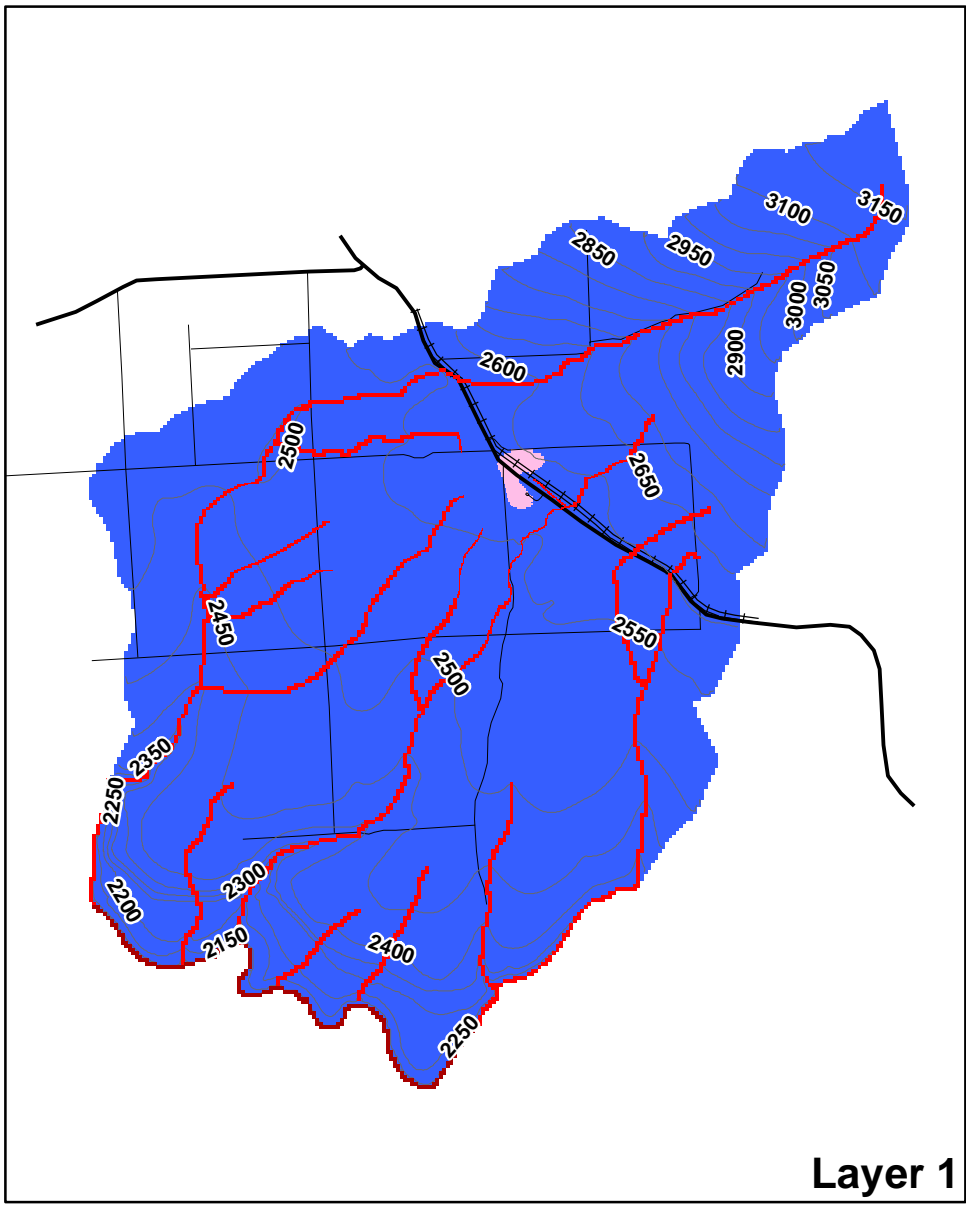


Layer 7:

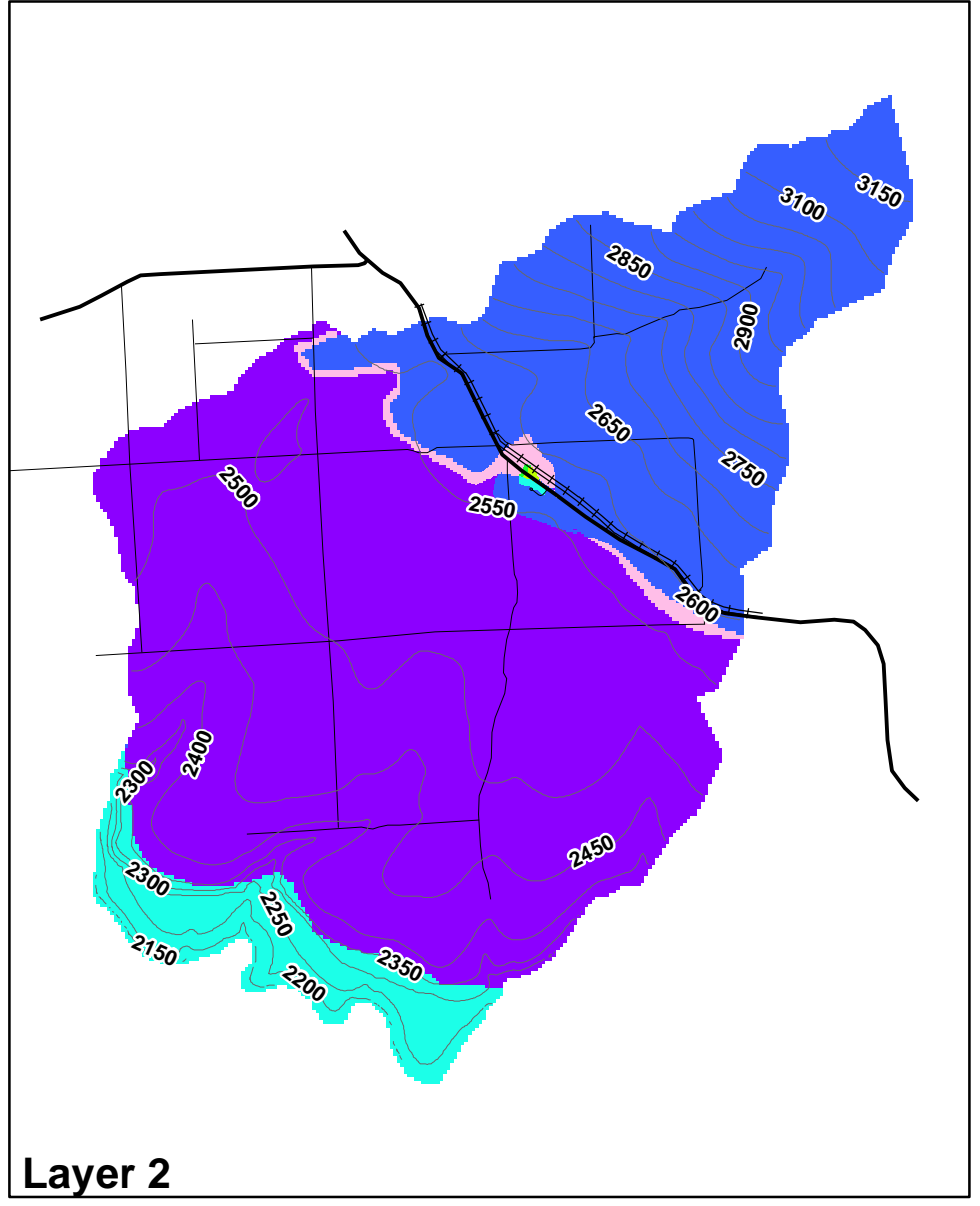


Layer 6 wells

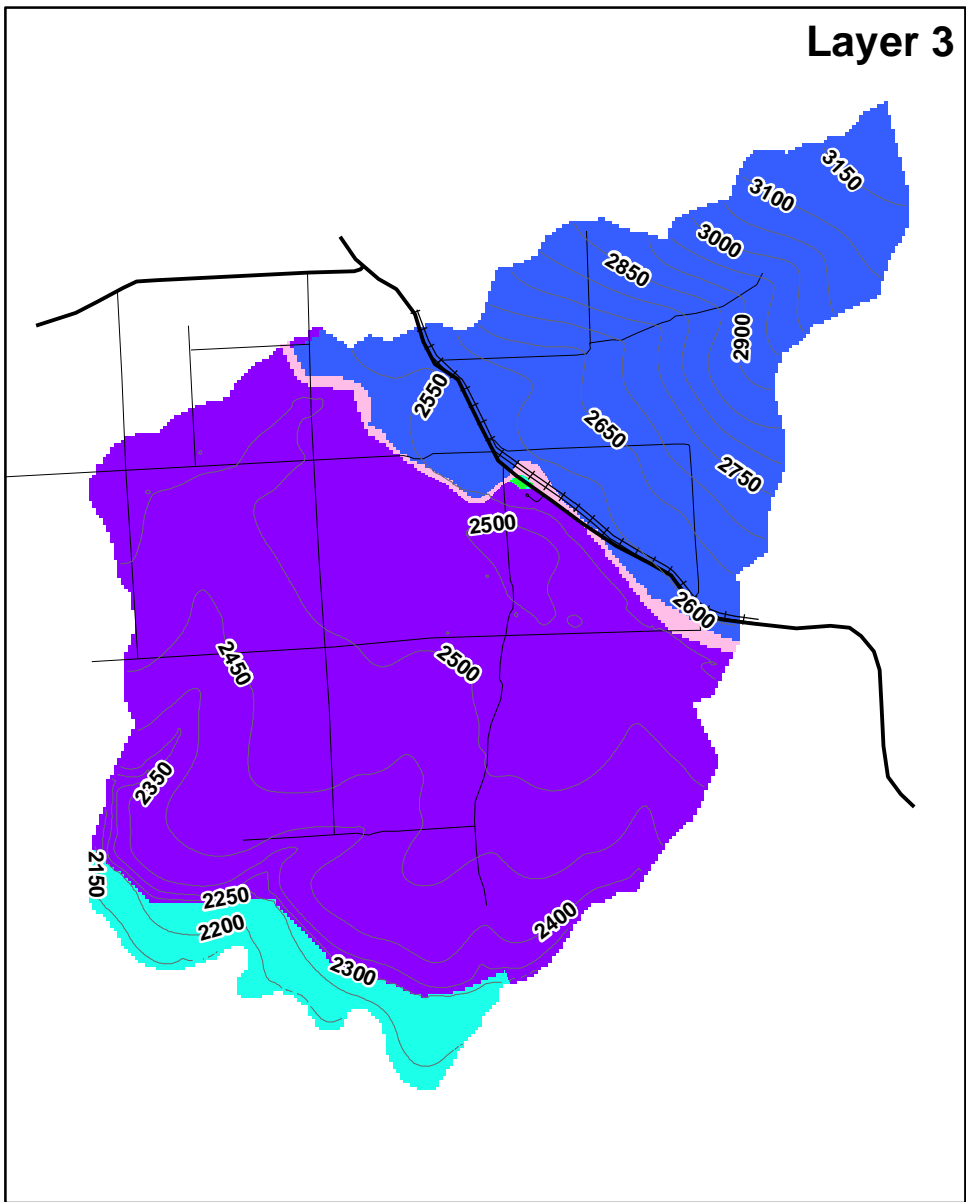
Figure 4-6E
Observed and Simulated
Groundwater Elevations
Model Layers 6 and 7
 2019 Groundwater
 Modeling Report
Grain Handling Facility at Freeman
Freeman, Washington



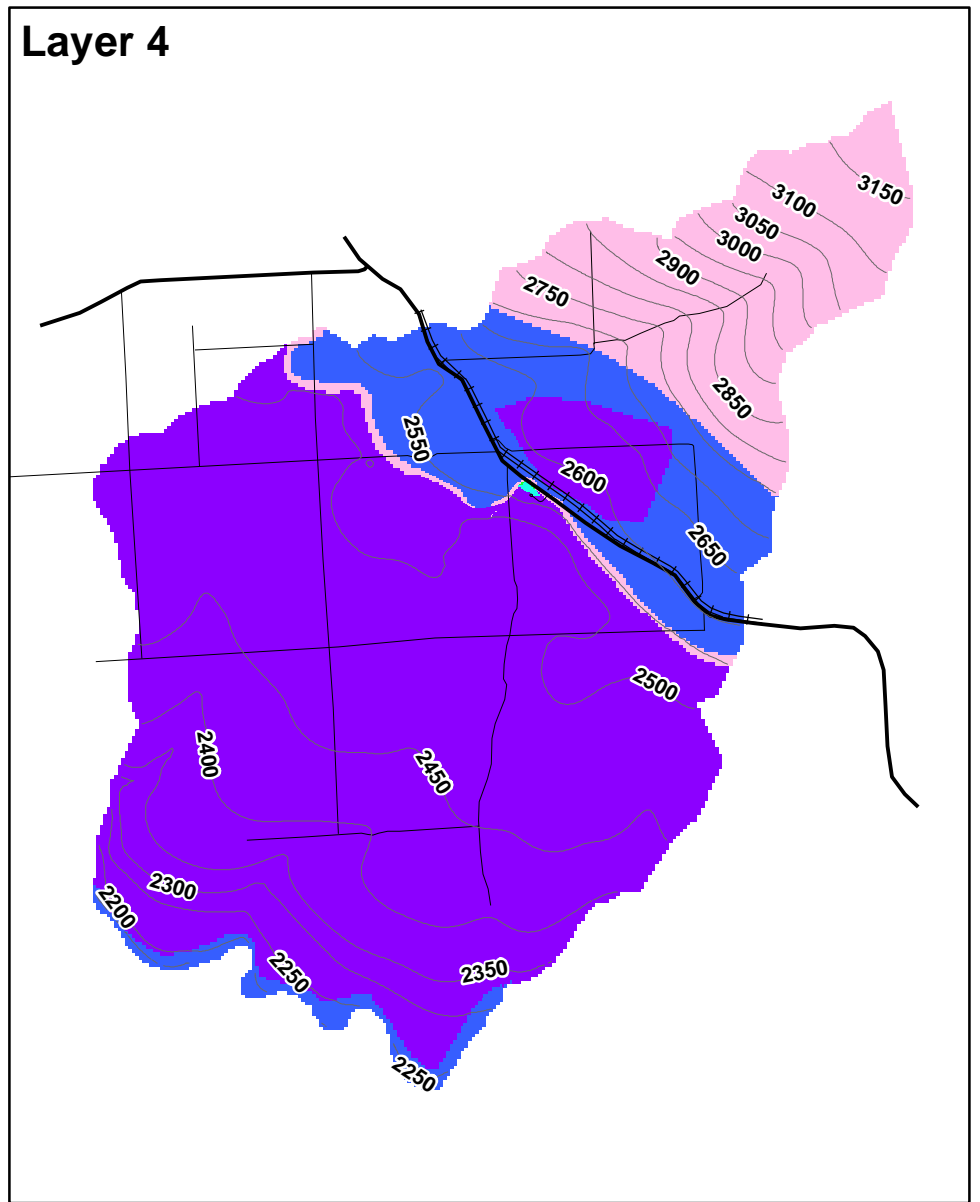
Layer 1



Layer 2



Layer 3



Layer 4

Legend

- | | |
|--|--------------------------------------|
| — Simulated Groundwater Elevation (ft) | Hydraulic Conductivity (ft/d) |
| — HWY | 0.001 to 0.01 |
| ≡≡≡ RR | > 0.01 to 0.1 |
| — Road | > 0.1 to 1 |
| Boundary Conditions | > 1 to 5 |
| █ Drain | > 5 to 25 |
| █ River | > 25 to 50 |
| □ No Flow | > 50 to 75 |
| | > 75 to 100 |
| | > 100 to 125 |

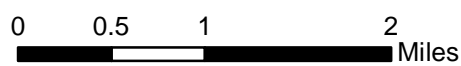
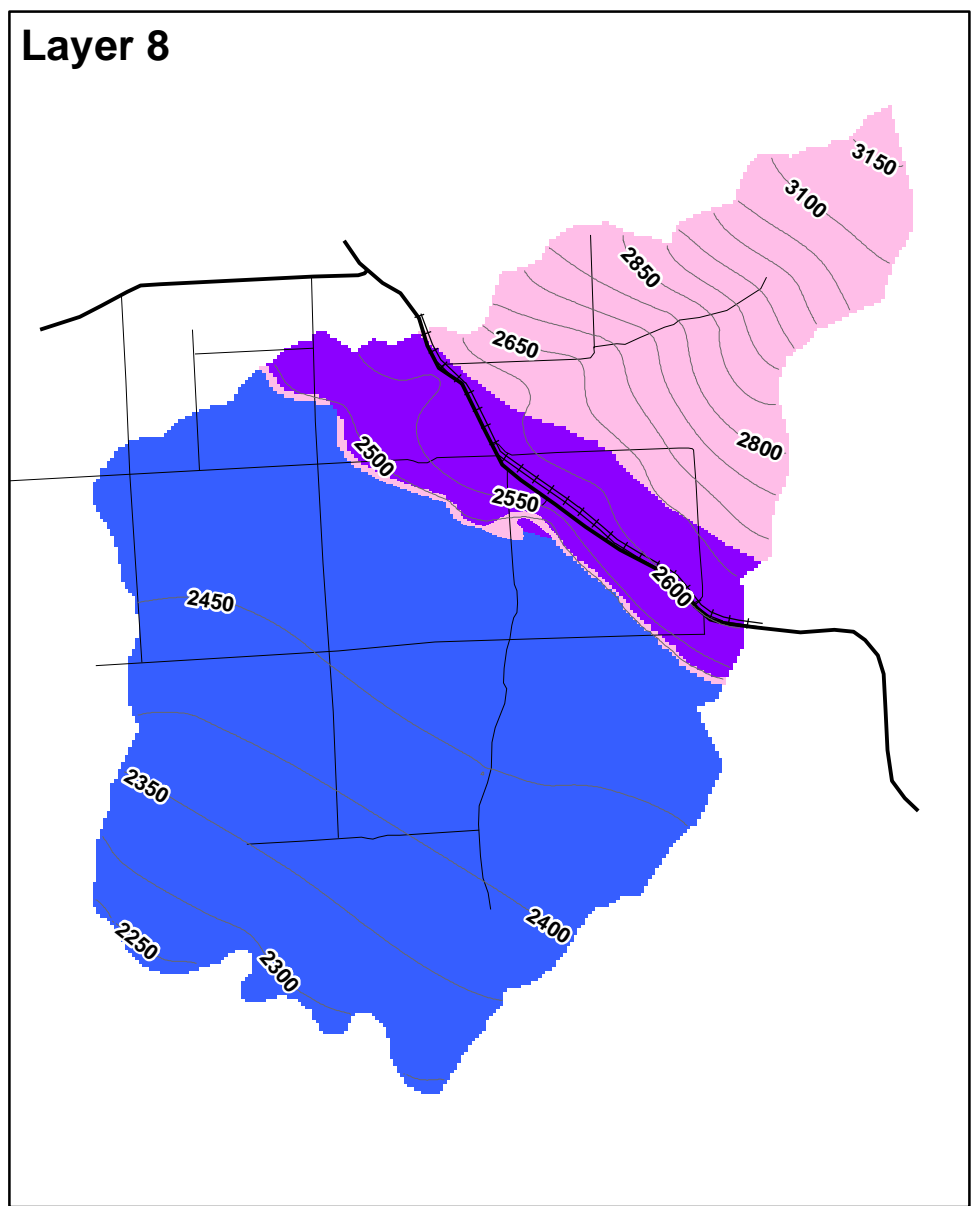
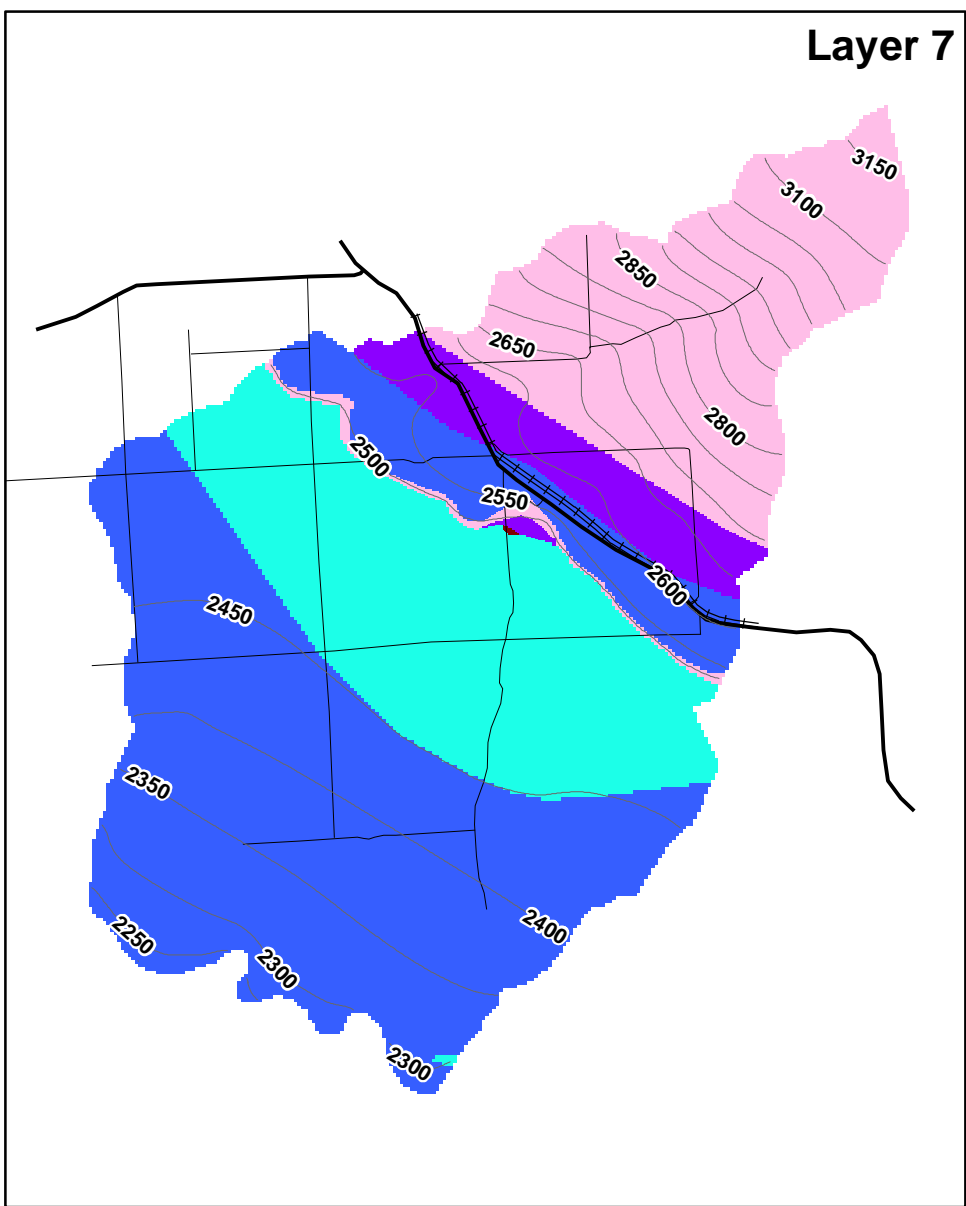
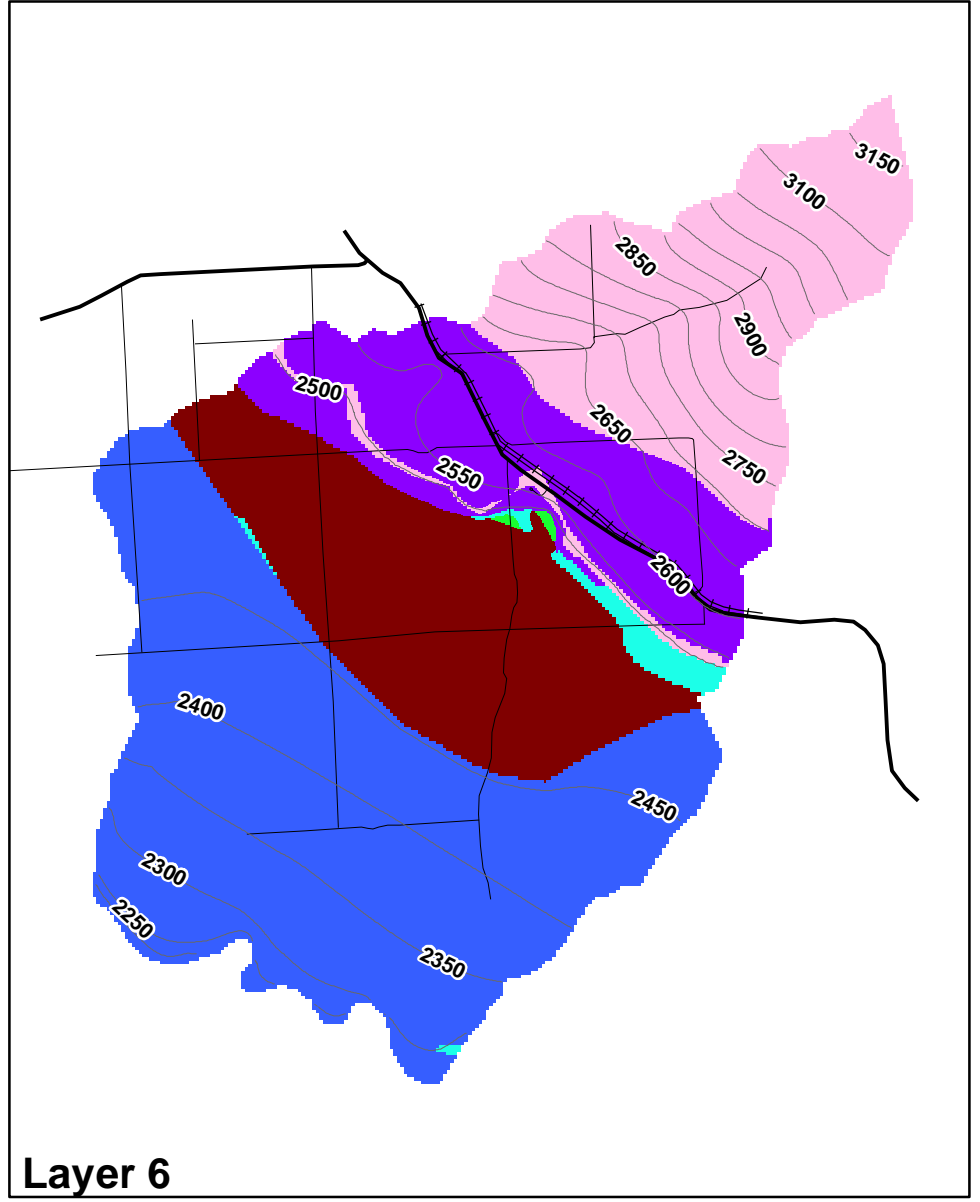
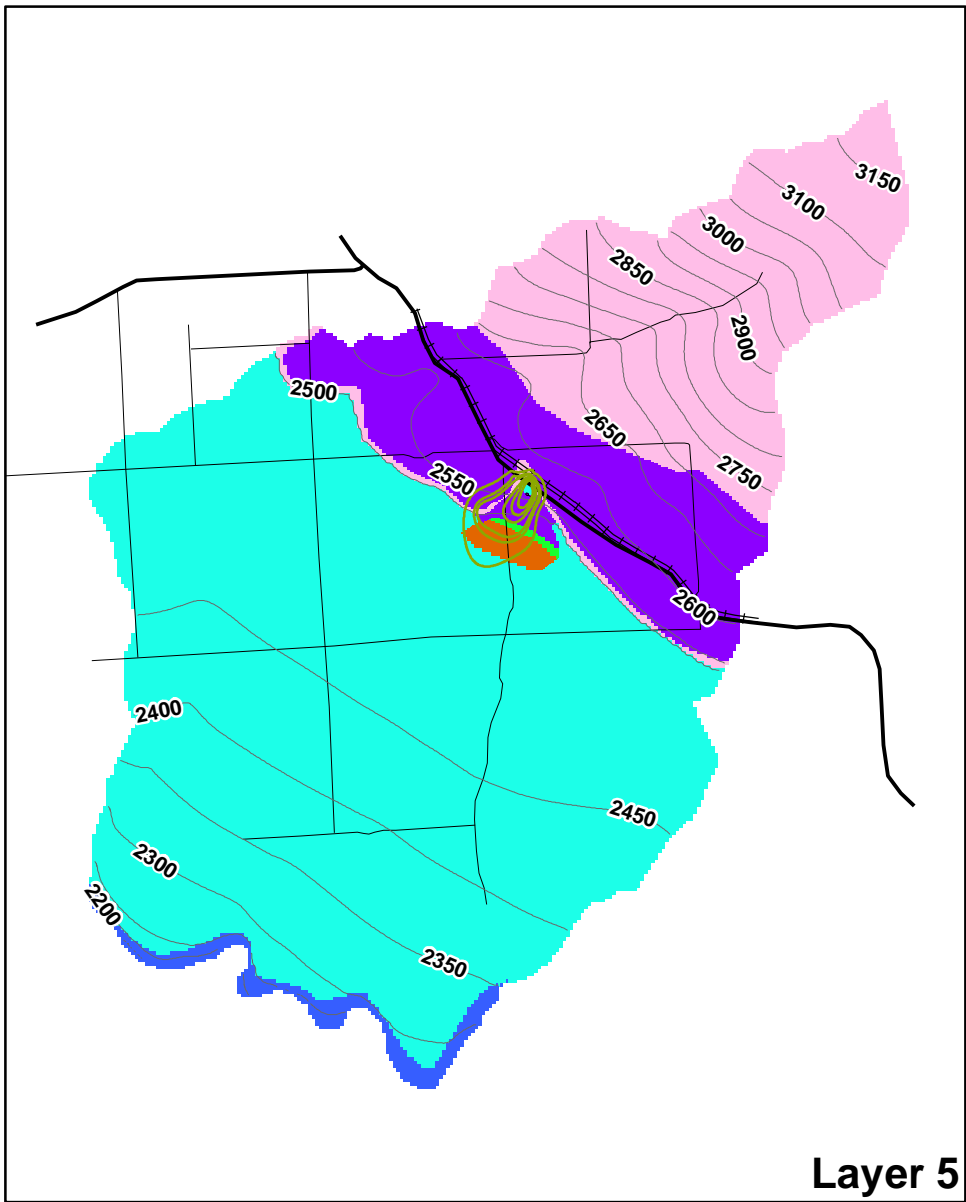


Figure 4-7A
Horizontal Hydraulic Conductivity
Distribution, Layers 1-4
 2019 Groundwater
 Modeling Report
 Grain Handling Facility at Freeman
 Freeman, Washington



Legend

- | | |
|--|--------------------------------------|
| — Simulated Groundwater Elevation (ft) | Hydraulic Conductivity (ft/d) |
| — HWY | 0.001 to 0.01 |
| ≡≡≡ RR | > 0.01 to 0.1 |
| — Road | > 0.1 to 1 |
| Boundary Conditions | > 1 to 5 |
| □ No Flow | > 5 to 25 |
| | > 25 to 50 |
| | > 50 to 75 |
| | > 75 to 100 |
| | > 100 to 125 |

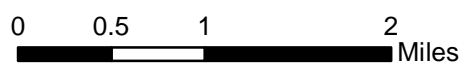
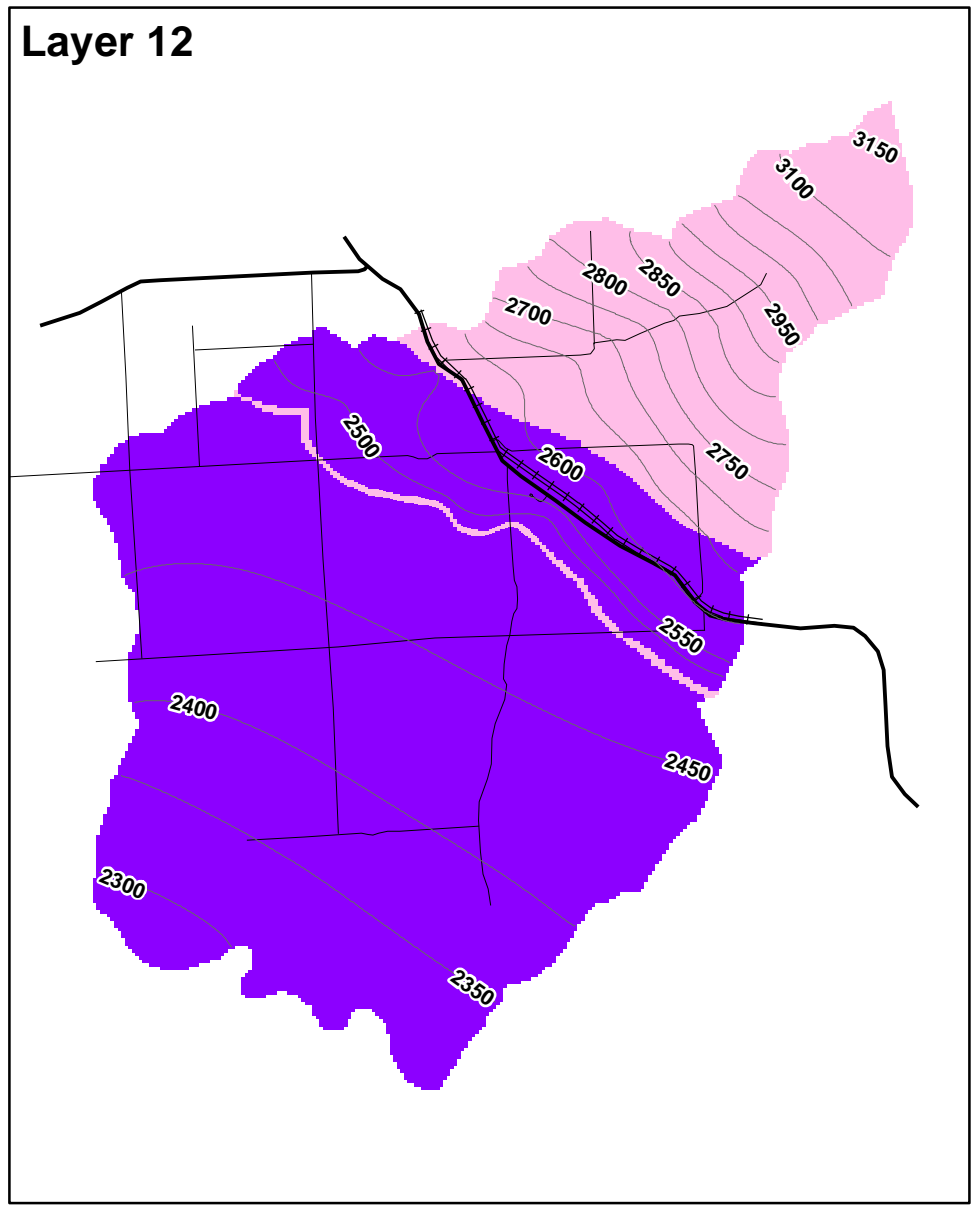
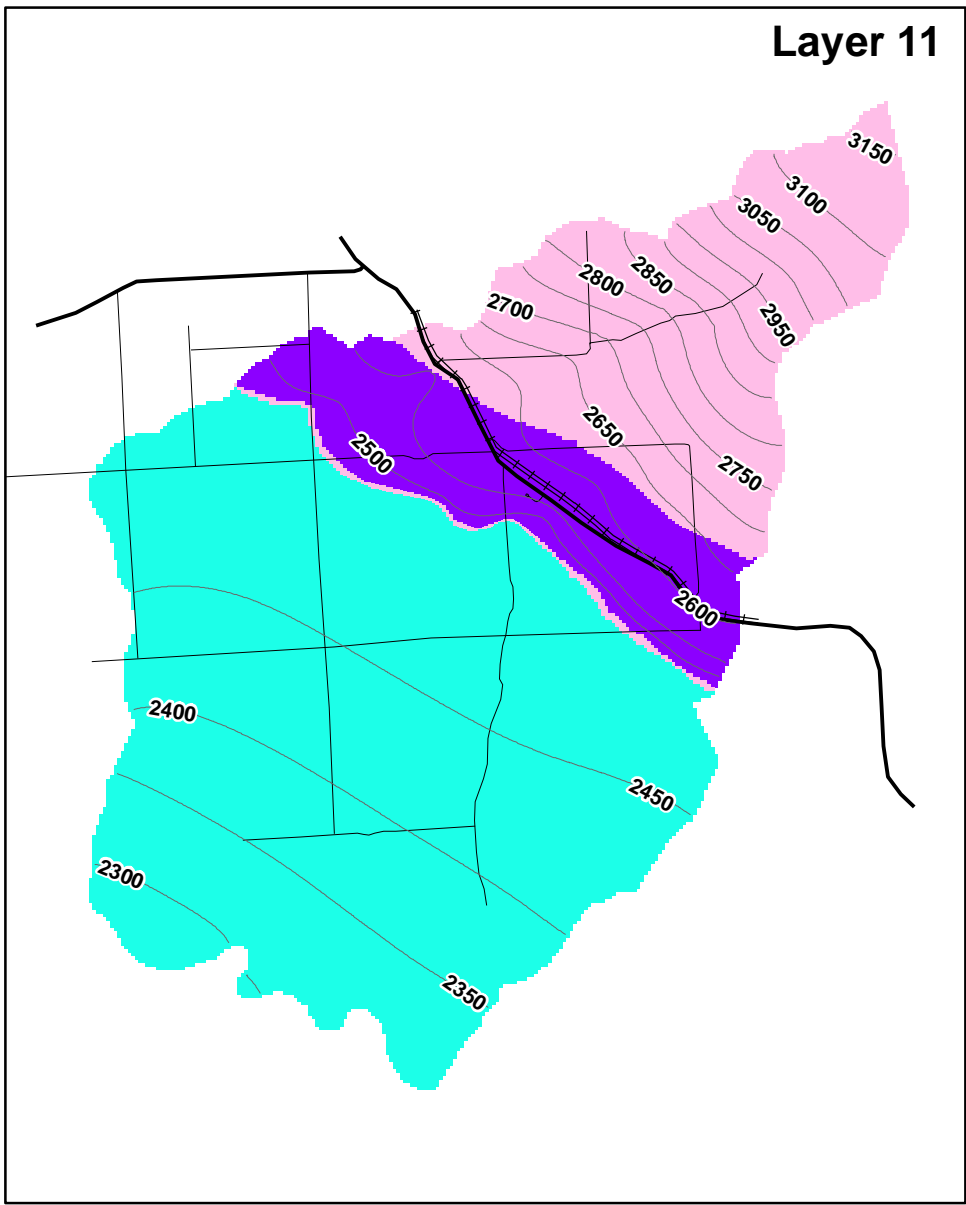
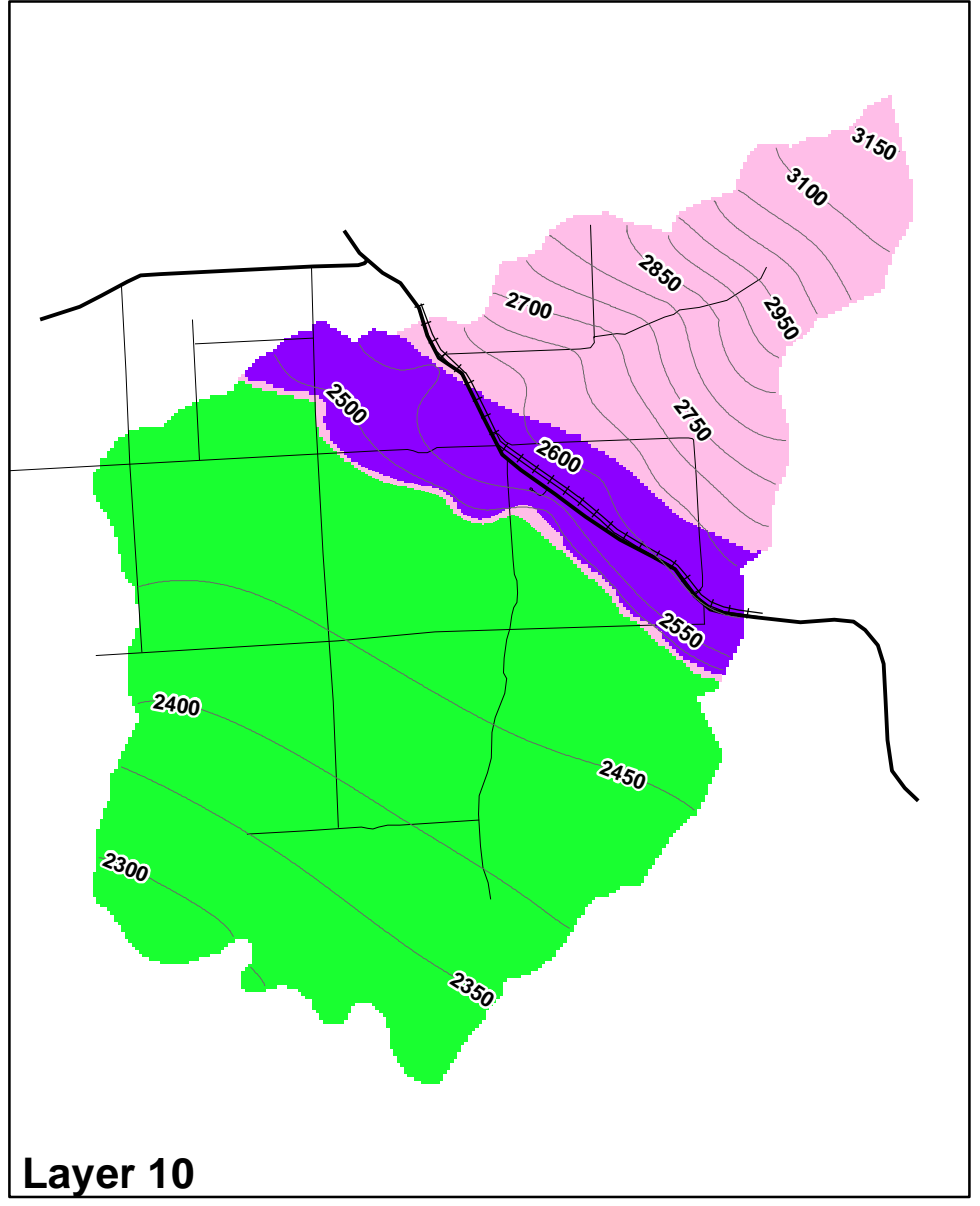
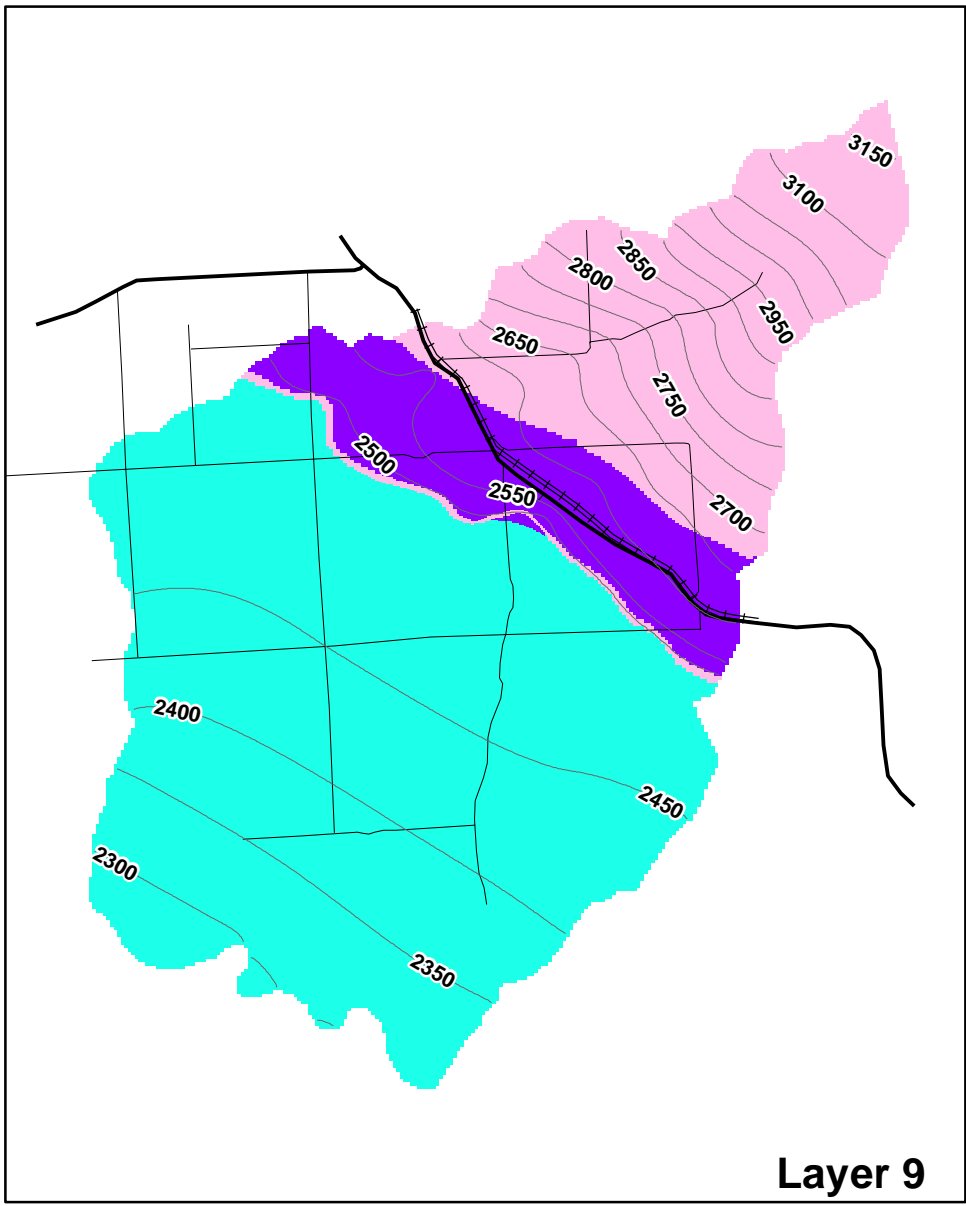


Figure 4-7B
Horizontal Hydraulic Conductivity
Distribution, Layers 5-8
 2019 Groundwater
 Modeling Report
 Grain Handling Facility at Freeman
 Freeman, Washington

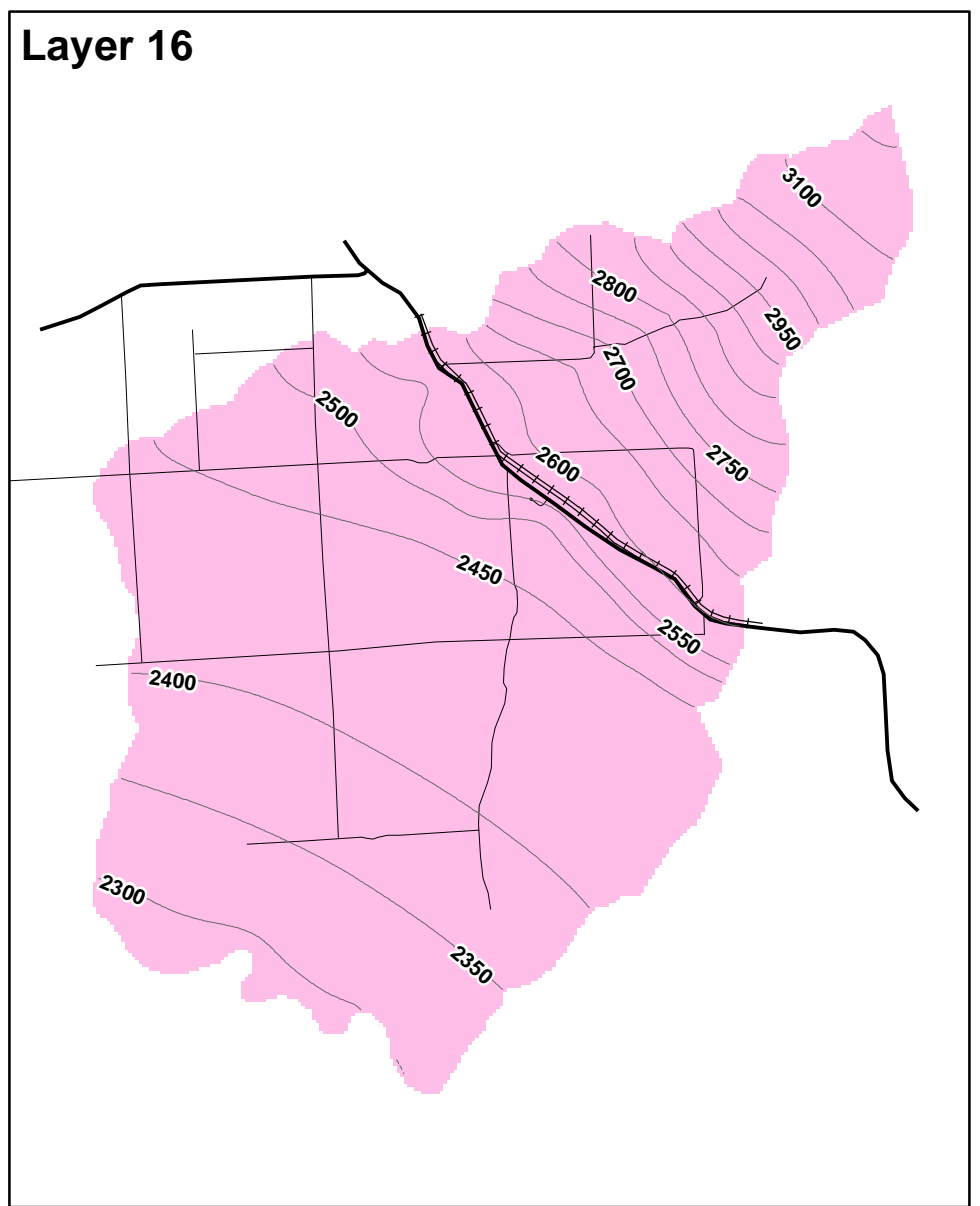
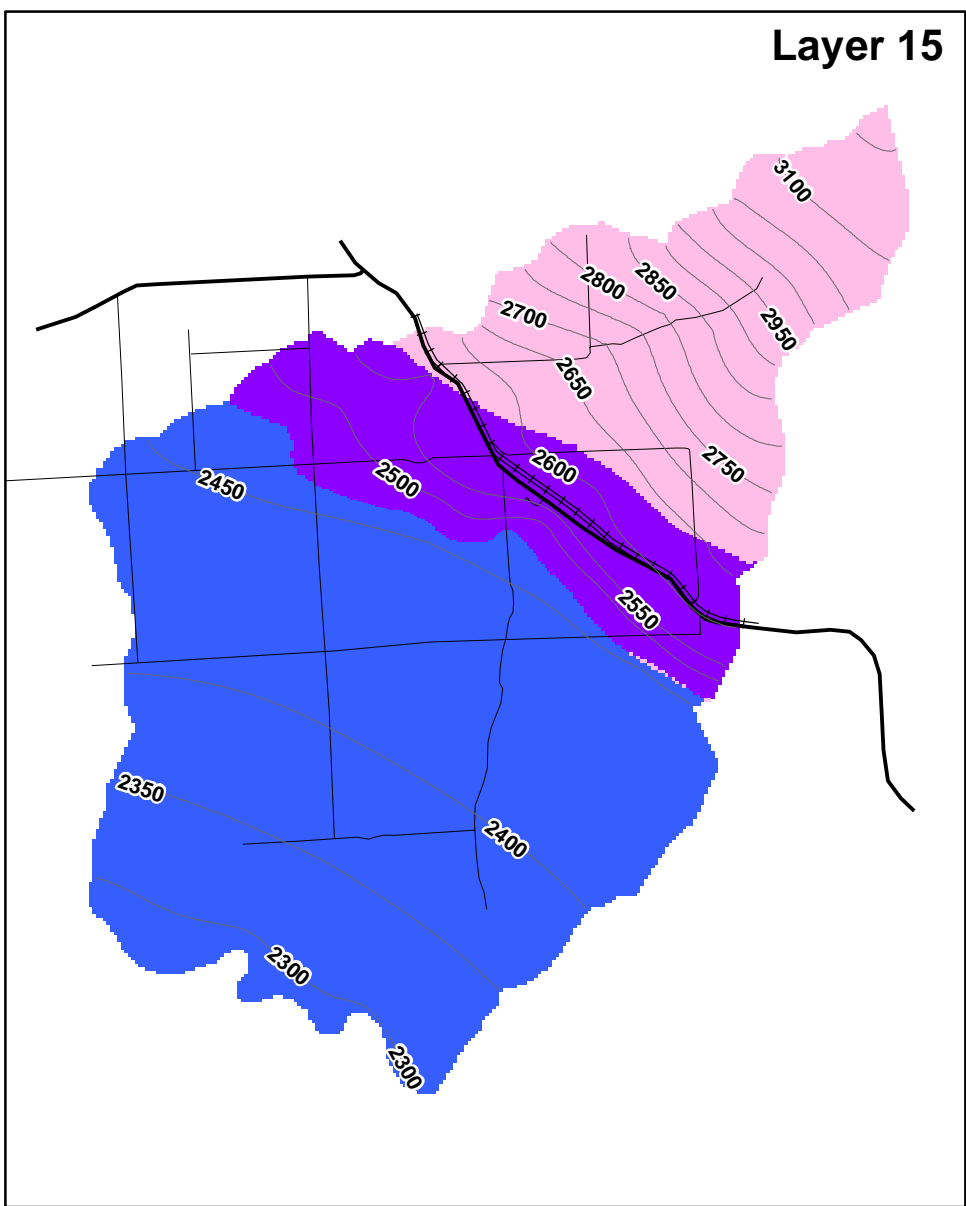
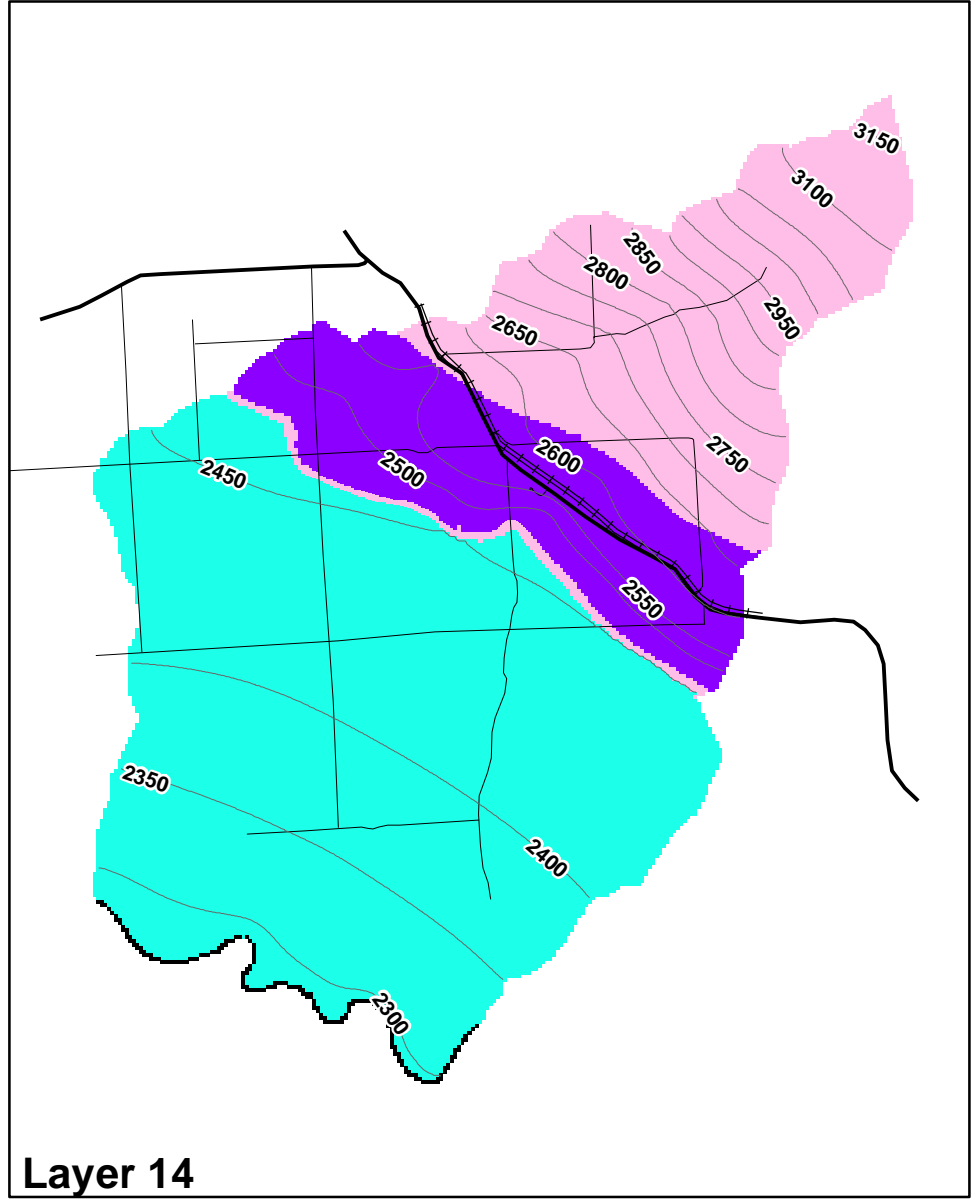
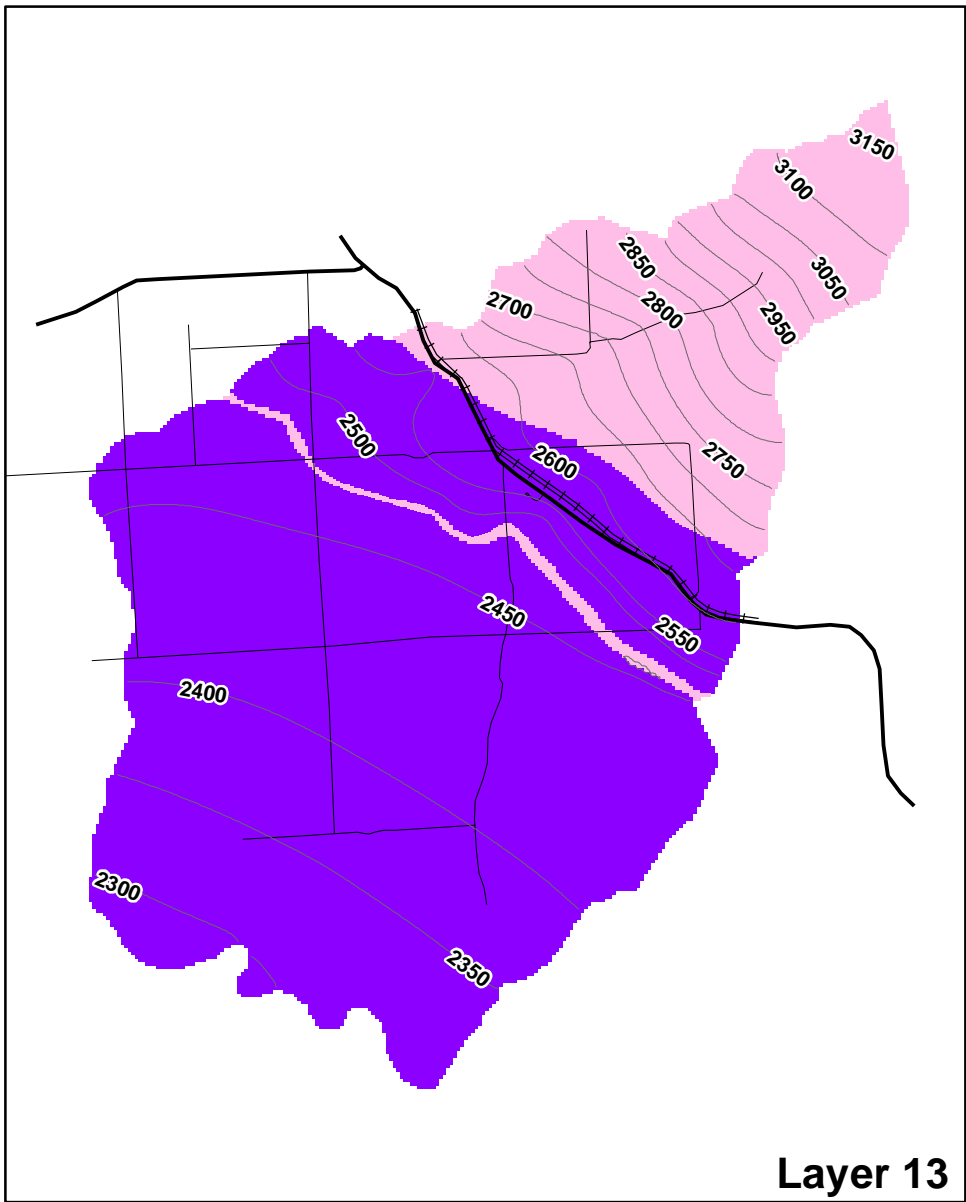


Legend

- Simulated Groundwater Elevation (ft)
 - HWY
 - ≡≡≡ RR
 - Road
- Boundary Conditions**
- No Flow
- Hydraulic Conductivity (ft/d)**
- 0.001 to 0.01
 - > 0.01 to 0.1
 - > 0.1 to 1
 - > 1 to 5
 - > 5 to 25
 - > 25 to 50
 - > 50 to 75
 - > 75 to 100
 - > 100 to 125



Figure 4-6C
Horizontal Hydraulic Conductivity
Distribution, Layers 9-12
 2019 Groundwater
 Modeling Report
 Grain Handling Facility at Freeman
 Freeman, Washington



Legend

- Simulated Groundwater Elevation (ft)
 - HWY
 - ≡≡≡ RR
 - Road
 - Boundary Conditions**
 - No Flow
 - Constant Head
- Hydraulic Conductivity (ft/d)**
- 0.001 to 0.01
 - > 0.01 to 0.1
 - > 0.1 to 1
 - > 1 to 5
 - > 5 to 25
 - > 25 to 50
 - > 50 to 75
 - > 75 to 100
 - > 100 to 125

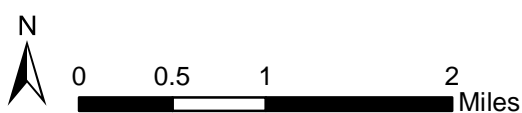
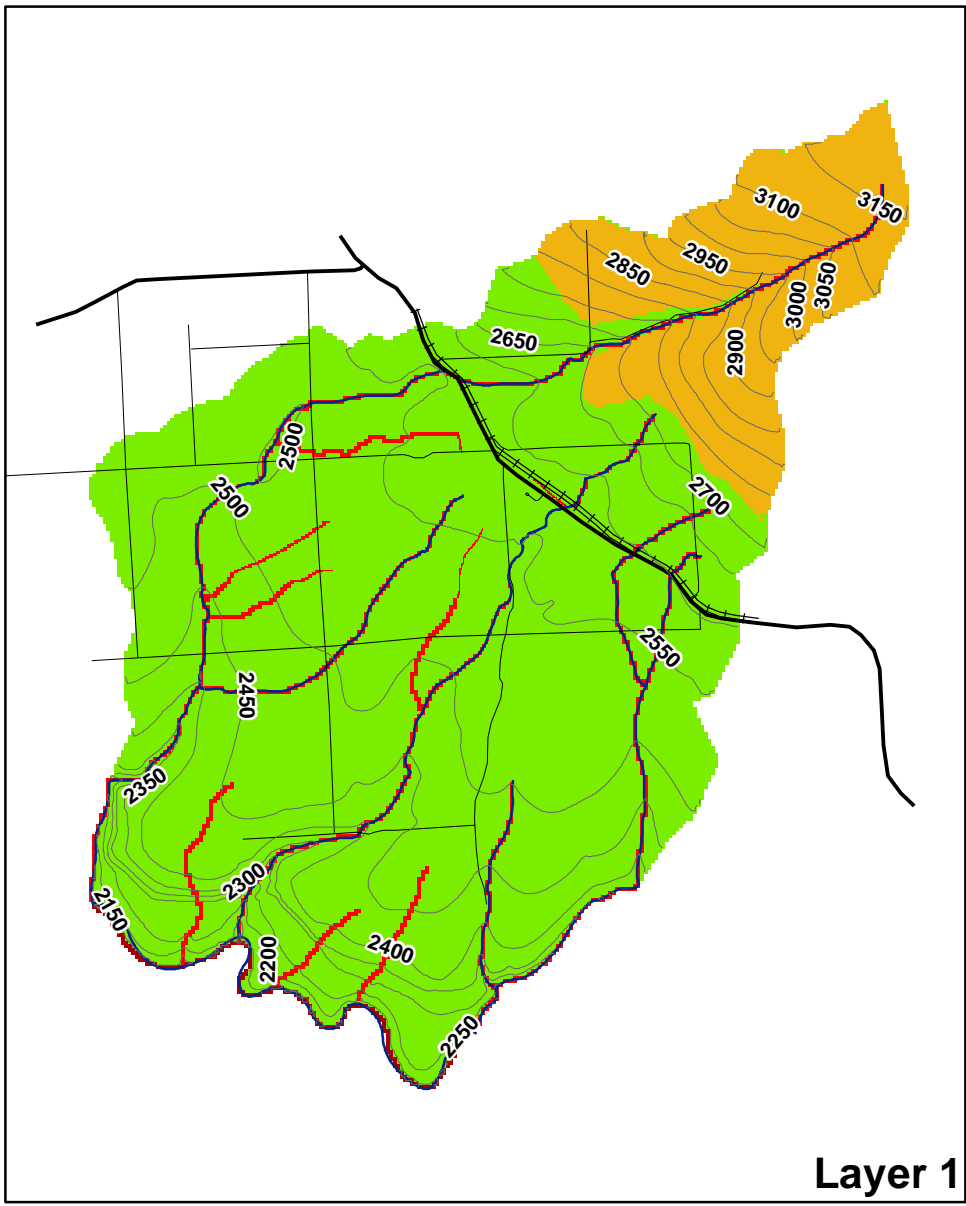
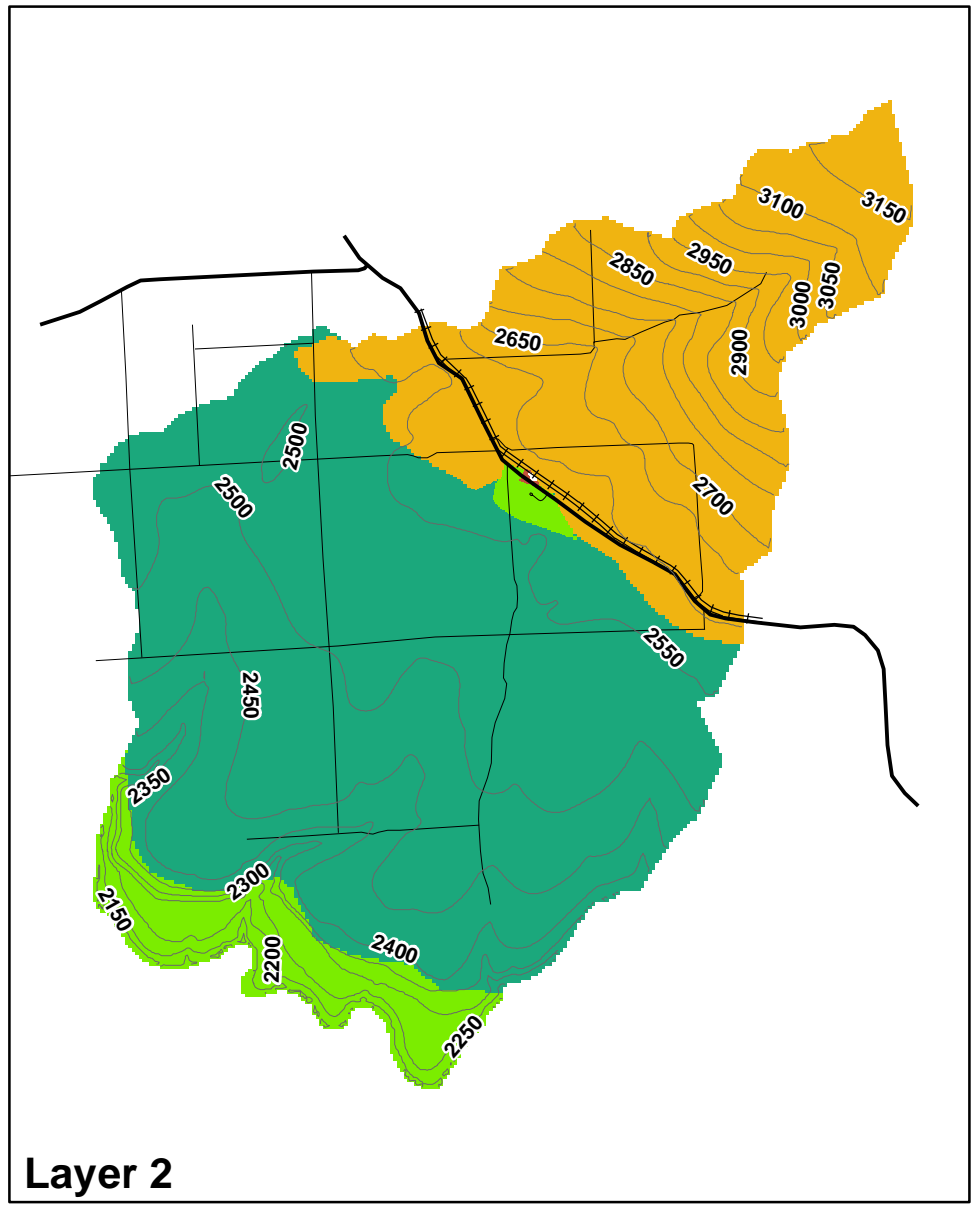


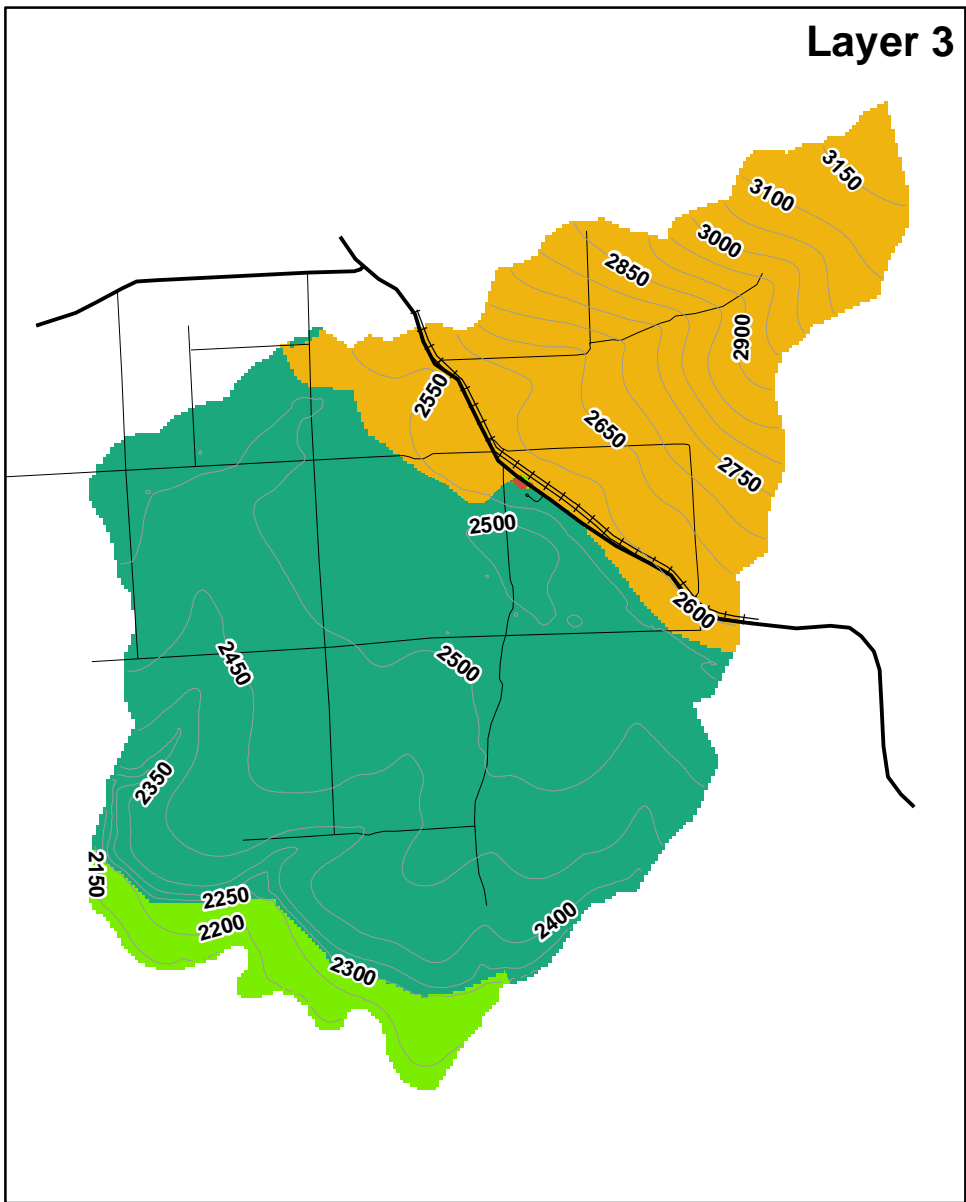
Figure 4-7D
Horizontal Hydraulic Conductivity
Distribution, Layers 13-16
 2019 Groundwater
 Modeling Report
 Grain Handling Facility at Freeman
 Freeman, Washington



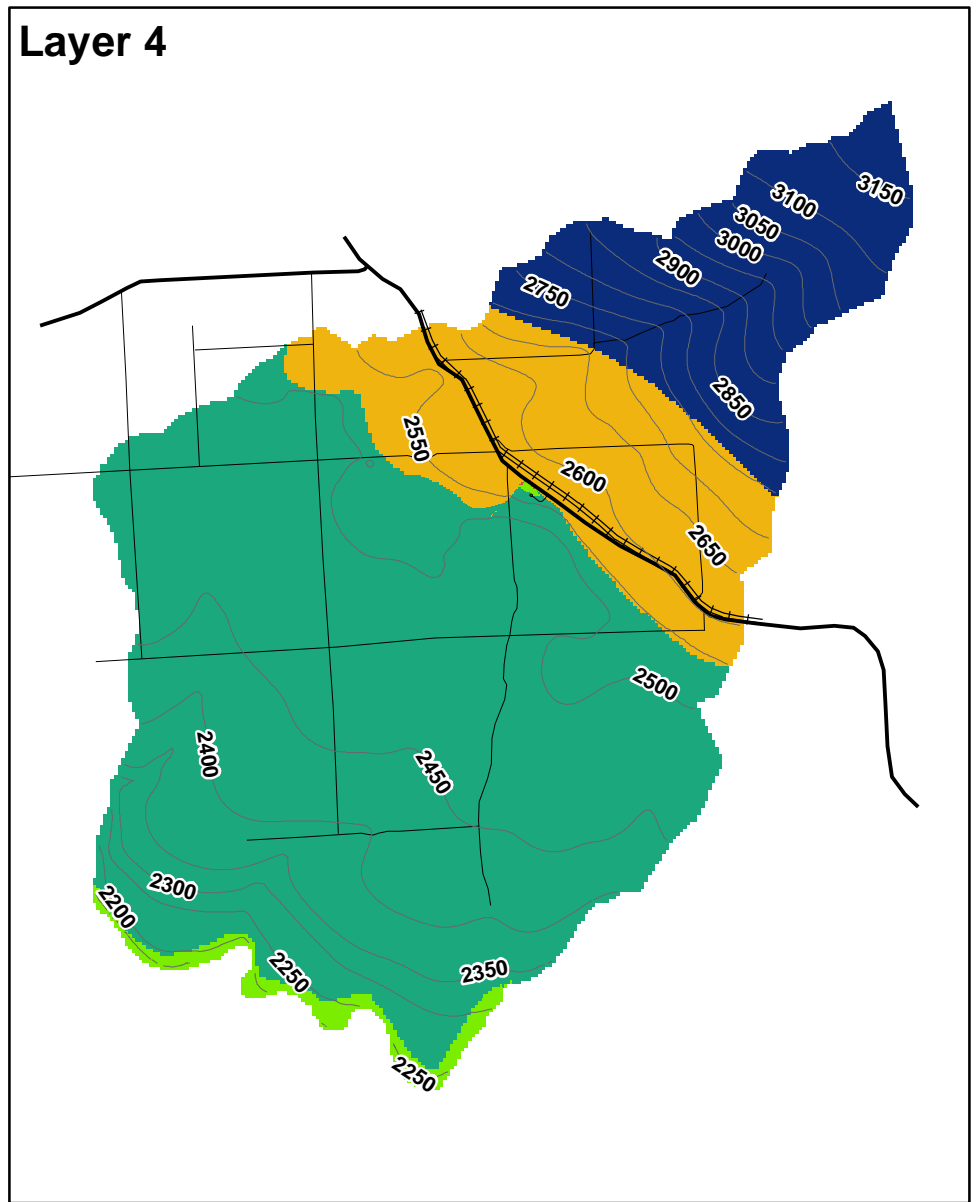
Layer 1



Layer 2



Layer 3



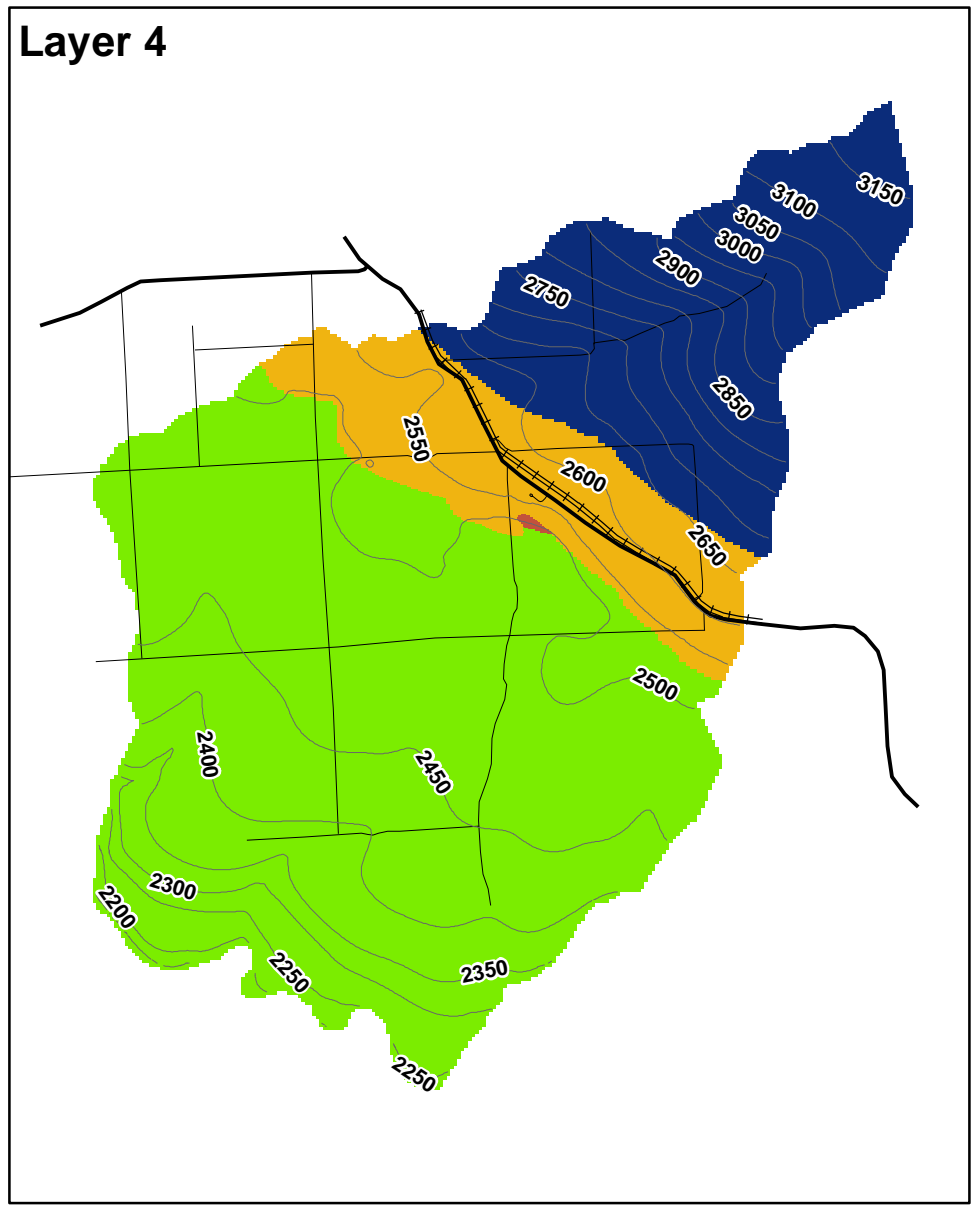
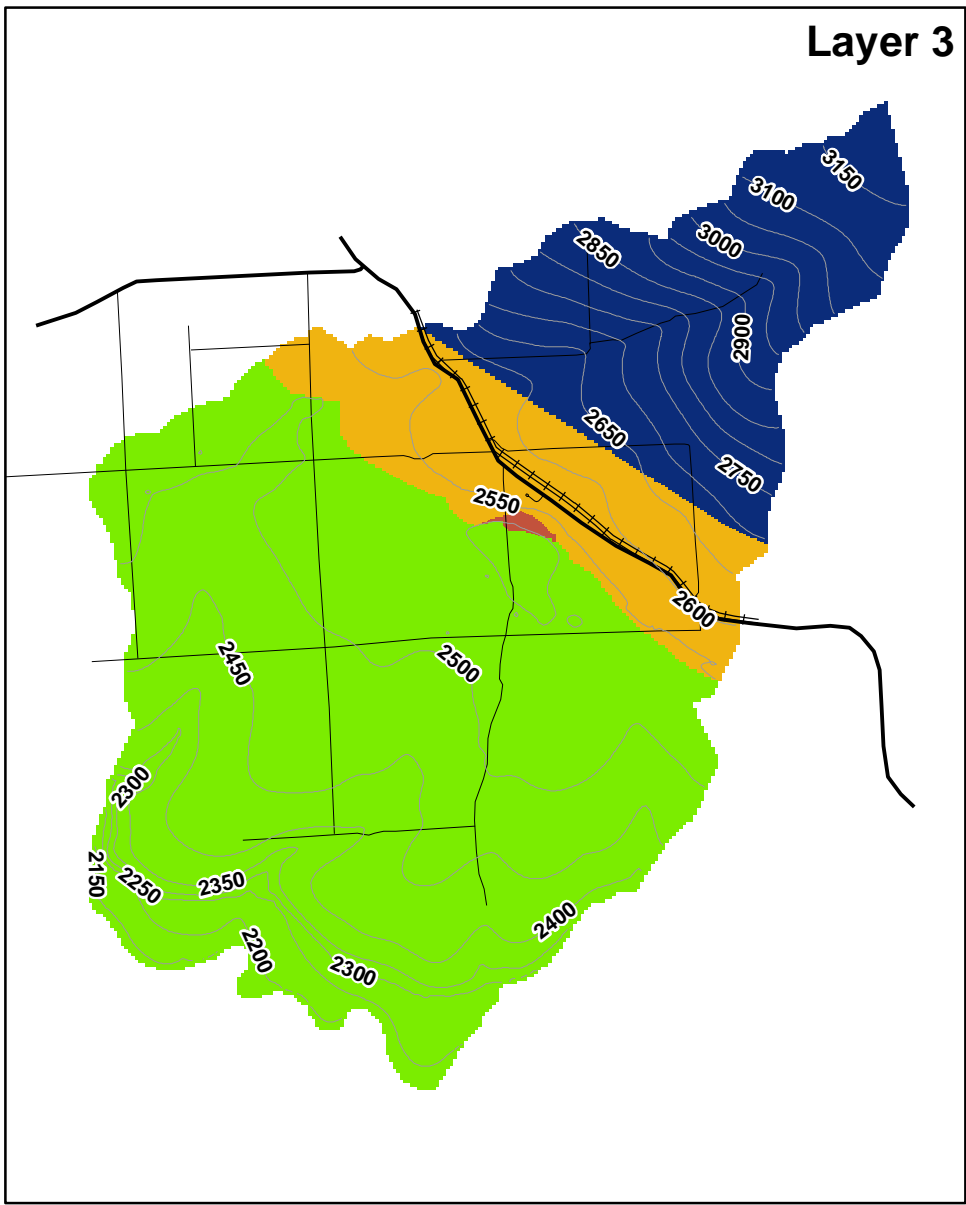
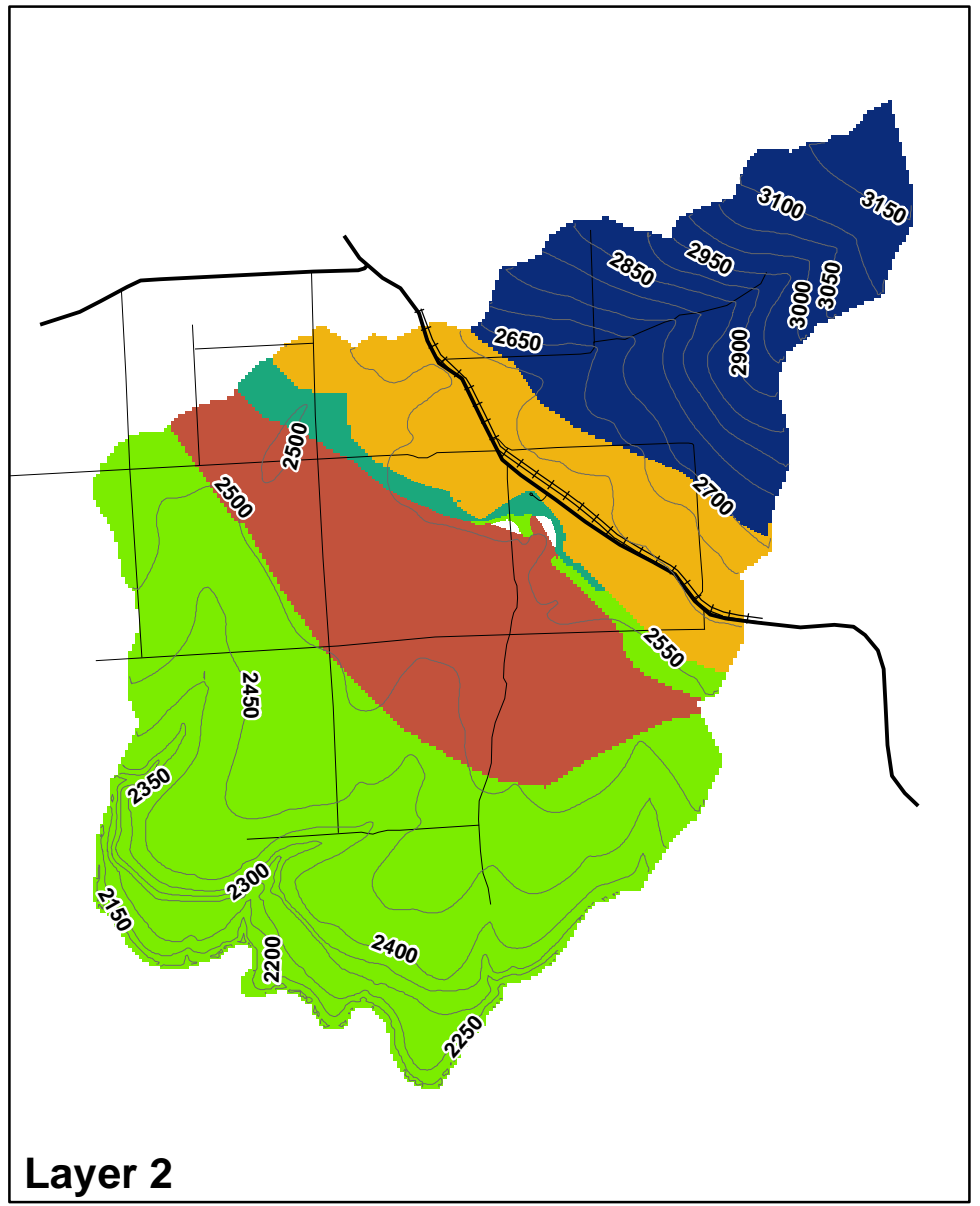
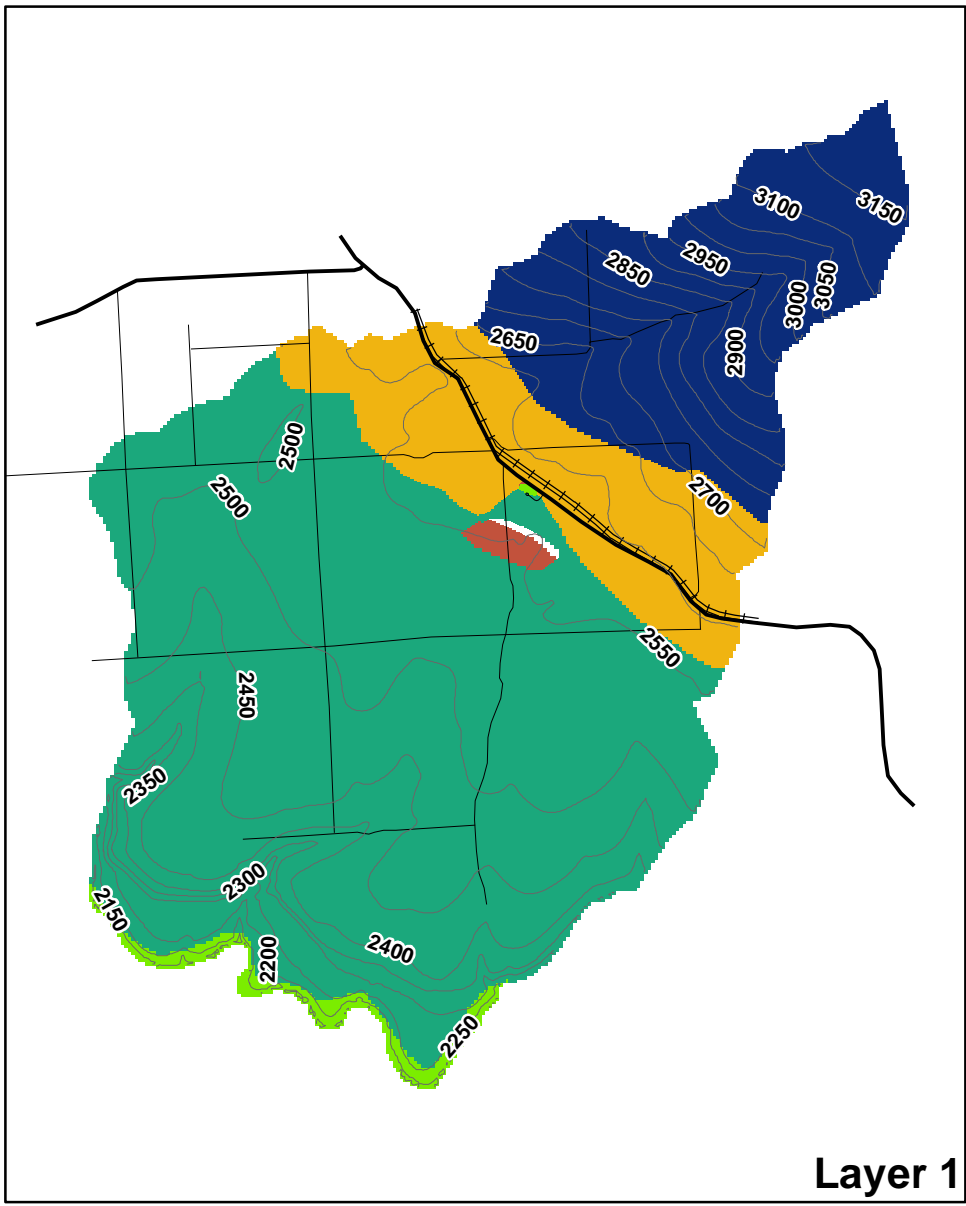
Layer 4

Legend

- | | |
|--|---|
| — Simulated Groundwater Elevation (ft) | Vertical Hydraulic Conductivity (ft/d) |
| — HWY | 0.0001 |
| ≡≡≡ RR | > 0.0001 to 0.006 |
| — Road | > 0.006 to 0.02 |
| — Streams | > 0.02 to 0.05 |
| Boundary Conditions | > 0.05 to 1.25 |
| ■ Drain | |
| ■ River | |
| □ No Flow | |



Figure 4-8A
Horizontal Hydraulic Conductivity
Distribution, Layers 1-4
 2019 Groundwater
 Modeling Report
 Grain Handling Facility at Freeman
 Freeman, Washington

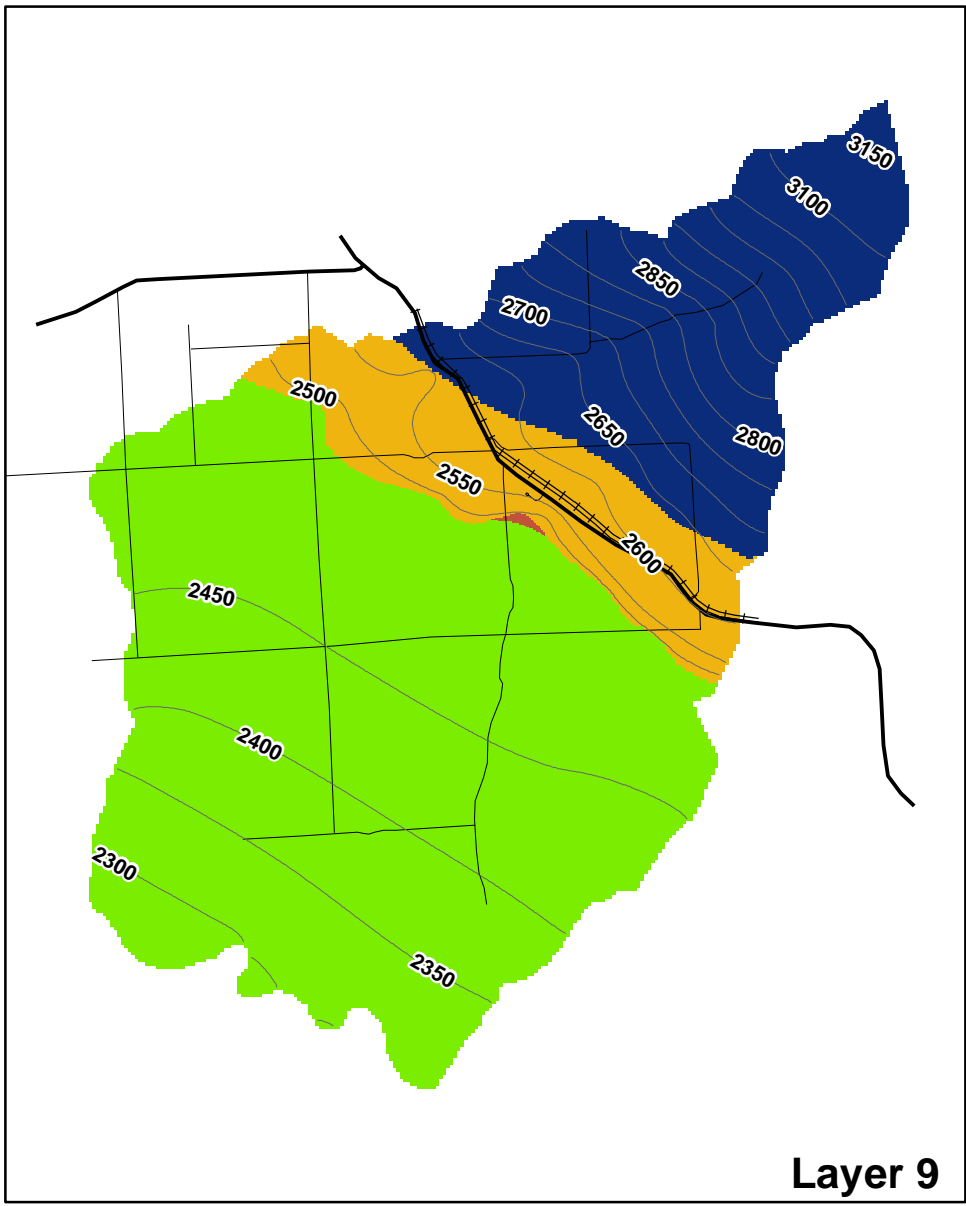


Legend

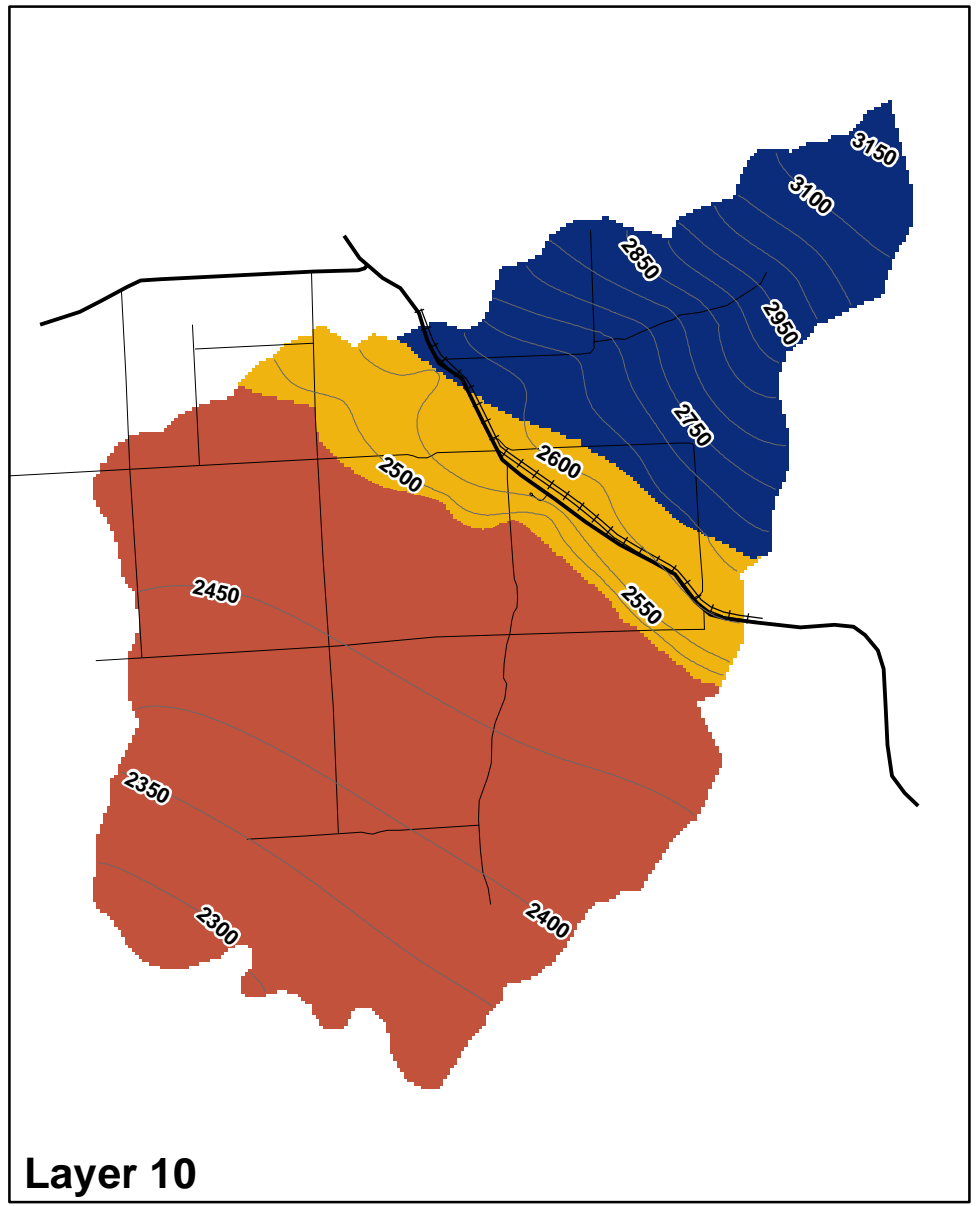
- | | |
|--|---|
| — Simulated Groundwater Elevation (ft) | Vertical Hydraulic Conductivity (ft/d) |
| — HWY | 0.0001 |
| ≡≡≡ RR | > 0.0001 to 0.006 |
| — Road | > 0.006 to 0.02 |
| Boundary Conditions | > 0.02 to 0.05 |
| □ No Flow | > 0.05 to 1.25 |



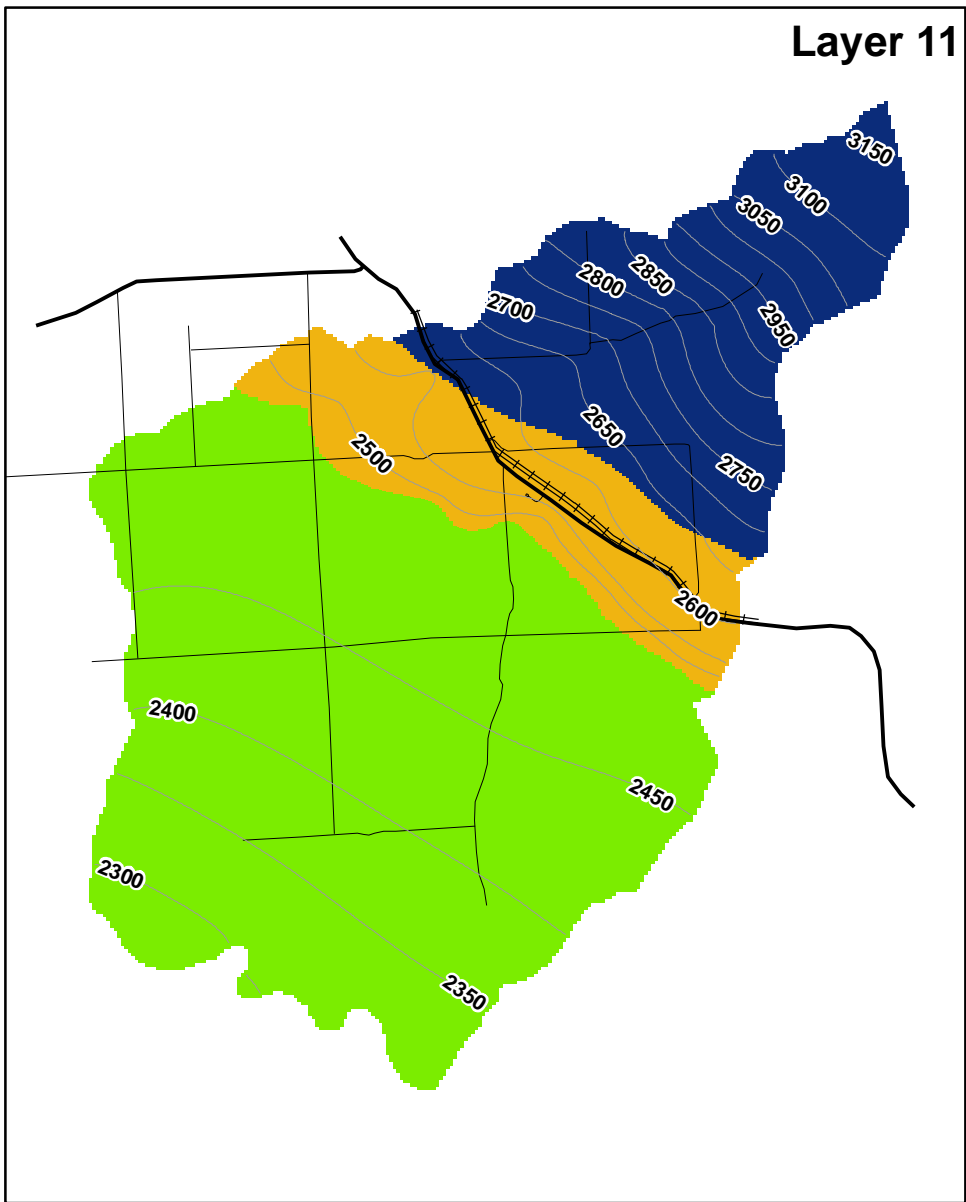
Figure 4-7B
Vertical Hydraulic Conductivity
Distribution, Layers 5-8
 2019 Groundwater
 Modeling Report
 Grain Handling Facility at Freeman
 Freeman, Washington



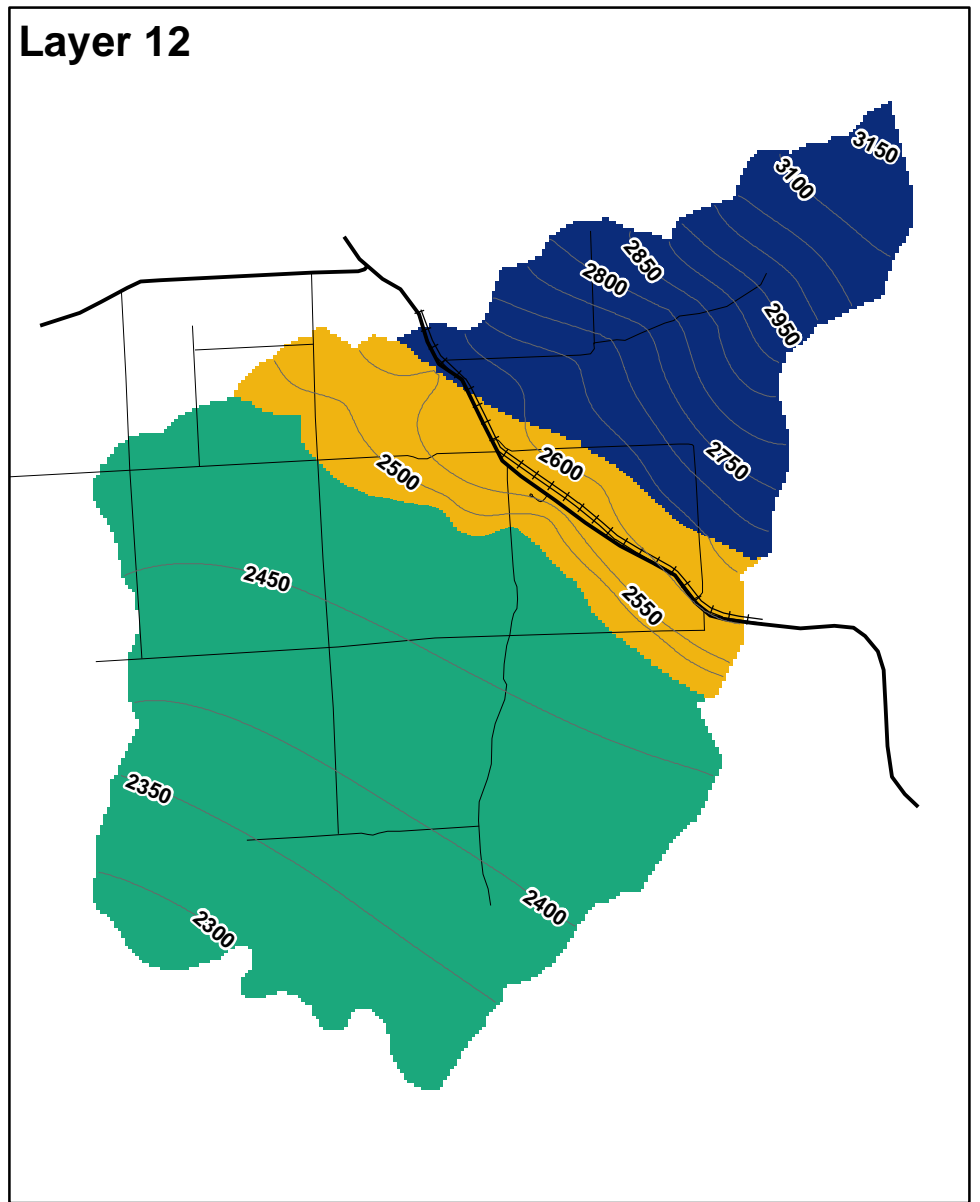
Layer 9



Layer 10



Layer 11



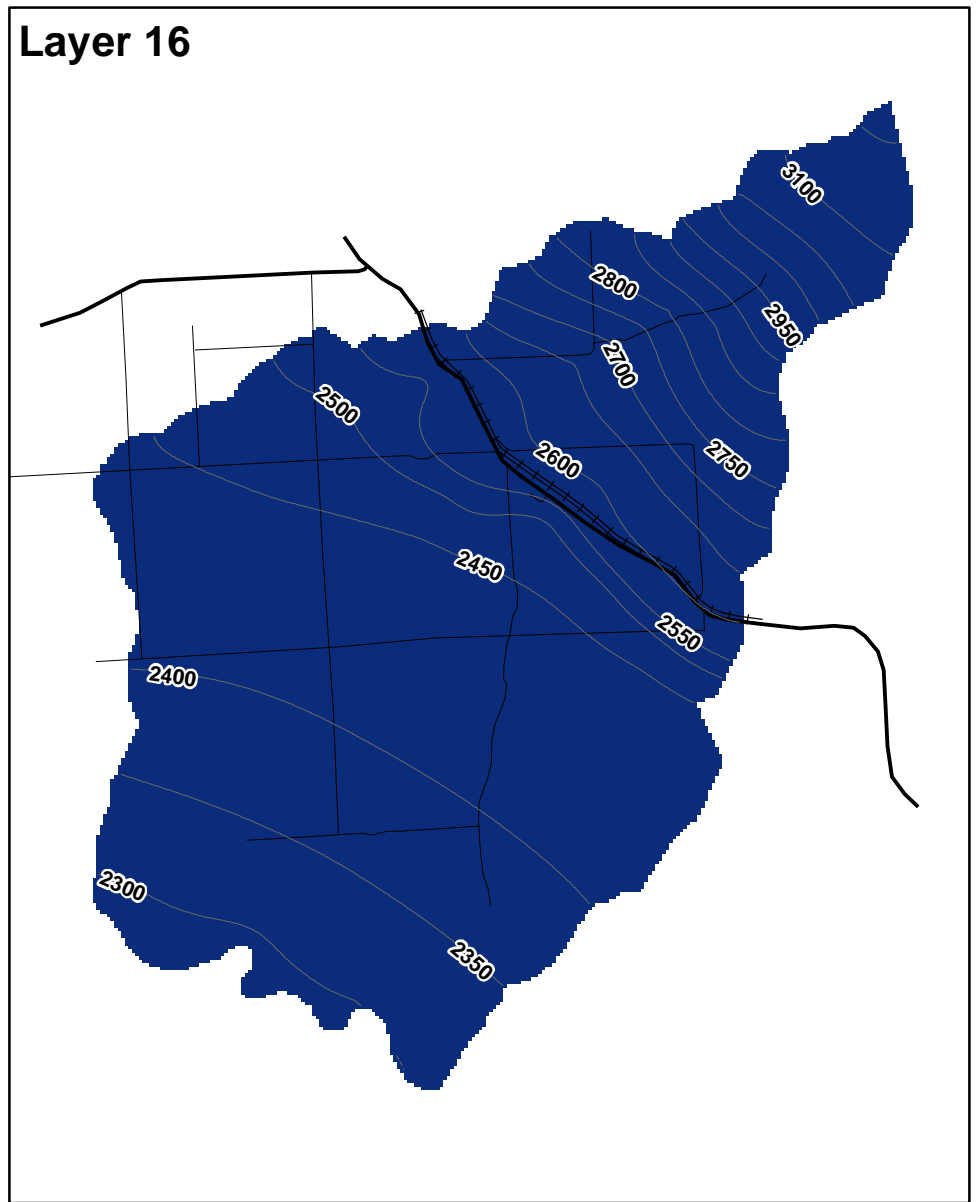
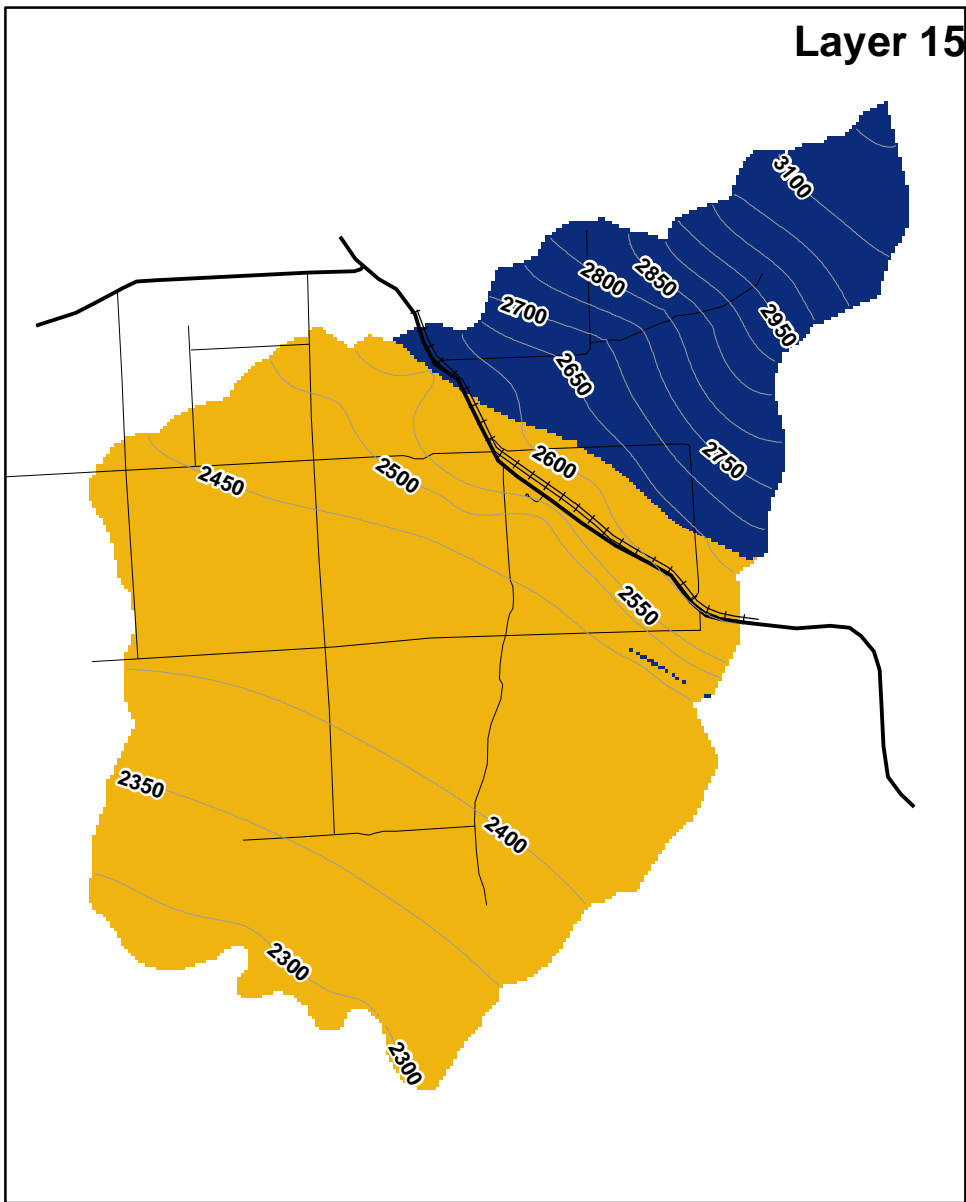
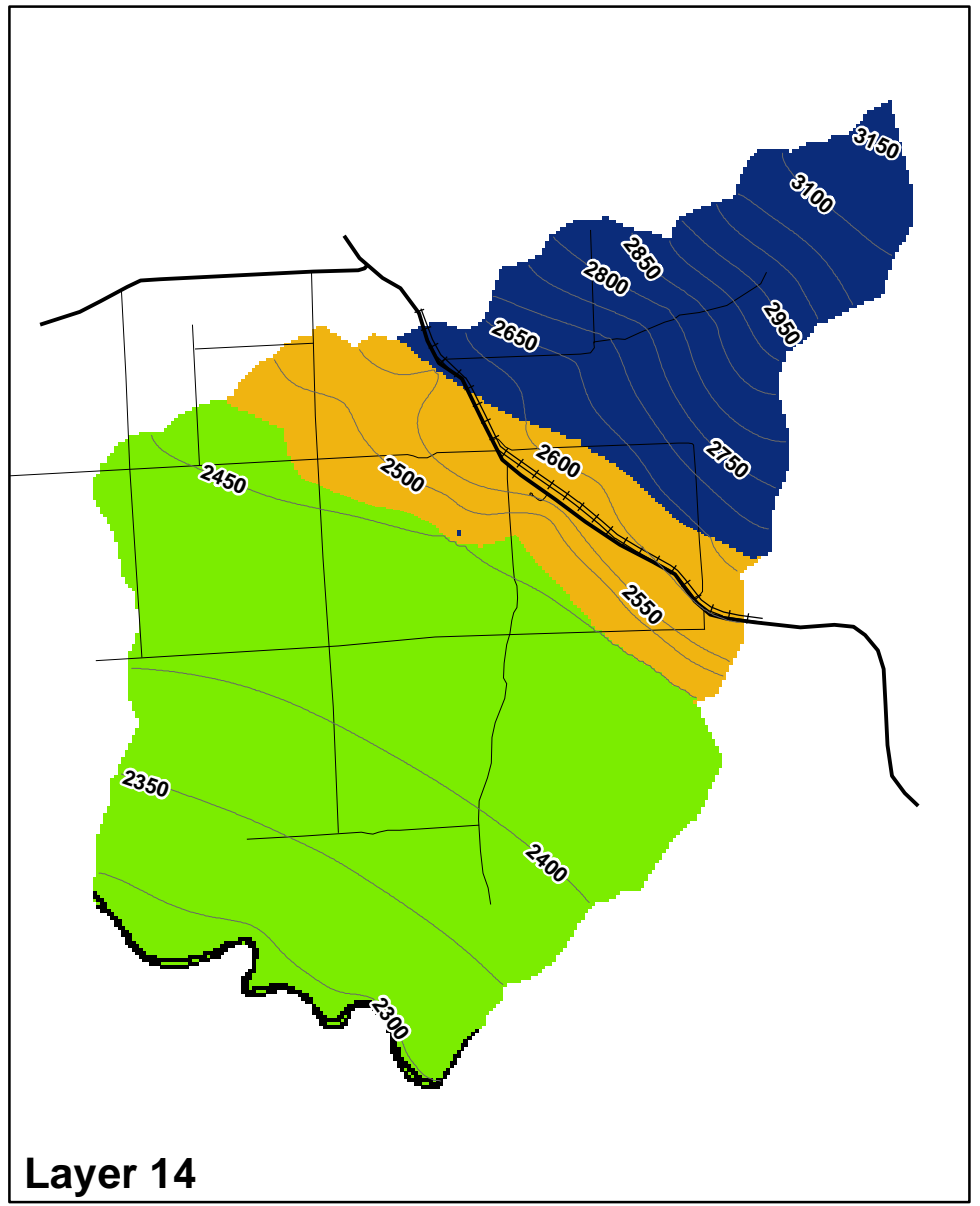
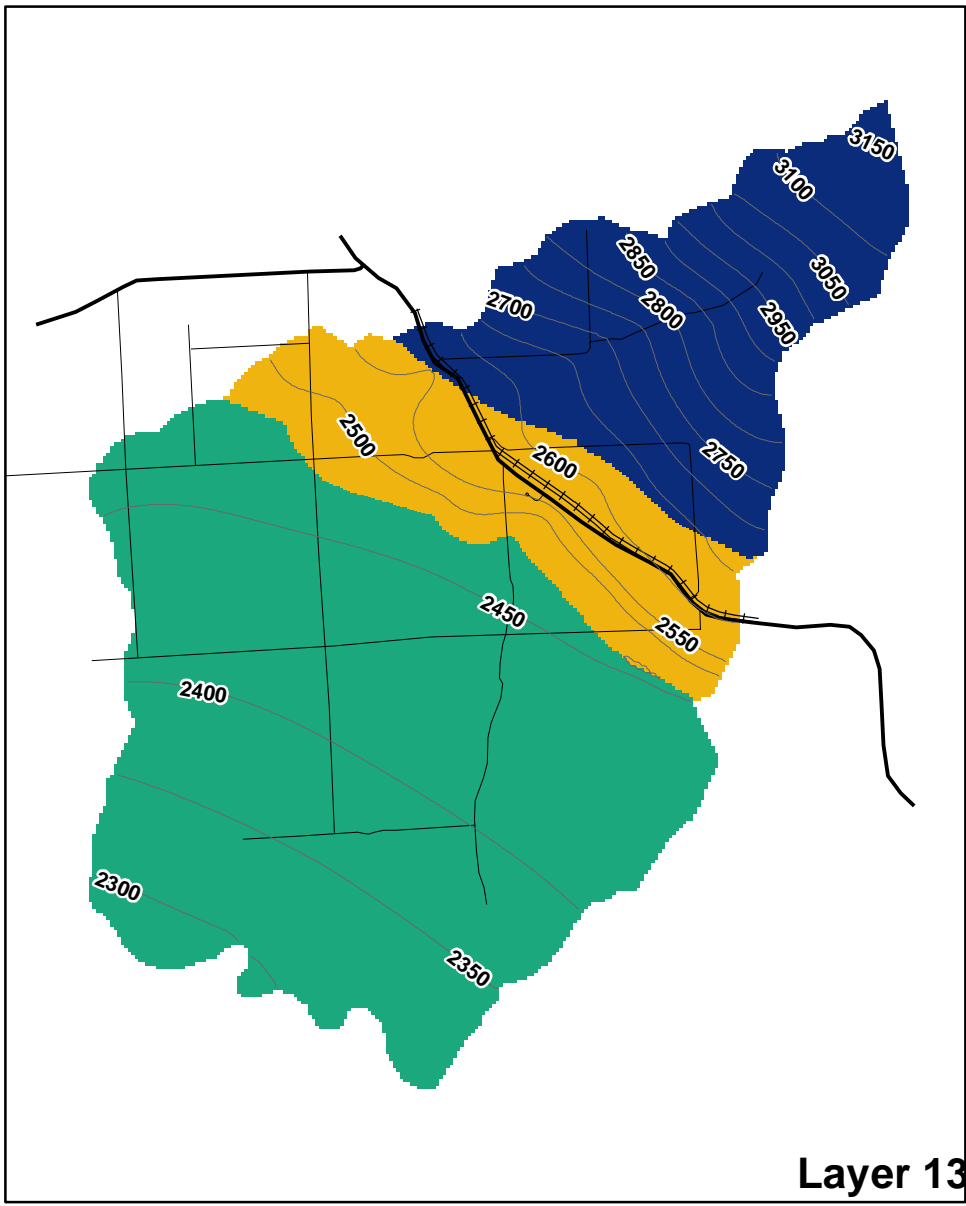
Layer 12

Legend

- Simulated Groundwater Elevation (ft)
 - HWY
 - RR
 - Road
 - Boundary Conditions**
 - No Flow
- | Vertical Hydraulic Conductivity (ft/d) | |
|--|-------------------|
| | 0.0001 |
| | > 0.0001 to 0.006 |
| | > 0.006 to 0.02 |
| | > 0.02 to 0.05 |
| | > 0.05 to 1.25 |



Figure 4-7C
Vertical Hydraulic Conductivity
Distribution, Layers 9-12
 2019 Groundwater
 Modeling Report
 Grain Handling Facility at Freeman
 Freeman, Washington



Legend

- | | |
|--|---|
| — Simulated Groundwater Elevation (ft) | Vertical Hydraulic Conductivity (ft/d) |
| — HWY | ■ 0.0001 |
| ≡≡≡ RR | ■ > 0.0001 to 0.006 |
| — Road | ■ > 0.006 to 0.02 |
| Boundary Conditions | ■ > 0.02 to 0.05 |
| □ No Flow | ■ > 0.05 to 1.25 |
| ■ Constant Head | |



Figure 4-7D
Vertical Hydraulic Conductivity
Distribution, Layers 13-16
 2019 Groundwater
 Modeling Report
 Grain Handling Facility at Freeman
 Freeman, Washington

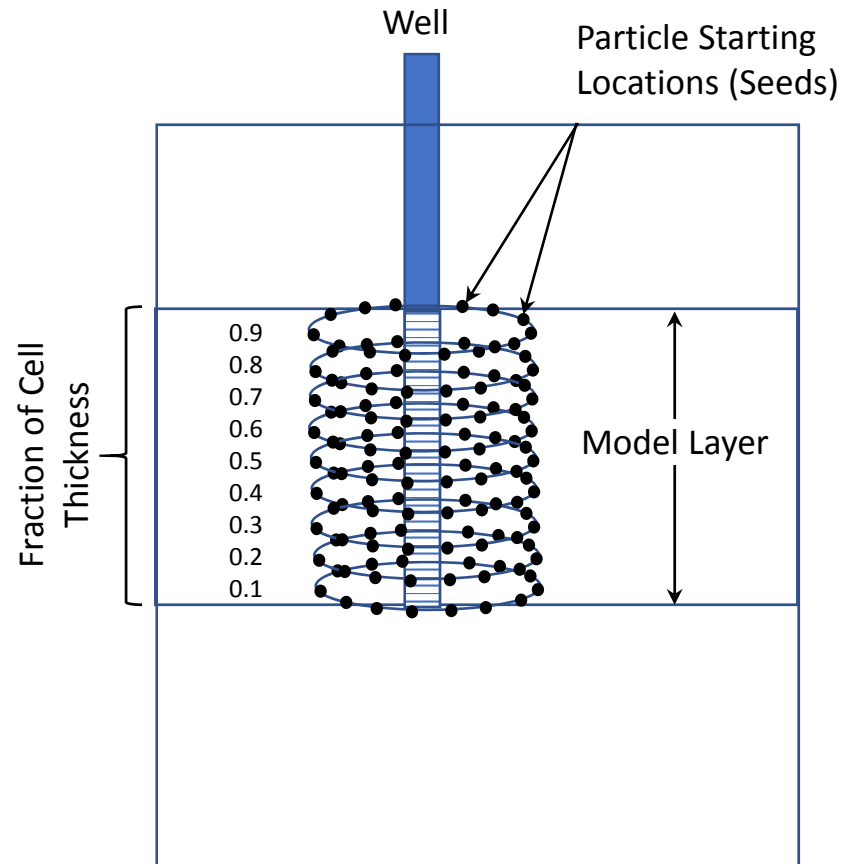


Legend

- ⊕ Monitoring Wells
- Pumping Wells**
- ⬠ Injection
- Extraction
- School Supply



Figure 5-1
Remedial Scenario
Well Locations
 2019 Groundwater
 Modeling Report
 Grain Handling Facility at Freeman
 Freeman, Washington



Notes:

The diagram illustrates the particle seeding or starting locations for reverse particle tracking

- 9 rings of particles per layer, surrounding well
- 24 particles per ring
- 15-ft radius
- 216 particles per layer

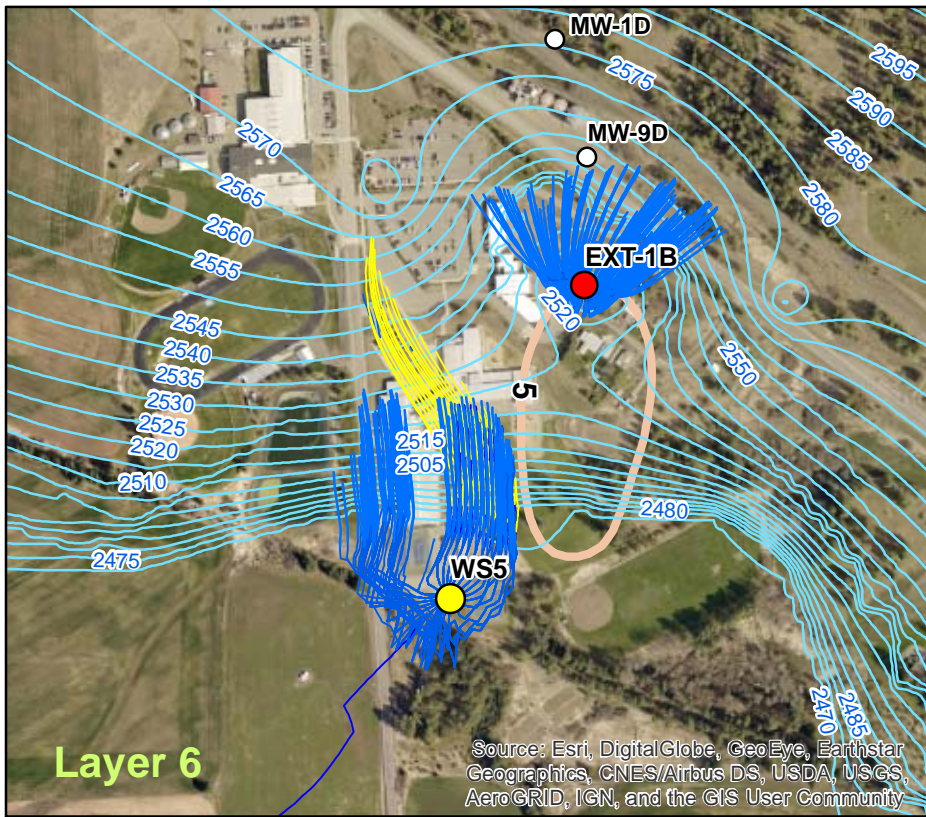
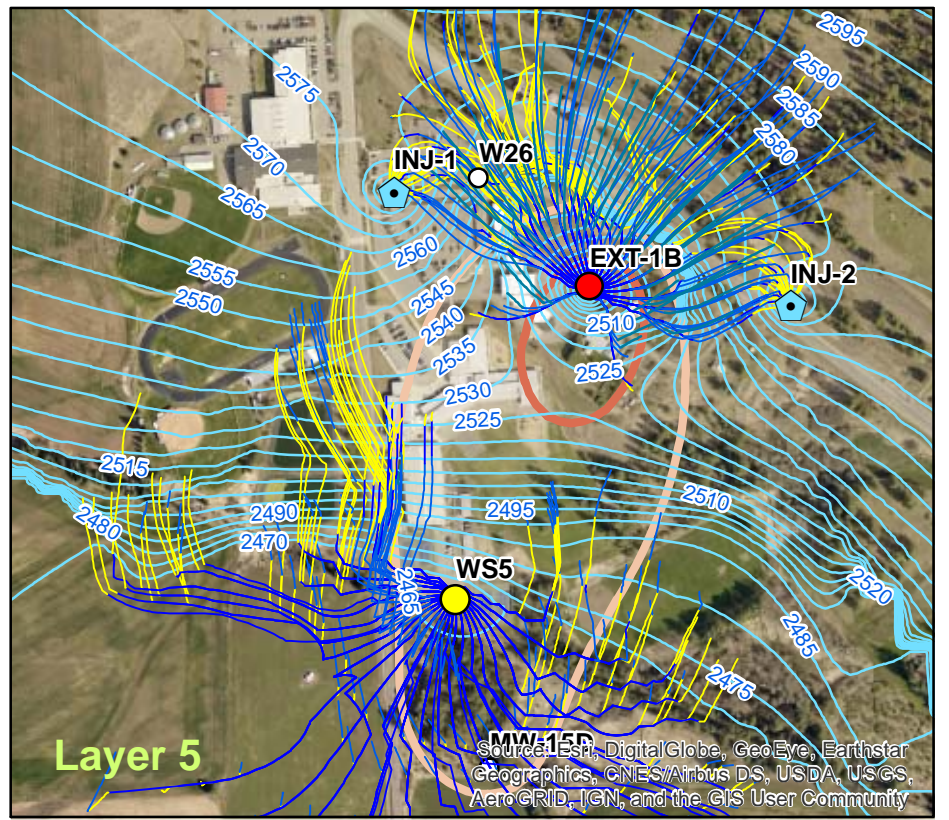
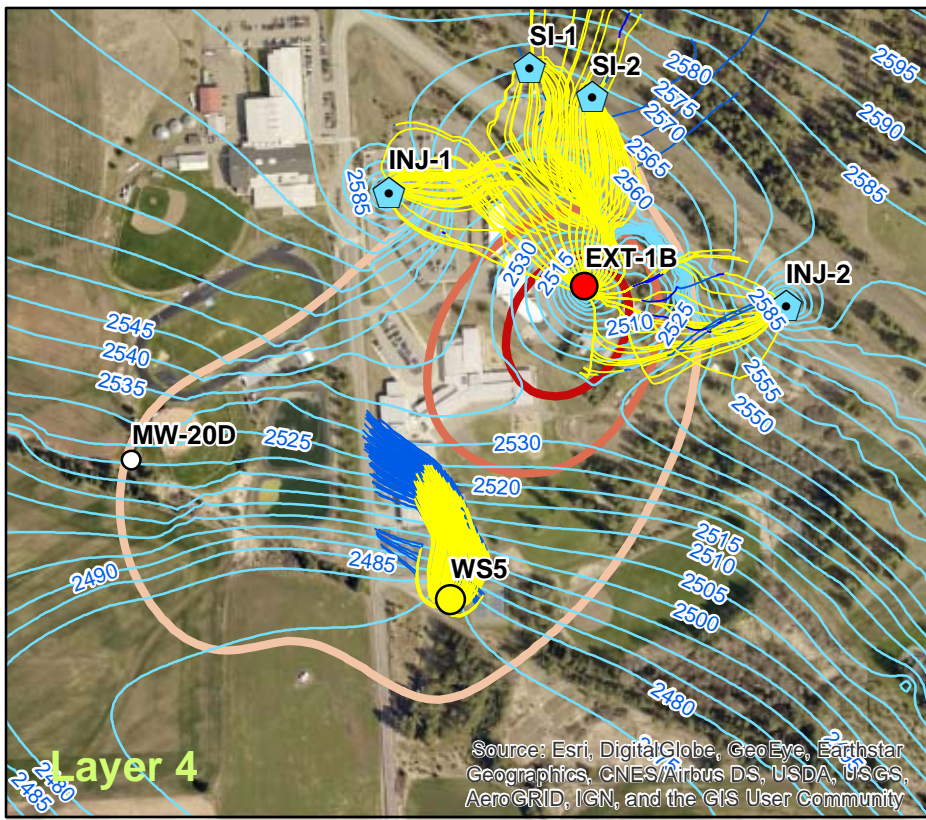
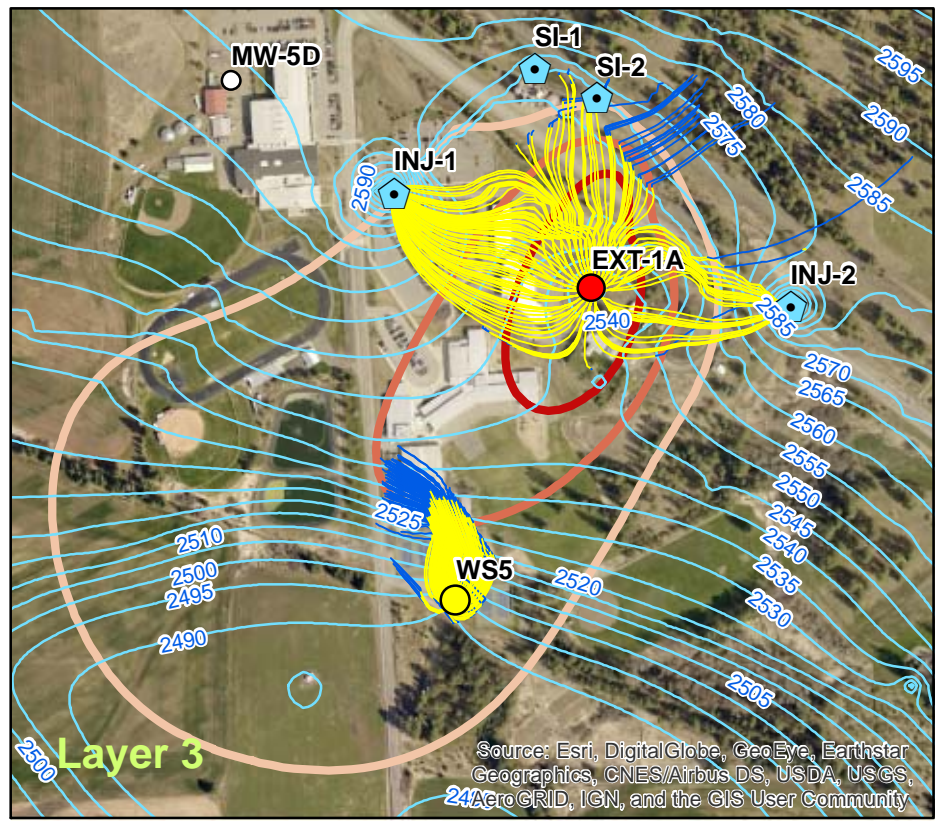
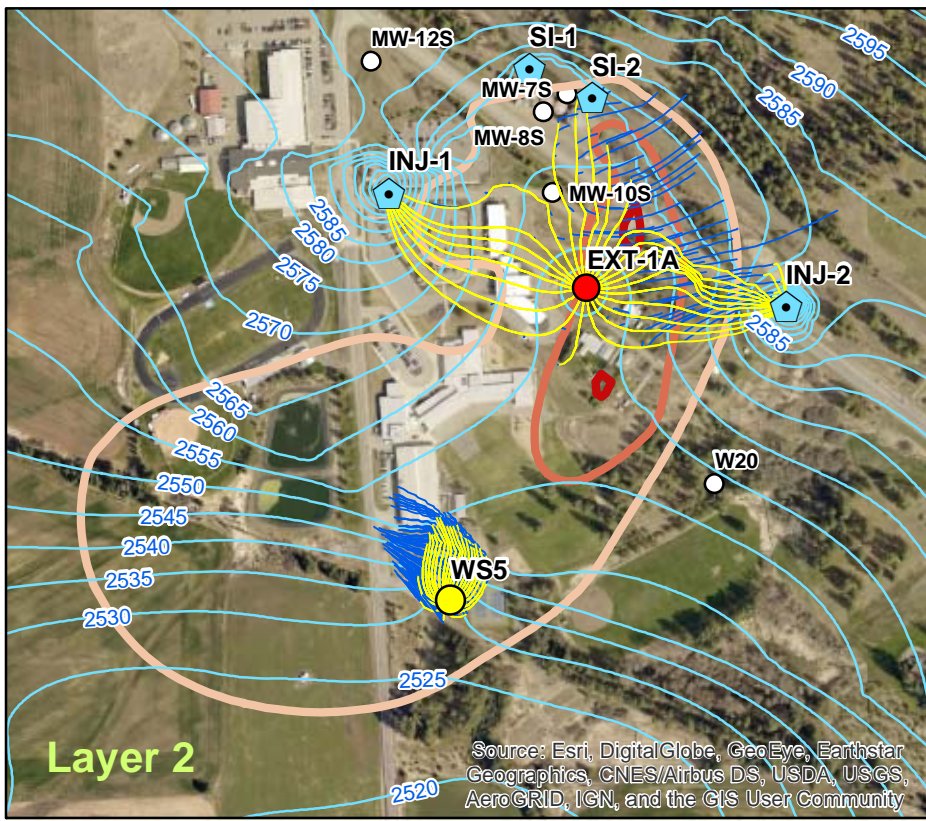
“Seed” location is where the particle is started (i.e., a well)

“Origin” is where the modeled GW originated from (where the particle reverses back to)

Figure 5-2
Reverse Particle Starting
Location Protocol

2019 Groundwater
 Modeling Report

Grain Handling Facility at Freeman
Freeman, Washington



Legend

- Monitoring Wells
- Pumping Wells**
 - ⬢ Injection
 - Extraction
 - School Supply
- Modeled Groundwater Contours (feet)
- CCI4 (ug/L) Contours**
 - 5
 - 50
 - 200
- Particle Pathlines**
- Particle Location**
 - Layers 1 - 4
 - Layers 5 - 7

Notes:
 Each panel displays particle tracks released in the respective layer.
 Reverse particles were started in rings surrounding the School Well (WS5), EX-1A and 1B.
 Ring radius: 15 ft.
 Rings per layer: 9
 Particles per ring: 24
 Total particles per layer per well: 216

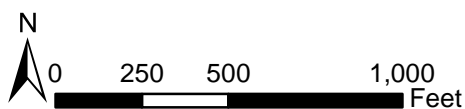
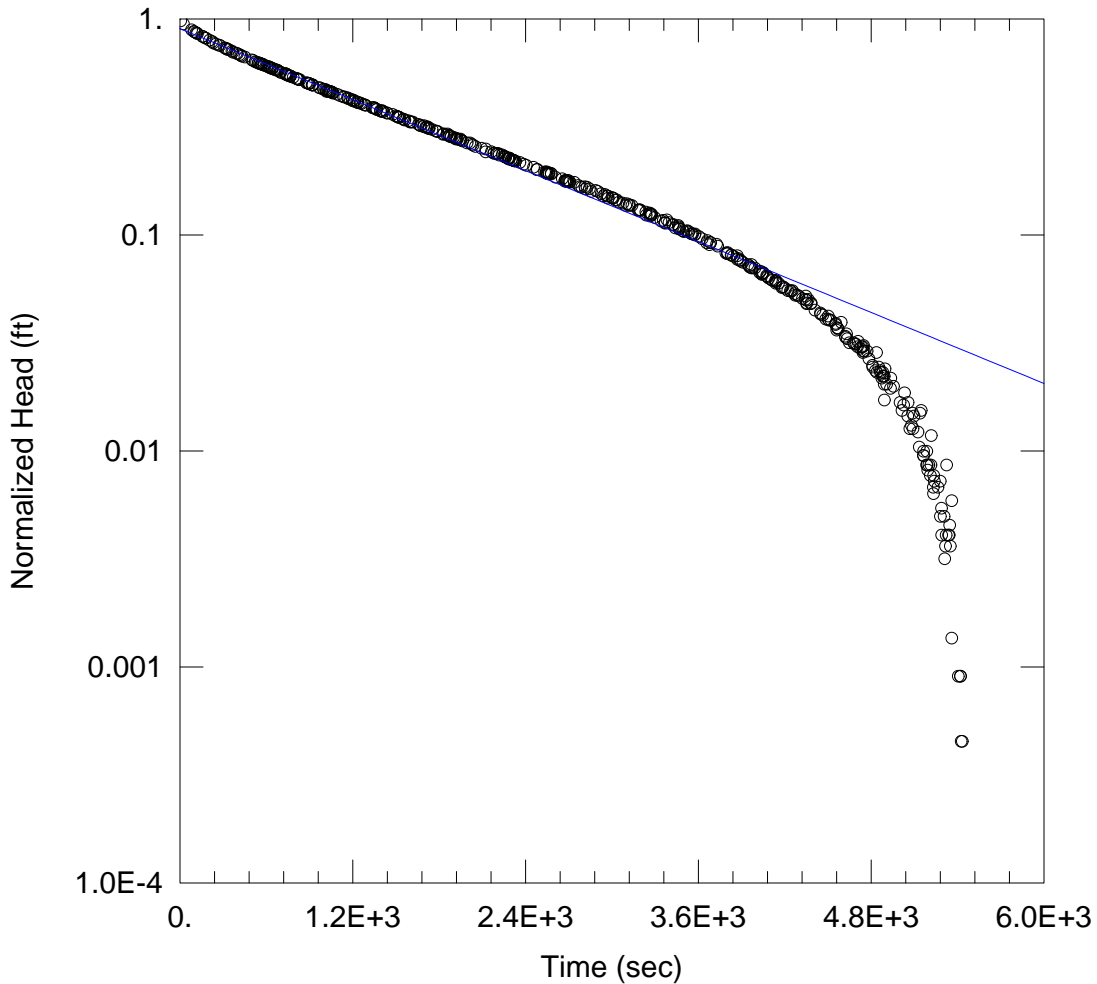


Figure 5-3
Remedial Scenario Results
Groundwater Elevations
and Particle Pathlines
 2019 Groundwater
 Modeling Report
 Grain Handling Facility at Freeman
 Freeman, Washington

Appendix A
2019 Slug Test AQTESOLV Results



WELL TEST ANALYSIS

PROJECT INFORMATION

Company: JACOBS
 Test Well: MW-27
 Test Date: 9-12-2019

AQUIFER DATA

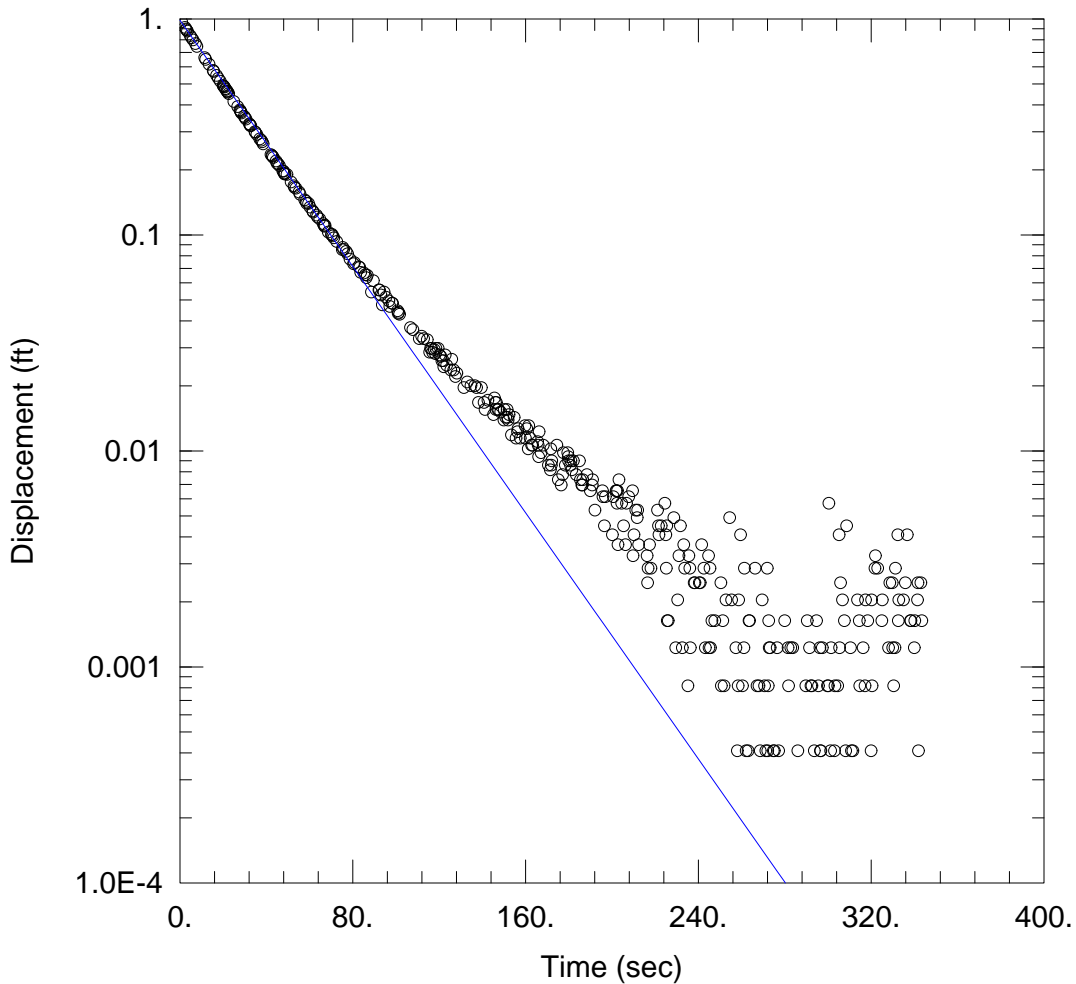
Saturated Thickness: 175.4 ft Anisotropy Ratio (Kz/Kr): 1.

WELL DATA (MW-27)

Initial Displacement: 2.47 ft Static Water Column Height: 175.4 ft
 Total Well Penetration Depth: 175.4 ft Screen Length: 10. ft
 Casing Radius: 0.083 ft Well Radius: 0.25 ft

SOLUTION

Aquifer Model: Unconfined Solution Method: Bouwer-Rice
 K = 9.636E-7 ft/sec y0 = 0.9008 ft



WELL TEST ANALYSIS

PROJECT INFORMATION

Company: JACOBS
 Test Well: MW-28
 Test Date: 9-12-2019

AQUIFER DATA

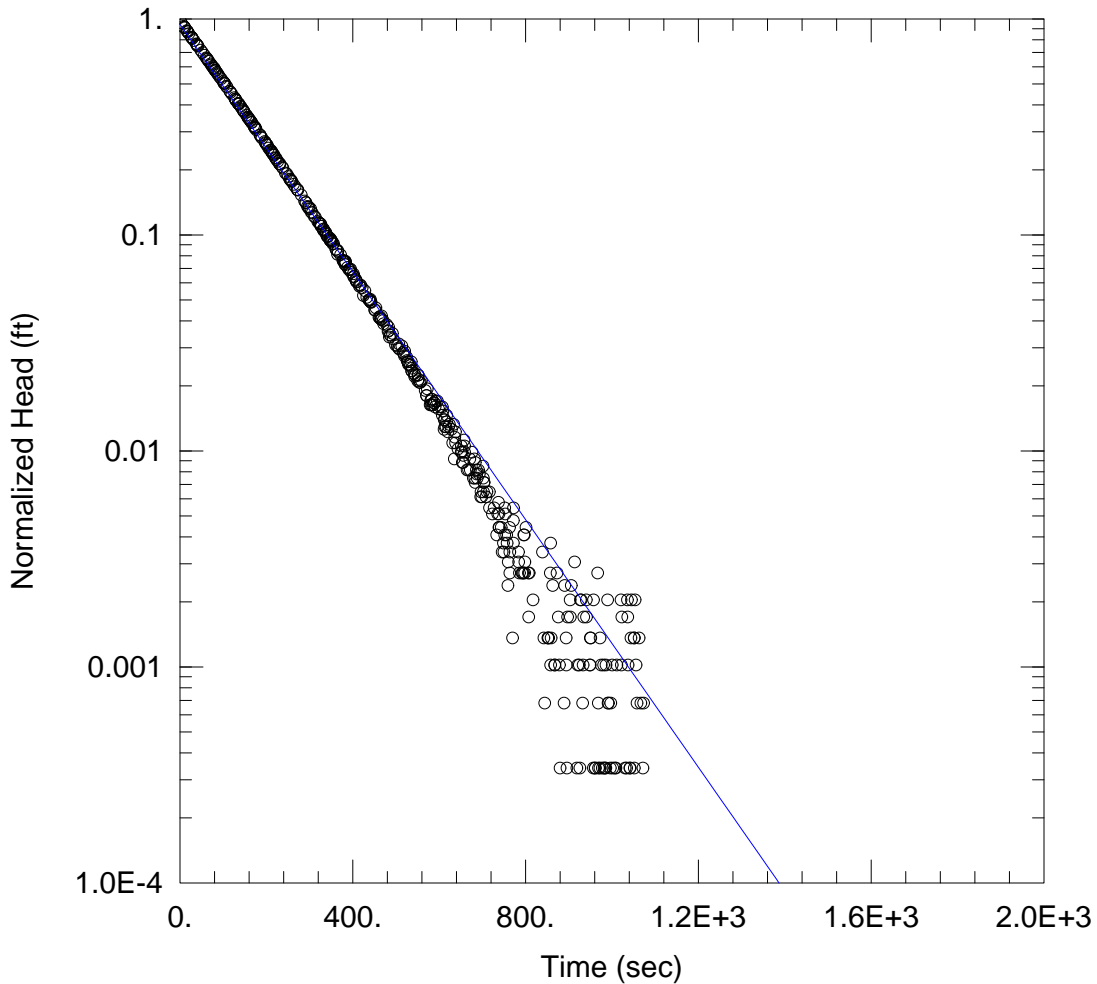
Saturated Thickness: 131.3 ft Anisotropy Ratio (Kz/Kr): 1.

WELL DATA (MW-28)

Initial Displacement: 2.439 ft Static Water Column Height: 131.1 ft
 Total Well Penetration Depth: 131.1 ft Screen Length: 10. ft
 Casing Radius: 0.083 ft Well Radius: 0.25 ft

SOLUTION

Aquifer Model: Unconfined Solution Method: Bouwer-Rice
 K = 4.667E-5 ft/sec y0 = 0.9859 ft



WELL TEST ANALYSIS

PROJECT INFORMATION

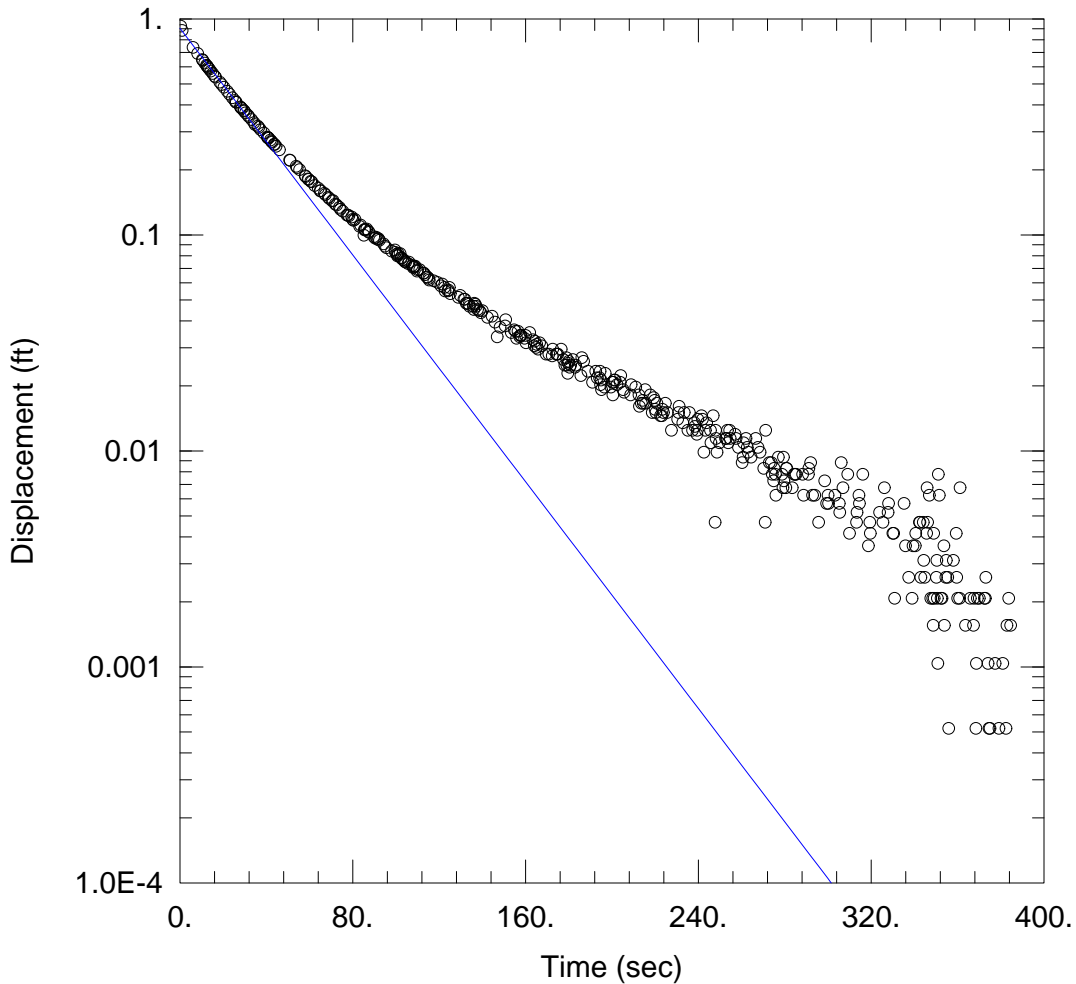
Company: JACOBS
 Test Well: MW-29
 Test Date: 9-12-2019

WELL DATA (MW-29)

Initial Displacement: 2.97 ft Static Water Column Height: 81.6 ft
 Total Well Penetration Depth: 81.6 ft Screen Length: 20. ft
 Casing Radius: 0.083 ft Well Radius: 0.25 ft

SOLUTION

Aquifer Model: Unconfined Solution Method: Bower-Rice
 K = 4.817E-6 ft/sec $y_0 =$ 0.9447 ft



WELL TEST ANALYSIS

PROJECT INFORMATION

Company: JACOBS
 Test Well: MW-30
 Test Date: 9-12-2019

AQUIFER DATA

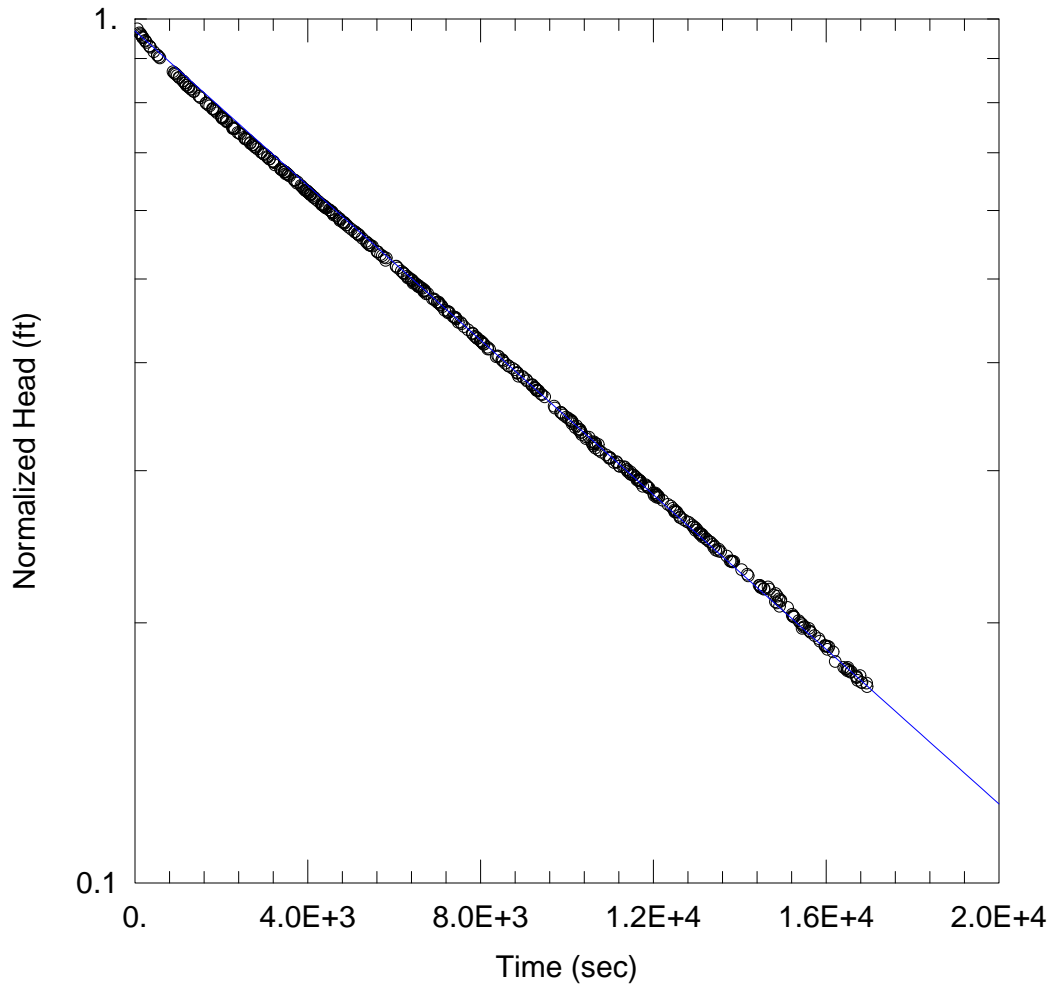
Saturated Thickness: 41.94 ft Anisotropy Ratio (Kz/Kr): 1.

WELL DATA (MW-30)

Initial Displacement: 1.945 ft Static Water Column Height: 41.94 ft
 Total Well Penetration Depth: 41.94 ft Screen Length: 20. ft
 Casing Radius: 0.083 ft Well Radius: 0.25 ft

SOLUTION

Aquifer Model: Unconfined Solution Method: Bouwer-Rice
 K = 1.996E-5 ft/sec y0 = 0.9053 ft



WELL TEST ANALYSIS

PROJECT INFORMATION

Company: JACOBS
 Test Well: MW-31
 Test Date: 9-12-2019

AQUIFER DATA

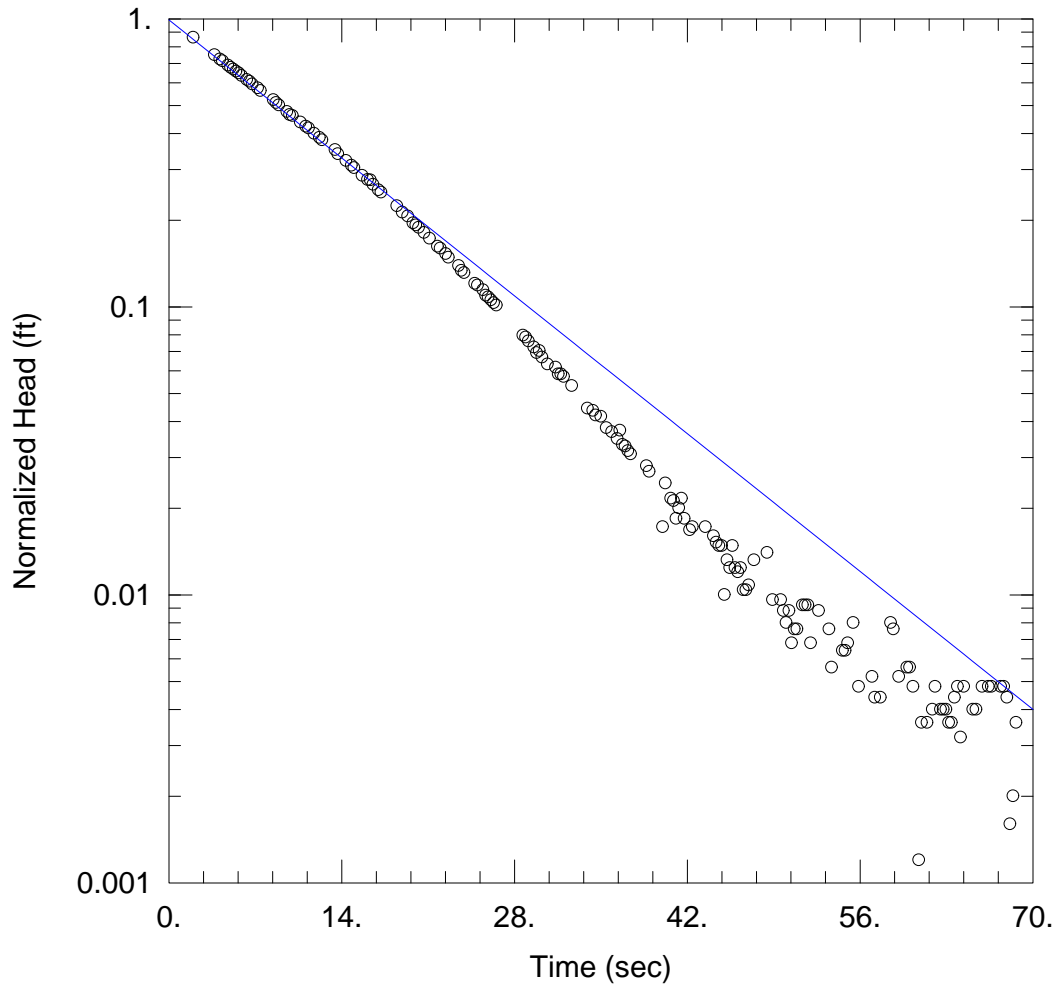
Saturated Thickness: 285.8 ft Anisotropy Ratio (K_z/K_r): 1.

WELL DATA (MW-31)

Initial Displacement: 2.644 ft Static Water Column Height: 285.8 ft
 Total Well Penetration Depth: 285.8 ft Screen Length: 5. ft
 Casing Radius: 0.083 ft Well Radius: 0.25 ft

SOLUTION

Aquifer Model: Confined Solution Method: Hvorslev
 $K = 2.618E-7$ ft/sec $y_0 = 0.9685$ ft



WELL TEST ANALYSIS

PROJECT INFORMATION

Company: JACOBS
 Test Well: MW-32
 Test Date: 9-10-2019

AQUIFER DATA

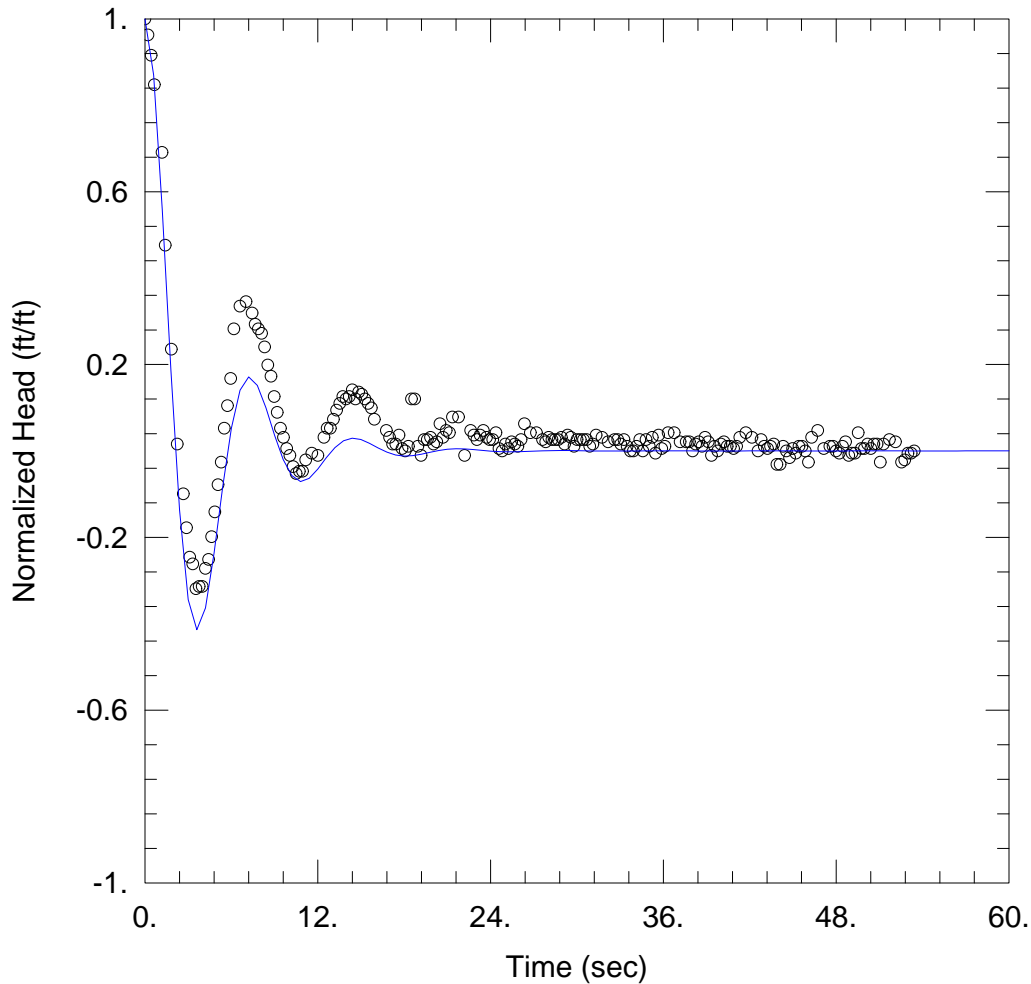
Saturated Thickness: 169.9 ft Anisotropy Ratio (K_z/K_r): 1.

WELL DATA (MW-32)

Initial Displacement: 2.493 ft Static Water Column Height: 169.9 ft
 Total Well Penetration Depth: 169.9 ft Screen Length: 10. ft
 Casing Radius: 0.083 ft Well Radius: 0.25 ft

SOLUTION

Aquifer Model: Confined Solution Method: Hvorslev
 $K = 0.0001189$ ft/sec $y_0 = 0.9914$ ft



WELL TEST ANALYSIS

PROJECT INFORMATION

Company: JACOBS
 Test Well: MW-36
 Test Date: 9-11-2019

AQUIFER DATA

Saturated Thickness: 54.93 ft Anisotropy Ratio (Kz/Kr): 1.

WELL DATA (MW-36)

Initial Displacement: 0.97 ft Static Water Column Height: 54.93 ft
 Total Well Penetration Depth: 54.93 ft Screen Length: 15. ft
 Casing Radius: 0.083 ft Well Radius: 1. ft

SOLUTION

Aquifer Model: Unconfined Solution Method: Springer-Gelhar
 K = 0.001023 ft/sec Le = 39.6 ft